LCC FIBER REINFORCED ‘GREEN’ COMPOSITES DERIVED FROM RAW PLANTAIN STARCH

A thesis

Presented to the Faculty of the Graduate School

of Cornell University

in partial fulfillment of the requirements for the Degree of

Master of Science

By

Vaibhavi Rajendra Vaidya

February 2016

ABSTRACT

Significant research is being conducted to derive environment-friendly, sustainable and fully biodegradable polymers and composites. These help avoid the environmental pollution created by the conventional non-degradable plastics that end up in landfills. Starch is a yearly renewable plant-based resource that is most abundantly available around the world. Increasing number of scientists have modified starches from potato, corn, rice, etc., to create resins that can replace the more common petroleum based ones.

Understanding the gravity of the situation, the major objectives of this research are as follows:

1. To develop a fully 'green' resin using raw plantain starch and banana microfibrils with the help of minimal and green/ food grade chemicals.
2. To study the effects of chemical and mechanical treatments on morphology, orientation, crystallinity and ultimately tensile strength of the inherently strong liquid crystalline cellulose fibers.
3. To devise an easy to scale up method for fabricating advanced 'green' fiber reinforced composites as a contribution to the greener world.

On these lines, starch was isolated from raw plantain pulp using alkaline and non-alkaline methods. A comparative study of the processes used and resulting starch contents was carried out. Starch content of above 80% was successfully isolated from the plantain fruit by alkaline steeping method using Sodium bisulfite ($NaHSO_3$), a food grade chemical. The physical and mechanical properties of the obtained starch were characterized and compared with the conventional starches. An environment-friendly cross linker 1,2,3,4-butane tetracarboxylic acid

(BTCA) along with a catalyst, Sodium hypophosphite-monohydrate (SHP), was used to crosslink the plantain starch into a thermoset resin. Further, banana stem fibers were harnessed to extract cellulosic microfibrils and used as the reinforcing element to enhance the modulus (stiffness) of the resin and make it truly ‘green’.

Liquid Crystalline Cellulose fibers were used as fillers to make a fiber reinforced composite using RP starch based resin. These fibers were characterized for their tensile properties, diameter and crystallinity in order obtain control data and device methods to improve them further. The fibers were subjected to physical (tension) and chemical treatments to enhance their mechanical properties and make them high strength. Various parameters like treatment chemical, load value, duration were varied to carry out a deep study of their effect on the mechanical properties of LCC fibers.

A gradual increase in the percentage crystallinity and mechanical properties was seen on optimizing each parameter. A dramatic increase compared to the control fibers was obtained in the tensile modulus and strength on testing the Sodium bisulfite treated fibers under tension at optimum parameters.

In summary, a convenient and easy to scale up process was developed to obtain a fiber reinforced composite from plantain-based resin using its pulp, banana stem fibers and LCC yarns. The mechanical and physical properties of this starch suggest that it can be used in place of conventional starch based resins. In addition, the developed process allows using large quantities of raw cull plantains and potentially eliminating the waste problem created by excess production as well as damage caused during their harvest and transportation.

BIOGRAPHICAL SKETCH

Vaibhavi R. Vaidya was born on 27th September 1991, in Pune, Maharashtra, India. Having keen interest in sciences, she was a recipient of State level talent search scholarship. After completing her schooling in Pune, she got admitted to the Institute of Chemical Technology, (formerly UDCT), Mumbai, India. She received her bachelors (B. Tech.) with a major in Fiber and Textile processing technology in May, 2013. Her eagerness for higher education brought her to Cornell University for graduate studies. She earned a Master of Science degree with a major in Fiber science at Cornell University under the guidance of Professor. Anil. N. Netravali.

Dedicated to my parents Rajendra and Ranjana, my sister Mrunal and my family for their unconditional support.

ACKNOWLEDGEMENTS

I thank my advisor, Professor Anil N. Netravali for his guidance and motivation that was extremely helpful during my graduate education and research. I thank my minor advisor Dr. Meredith Silberstein for her invaluable suggestions that helped complete my research work.

I thank Xia Zeng, Maura Weathers and Don Werder for providing me training and technical assistance with various research instruments. I thank Dr. H. Boerstoel, Teijin Twaron BV (Arnhem, The Netherlands) and CSIR- North East Institute of Science and Technology (NEIST), Jorhat, India for providing multifilament LCC yarns and mechanically extracted banana stem fibers respectively that were very useful for my research. I thank Cornell Center of Materials Research (CCMR) for allowing me to use various facilities and characterization equipment. I also thank the National Science Foundation (NSF) and The Wallace Foundation for providing financial aid for my research.

I thank my fellow colleagues Maksud Rahman, Namrata Patil, Yidong Zhong and Dr. Dipul Kalita for their help and discussions about my research work. A special thanks to my friends Pooja, Sarang, Kritika, Purujit and Ojas for proof reading my thesis. Last but not the least I thank the FSAD staff and my friends for making my stay at Cornell a pleasant experience.

TABLE OF CONTENTS

LIST OF FIGURES

LIST OF TABLES

1. INTRODUCTION

The motivation behind this study was to take a step towards a greener world. The best way to go green is to return back what we get from nature in a responsible and sustainable manner. Thus, composite materials such as wood and bones that are developed by nature have inspired the present research. It is well understood that wood and bones as composite materials have been used for generations for multiple structural and functional applications [1]. In fact, they have proven to be the perfect examples of superior quality, fiber reinforced composites.

To fabricate similar composites, it is important to understand the properties of bones and wood. The basic building block of a bone is hydroxyapatite reinforced collagen fiber composite and different types of bones are obtained from the change in orientation and arrangements of the collagen fibers [1]. Similarly, wood is a composite comprising of lignin as matrix (binding resin) and spirally oriented cellulose fibers (fibrils) [1]. The overall orientation and packing of constituent materials at the microscopic level impart exceptional stiffness and load bearing strength to these naturally occurring composites. Mechanical properties of such high orders are challenging but have been achieved for synthetic engineering composites using high strength fibers. Currently, advanced engineering composites are mostly produced by using synthetic petroleum based resins and fibers.

Table 1.1 presents the 2013 and 2014 statistics of resin production and sales in the USA. The data indicate that the yearly production of these plastics crossed 100,000 million pounds in the USA alone [2]. It can also be seen from Table 1.1 that thermoplastics occupy the majority share of the resin market. However, due to the difficulties associated with their recyclability and reusability, thermosets create a greater environmental impact than thermoplastics [3]. Figure 1.1

[4] illustrates the current and expected demand in carbon fiber reinforced plastics (CRP). The Figure 1.1 also shows an exponential rise in demand for previous years. The increase in the demand of CRPs because of the ever-expanding applications has led to large-scale production of non-biodegradable or non-compostable composites today. Majority of the current composites are petroleum based and most of them end up in landfills because no environment friendly solution for disposing them has been found as of today. In fact, over 94% of the composites end up in landfills because they are difficult to recycle or reuse [5]. This is a rising concern due to depletion of available land resources and ever increasing land, air and marine pollution [6].

Table 1.1 US resin production for the years 2013 and 2014 [2]

Resin	**Production**	
	2013	**2014**
Thermosets	**14,975***	**15,814**
Thermoplastics	**92,547**	**92,298**
Grand Total Plastics	**107,522**	**108,112**

*(Values in Million pounds, on dry weight basis)

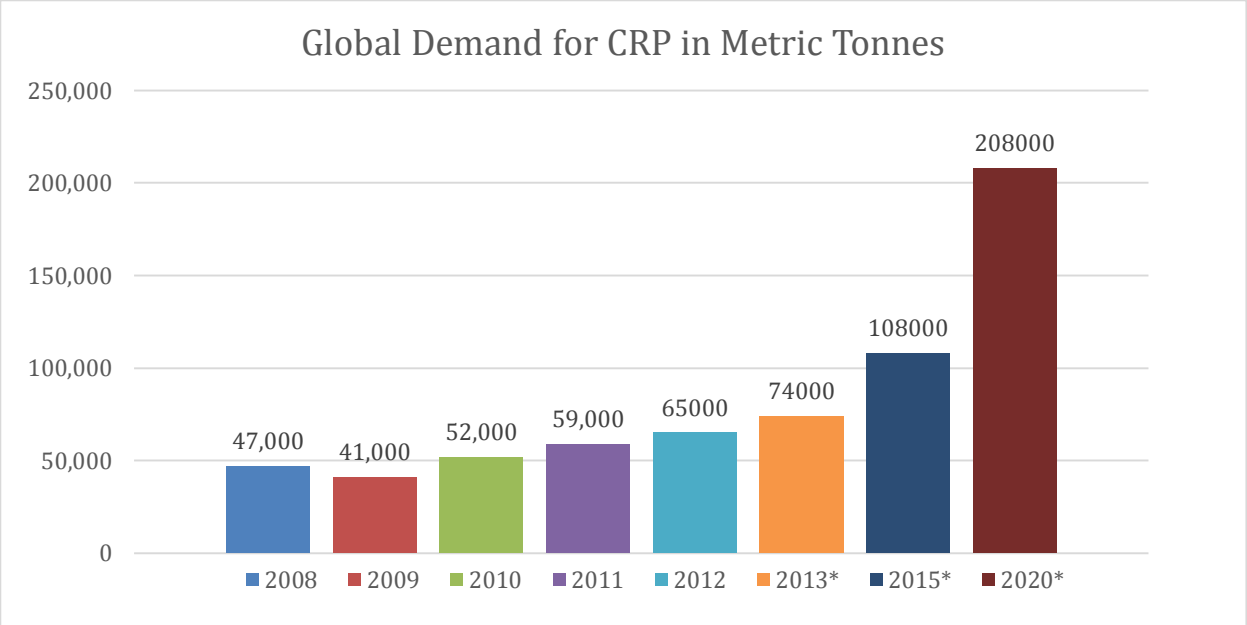

*(Estimated values)

Figure 1.1 Current and estimated demand for Carbon reinforced plastics (CRP) in the world [4]

Similar to the rise in demand for the resins, the demand for the petroleum based resources has increased by 400% from 1970 to 1990 and is soon expected to supersede the supply due to their exhaustible nature [6]. As a result, the prices of utilizing these sources are expected to rise significantly in the coming years [7]. These challenges can be dealt with efficiently by using biobased replacements that are abundantly available and easy to biodegrade or compost, eliminating the need to landfill them. The world's yearly production of biomass is large and estimated to generate 6.9 $*10^{17}$ kcal of available energy [7]. Moreover, this is a yearly renewable resource, replenished on a continuous basis and, hence, eliminates the probability of exhaustion of biomass in the near future. In spite of its abundant availability in nature, only 7% of the produced biomass is utilized today[7]. All the above mentioned statistics state the

potential in using biobased materials for a wide variety of applications apart from food and feed stock. Increasing number of laws and regulations enacted by governments around the world and rising environmental awareness among people have started to create a paradigm shift in the design of materials and raw material sources. This has led to developing more environment friendly materials [8]. Based on the consumer demand, big manufacturers are now innovating and producing sustainable goods that would be beneficial to the environment in the long run.

Table 1.2 illustrates the yearly usage of categories of plant based materials used in various industrial applications [9].

Table 1.2 Yearly usage of categories of plant materials for industrial applications [9]

Inputs	Usage*	Applications
Wood	**80.9**	**Paper, Boards, Lignocellulose, Composites**
Industrial Starch	**3.0**	**Adhesives, Polymers, Resins**
Vegetable Oil	**1.0**	**Surfactants, Inks, Resins**
Natural Rubber	**1.0**	**Tires, Household Goods**
Wood Extractives	**0.9**	**Oils, Gums**
Cellulose	**0.5**	**Textiles, Polymers**
Lignin	**0.2**	**Adhesives, Tanning**

*(Values in Million metric tons)

It is evident from the Table 1.2 that wood and wood based products occupy the largest share of the market. Other biobased materials such as proteins, starches, cellulose and lignin also have scope to improve their utilization by a significant margin. In fact, environment friendly composites fabricated using plant based resins and biobased fiber reinforcements can be called the next novel materials of the 21st century [3]. Biobased materials have attracted attention of many researchers and manufacturers and are now capable of competing with commercially available resins due to their desirable mechanical and thermal properties and environment friendly nature. Composites made using biobased resins and fibers that are fully biodegradable, sustainable and can be composted at the end of their lifecycle have been termed as 'green' composites.

The above mentioned 'green' composites use polymeric resins derived from starch extracts, microbial synthesized extracts or protein extracts [3]. Of these, starch based resins are more compatible for cellulose fiber reinforced composite applications due to their high adhesion property arising from their common chemistry that results in strong hydrogen bonding capacity.

The starch based resins can be derived from various biobased materials that are commonly available. For example, starches can be easily isolated from potato, rice, and corn. The starch used in the present research was isolated from plantain fruit and reinforced with banana stem microfibrils to enhance its stiffness as a potential resin for composites. Plantain and banana belong to the *Musaceae* family of crops and are produced extensively in Asia, Africa, Hawaii and South America. However, it has been recorded that these fruits go waste on a significantly large scale due to lack of storage and transportation facilities in the producing countries [10]. For example, about 50% of weekly plantain production is wasted in Agogo, Ghana [10]. Similarly, large quantities of plantains are thrown in river beds in Taiwan [11].

Large quantities of green cull bananas and plantain waste can be harnessed to obtain functional products by converting them to useful biobased resins and further into green composites. Additionally, the stem wastes can be used to produce high strength cellulose microfibrils as enhancers of mechanical properties of biobased materials. In the present research, the isolated plantain starch has been crosslinked using 1,2,3,4 butane tetracarboxylic acid (BTCA), a green crosslinker, in the presence of sodium hypophosphite as a catalyst. Additionally, banana fiber micro cellulose was used to reinforce the resin.

Conventionally, various petroleum based high strength fibers such as carbon, Kevlar®, etc., are used to fabricate advanced composites for use in aerospace, sports and auto industry. Similar to these fibers, many plant based fibers such as cotton, hemp, sisal, ramie, etc., can also be used for making green composites [12-14]. Most of these fibers, unlike carbon, have relatively moderate mechanical properties and are susceptible to water, thus limiting their applications [15]. Plant based fibers have strength in the range of 300 to 900 MPa and Young's modulus in the range of 10 to 30 GPA [6]. As the mechanical properties of the composites are mainly dependent on the tensile properties of the reinforcing fibers, the present research has used liquid crystalline cellulose (LCC) fibers with inherently high stiffness and strength.

The high strength LCC fibers were further modified by using various chemical and physical (tension) treatments to enhance their stiffness and strength. Attempts were made to use modified LCC fibers as the reinforcing element in plantain starch based crosslinked (thermoset) resin to fabricate a fully biodegradable high strength 'advanced green composites'.

With developments happening all around the world the future of green and sustainable composites looks very promising. The U.S. Department of Energy (DOE) sponsored the vision

of ‘The Technological Roadmap for Plant/Crop based Renewable Resources-2020’. It is targeted to achieve the mark of at least 10% of basic chemical building block arising from plant derived renewables by 2020. Furthermore, development of concepts is expected to achieve the mark of 50% by 2050 [7].

With great research efforts undertaken in the area of biobased materials for industrial applications, advanced green composites are expected to be fabricated with high mechanical properties but environment friendly characteristics to compete with petroleum based products and eventually replace them in the near future.

2. LITERATURE REVIEW

2.1 Polysaccharides

Carbohydrate polymers are a class of polysaccharides that are synthesized by plants and animals for nutritional and structural purposes. They are abundantly available in nature and constitute long chains of monosaccharide units like glucose, fructose [16] and oligosaccharides with a general form $(CH_2O)_n$ connected together by glyosidic linkages. In general, polysaccharides are high molecular weight polymers that are represented with a general formula of $(C_6H_{10}O_5)_n$, where $40<n<15{,}000$. They have varied structural and functional properties due to their heterogeneous nature of repeat units.

The most common types of polysaccharides include cellulose, starch, hemicellulose and glycogen, all having the basic repeat unit of glucose, held together by distinct linkages [17]. Of these, starch and glycogen are easily broken down and digested and hence used for energy storage in plants and animals. Cellulose on the other hand, is a hydrophilic polymer imparting structural integrity to the cells and tissues. It is also used for nutritional purposes as dietary fiber due to the inability of plants and animals to digest it.

Taking advantage of the inherent properties and abundant availability of these polysaccharides in natural and processed forms, there is now a rising trend in utilizing them in industrial applications.

Natural and regenerated forms of cellulose are used in textile, paper, cosmetic and food industries. Similarly, cellulose in micro- and nano- forms such as MFC, bacterial cellulose and

nanocrystalline cellulose are used for structural applications in construction, aerospace and sport industry [5, 18, 19].

Following cellulose, starch is the second largest used polysaccharide, with a wide variety of applications from gelling systems in food to paper and adhesives [20].

2.2 Natural Starches

Starch is an inexpensive and abundantly available commodity, produced in almost all the countries [21]. It is one of the most common ingredients of human diet and is found as a deposition in plant tissues and organs including leaves, roots, fruits, grains and stems [22]. Different plant based sources can provide many varieties of starches. Of these, rice, maize, potato, wheat and tapioca are the most abundantly available starches. The overall growth rate of starch production in the US has been recorded at 4%/p.a. from 1995 till 2010 [23].

The sources of starch vary over the world depending on the climatic conditions and harvesting traditions. However, starch and derivatives from maize and potato have been of highest commercial interest [20]. Figure 2.1 illustrates the proportions of world starch production by crop, in 2010.

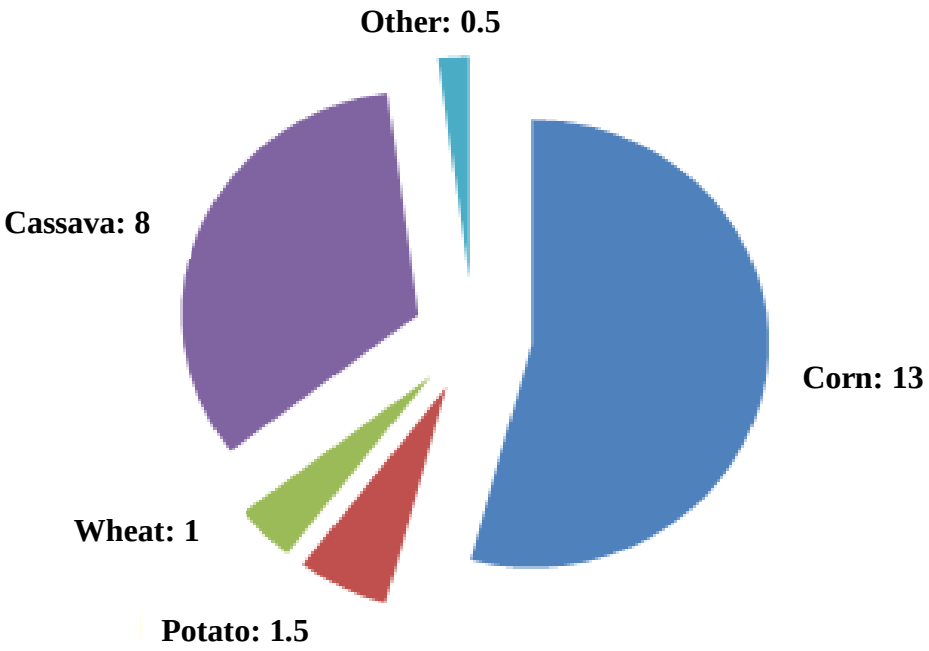

Figure 2.1 World starch production by crop, 2010, million tons [24]

It can be clearly seen that corn/maize is the largest source for starch and the other sources remain relatively less explored. Of the overall starch production, about 50% of starch is used for sweeteners and other food applications, 35% is used in native form whereas about 10% is modified for various other functional uses [23]. However, there is a rising concern among the consumers about modified starches in food production [25] due to the presence of chemical traces in them. Moreover, the lack of domestic starch production in many countries, has led to a need to isolate and characterize new varieties of starch that can be made available to the domestic population for food as well as industrial applications [25]. Therefore, in the present research, starch was isolated from raw plantain fruit, which is readily available in tropical areas all around the world. Presently, the excess production of plantains and bananas in the tropical

countries is discarded due to lack of export quality requirements making these fruits an ideal source to fulfil the demand for starch.

2.2.1 Chemistry of Starches

Starch, chemically, constitutes of two polymers namely amylose and amylopectin derived from D-glycopyranose. Figure 2.2 shows the linear structure of amylose, which is a helical polymer of α- D glucose units joined by α (1 → 4) glyosidic linkages. Figure 2.3 shows the branched structure of amylopectin. Amylopectin constitutes of both (1 → 4) and (1 → 6) glyosidic linkages which form the linear and branched regions in the polymer, respectively.

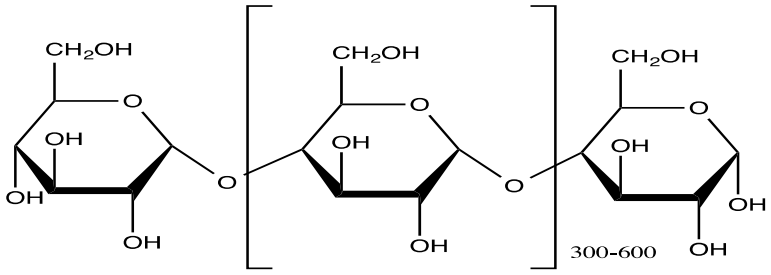

Figure 2.2 Linear structure of amylose

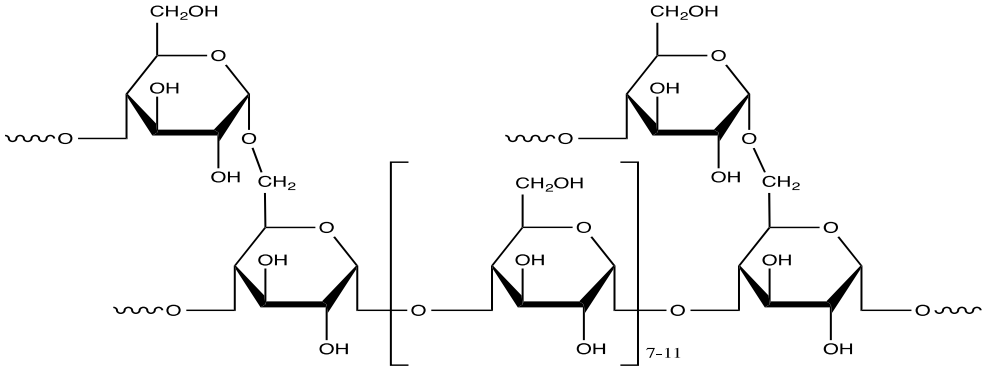

Figure 2.3 Branched structure of amylopectin

Table 2.1 Amylose content of various native and modified starches [26]

Source of Starch	% Amylose
Corn	**28-30**
Cassava	**17**
Wheat	**26**
Potato	**20**
Waxy Sorghum/ Waxy Rice/ Waxy Maize	**0-2**
High Amylose corn	**70**

Amylose is a low molecular weight polymer with 1,000-10,000 glucose repeating units, while amylopectin is a much larger molecule, that may have a degree polymerization (DP) above a million [27]. Due to a large difference between the two D-glycopyranose polymers, the properties of different starches are greatly affected by their constituent percentages. The solubility characteristics and bonding capability of amylopectin makes it desirable for industrial applications. Interestingly, it has been observed that each starch variety has a unique structure of amylose with a distinct branch chain length distribution profile [28, 29]. The average DP of amylopectin branch chain length was noted as around 18.8 for waxy starches whereas it was around 30.7 for high amylose starches [30]. Commonly, the native starches have amylose content around 20-30% and 70-80% of amylopectin.

However, new modified forms of starches with separation of the 2 contents; amylose and amylopectin are available commercially, to target the desired end use [12]. Table 2.1 gives summarized statistics of the amylose contents of various native and modified starches.

2.2.2 Functional Properties of Starches

Amylose and amylopectin content of starch is one of the main functional characteristics on which its suitability for a specific end use depends. Some of the other functional properties based on which the starch is selected for industrial applications include chemical composition, granule size [31], water solubility, gelatinization temperature and viscosity. Most of these physicochemical properties are closely linked to the botanical origin of the starch and the environmental conditions during processing and storage [32]. Starch is considered a semi crystalline polymer due to the existence of both crystalline and amorphous phases in its growing rings. These phases are obtained in complex arrangements in the amylopectin. There are helical intertwining chains with glucose repeat units, which represent the crystalline lamellae whereas the branching points act as the amorphous lamellae [28, 33]. For composite and resin applications, these phases are modified to form a polymer having desirable moisture resistance, biodegradability and thermal stability [13, 34, 35].

2.3 Raw Plantain Starch and Its Advantages

Raw plantain (RP) starch makes an attractive replacement for petroleum based polymers which are exhaustible, expensive and environmentally non-compatible. Polysaccharides and proteins together form the largest part of available biomass which is yearly renewable, biodegradable and inexpensive [18]. Starch is a form of polysaccharide that is present in multiple organs of the plants. Plantain and bananas are starch rich fruits obtained on a large scale all across the world.

As mentioned earlier, plantains belong to the *Musaceae* family known by the general term banana consisting of all species and hybrid varieties. It is known as the cooking variety of banana or vegetable-banana and has low water soluble sugar content compared to the fruit bananas.

Plantains are native to India and mainly produced in the tropical and subtropical areas of the world. They have an advantage of year round growth assuring a secured supply of nutrition and, for growers, as a source of continuous income. Table 2.2 gives the statistics of world production of banana family in 2003 by areas. The overall production in these areas is estimated at 102 million metric tons with a distribution of 32% plantains and 68% bananas of the total [36]. The production increased by more than 40% in 10 years. In 2013, the total production of bananas and plantains was recorded to be as high as 145 million metric tons of which about 27% constituted of plantains and the rest 73% were bananas.

Such large production of the crop generates considerable income for the producing regions through export as well as local sales. However, today there is a high rejection rate to the RP fruit from entering the market due to stringent quality restrictions on the size, shape and color as well as possibility of microbial infections on slightly damaged areas [10]. The high expectations of the consumers in terms of shape or color render a large amount of the produce useless in spite of it being healthy and edible. The discarded produce thus becomes readily available for starch isolation.

Table 2.2 Total world production statistics of banana and plantains in 2003 [36]

Area	Production*
Asia	**37,140**
Africa	**23,308**
Central America and Caribbean	**8,519**
Total Plantains	**32,974**

*(Values × 1000 MT)

There are many examples all across the world where banana and plantain rejection has risen and has become a great problem. It has been observed that 50% of the harvest is used as feed stock or is discarded in many African countries [10]. Some other examples include Costa Rica and Taiwan where the discarded harvest is thrown as cull in riverbeds. This leads to a high biochemical oxygen demand in the rivers, depleting the aquatic life in these regions [36]. Similarly, in a recent study it was found that 100,000 metric tons of bananas go waste every year in Australia. This waste is cut and spread over plantations as organic fertilizers or used as feedstock. Though these make up for fair uses of the discarded crop, the growers prefer to earn some revenue for their crop that does not make it to the market simply due to the strict regulations of size and color. The heavy wastage problem has created an interest amongst the researchers to explore avenues for the use of *Musaceae* family produce as a viable source of income. Some of these efforts are discussed below.

2.3.1 Starch Isolation Procedures

Among the multiple applications of the plantains other than food, starch isolation can be the easiest and most revenue yielding application due to its year round demand and easy processing. Currently researchers have used multiple processes to isolate starch from raw plantain. The isolation processes can be broadly categorized into alkaline and non-alkaline methods. Initially, starch was isolated by the conventional alkali steeping method using NaOH solution of 0.1 M or lower concentration [37]. After steeping further processing steps included blending or wet milling, filtering, washing and drying of the slurry [37].

Chung, Liang and Huang in 1982, were the first to produce banana starch on pilot scale [38]. In their research, Taiwan bananas were used with 0.5 M NaOH on a stone mill. Removal of peels was suggested due to their high content of pectin and presence of 21% of crude fiber which led to difficulty in material handling. Other non-alkaline methods of starch production include extraction with DI water [39]. It is the simplest procedure that includes, disintegrating sliced bananas in a blender, decanting and drying to obtain starch with highest purity but with a low yield [39]. However, in order to obtain a high yield, a green and cost efficient method of starch isolation was developed by using sodium bisulfite ($NaHSO_3$) using minimum processing chemicals, machinery and processing time [21]. It used banana/plantain pulp in 1% aqueous sodium bisulfite solution in the ratio 1 gm: 2 ml at a pH of around 4, for 4 hr at room temperature (RT). Sodium bisulfite is a food grade chemical used for preservation of wines and green leafy vegetables is nontoxic in low concentrations and makes the process green.

This method was identically repeated with raw plantains by replacing $NaHSO_3$ with NaOH which is less expensive. However, the results indicated that the yield with $NaHSO_3$ was greater than that obtained using NaOH by almost 13% [40].

Use of $NaHSO_3$ allows the endogenous enzymes present in the RP fruit to disintegrate the plant cell walls and release of starch granules into the aqueous solution [21]. Filtration of the steeped pulp leads to removal of these cell walls and the non-starchy matter, giving a high yield of pure starch.

In this research a comparative study of the isolated starch yield using alkaline and non-alkaline methods was conducted. The proximate analysis results confirmed the isolation of highest starch percentage using aqueous $NaHSO_3$ solution. $NaHSO_3$, being a green and highly productive steeping solvent, was selected for starch isolation and resin formation from raw plantain fruits.

2.3.2 Properties of RP Starch

It is pertinent to review numerous factors that affect the physicochemical properties and ultimately the functionality and usefulness of RP starch for industrial applications. In comparison to potato and other root starches, RP starch possesses properties that allow plenty of scope for modifications relevant for industrial usage. The granular size of plantain/banana starch is 10-45µm [41] which is similar to sago and other bean (lima, garbanzo, green pea) starches having a size range of 15-50 µm and 10-45µm, respectively. Raw plantain starch granules are irregularly shaped but mostly elongated spheres with ridges. Figure 2.4 shows the scanning electrons micrographs of starch granules from green and ripe Valery bananas [39].

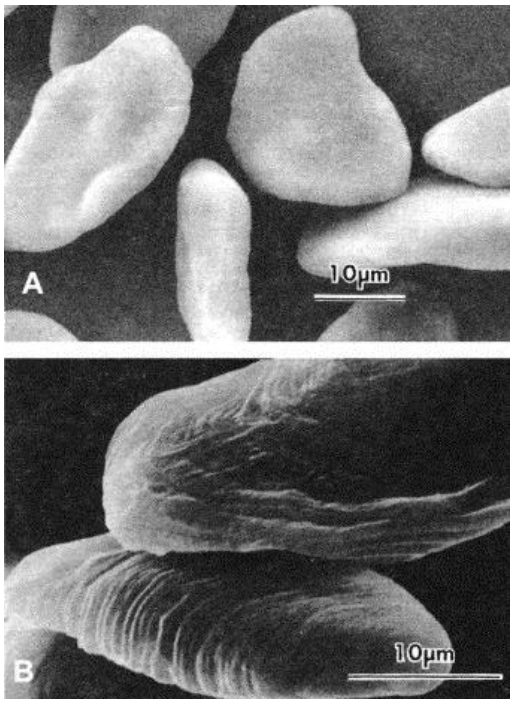

Figure 2.4 Scanning electron micrographs of starch granules from green (A) and ripe (B) Valery bananas [39]

The RP starch has an amylose content of 11-12% [29], whereas the amylose content of banana starch ranges from 15-40% [42, 43]. RP starch is a semi crystalline material with crystallinity depending on the amylose and amylopectin structure as explained earlier in section 2.2.2. Starches can be classified into 3 different patterns depending on their crystalline structure A, B and C. Most commonly, cereal starches belong to pattern A, amylomaize and tuber starches yield pattern B whereas root, bean and pea starches yield pattern C. Interestingly, in the case of plantain starches, both type B and C have been reported making it an unclear category [44].

Gelatinization characteristics of a starch are of prime importance for its use in bioplastic/adhesive industry. The natural process of starch gelatinization is a phase transition

that occurs when it is heated in excess of water over a characteristic range of temperatures [45]. On approaching the initial gelatinization temperature, it leads to swelling of starch granules, loss of birefringence, loss of crystallinity, water uptake by amorphous region, uptake of heat and ultimately leaching of amylose [36]. In case of RP starch, the gelatinization behavior is seen at temperatures between 70°C and 90°C with 14% swelling [46]. The density of plantain starch is around 1.6 ml/gm at 30°C [29]. It is pale white to yellow in color. The starch shows a non-Newtonian shear thinning character with increase in shear rate [45].

Bananas and plantains have a peculiar property of dramatic reduction of starch content with ripening of the fruit. Though it is an important fruit physiology, not much is known about the mechanism of this starch reduction phenomenon. Many researchers have studied the degradation rates as a function of humidity, temperature and other environmental factors [45]. It is seen that the average starch content drops from 70-80% in the pre-climacteric period to as low as 1% at the end of climacteric period. The degradation is mainly a conversion of the starch to soluble sugars in the form of sucrose in fruits with a high water content [47]. This process is said to occur due to multiple endogenous enzymes. Table 2.3 provides in detail the reduction of starch content (%) in bananas as a function of change in peel color upon ripening. Table 2.3 also summarizes the effect of ripening on the gelatinization temperature [37]. Apart from the changes in gelatinization temperature and sucrose content with ripening, there is also a distinct change in the structure of granules from oval to irregular [38].

Table 2.3 Reduction of starch content (%) in bananas as a function of change in peel color (Ripening)

Stage	Peel Color	Starch Content (%)	Sucrose Content (%)	Gelatinization Temperature (°C)
0	Green	61.7	1.2	74-81
1	Green	58.6	6	75-80
2	Green with Trace Of Yellow	42.4	18.4	77-81
3	More Green than Yellow	39.8	21.4	75-78
4	More Yellow than Green	37.6	27.9	76-81
5	Yellow with Green Tips	9.7	53.1	76-80
6	All Yellow	6.3	51.9	76-83
7	Yellow with Brown Spots	3.3	52	79-83
8	More Brown that Yellow	2.6	53.2	-

Plantains by composition have a much lesser moisture content (~65%) compared to bananas (~83%). This leads to reduction in the rate of conversion of starch to simple sugars making them a desirable source for starch isolation [42].

2.4 Nano-/Micro-Fibrillated Cellulose Based Reinforcements for Biobased Resins

Use of nano-/micro-fibrillar materials in resins has been a characteristic step that imparts stiffness to the resin making it desirable in high strength applications [19, 48]. Apart from the conventionally known nano- and micro-scale reinforcements such as carbon nanotubes, silicone

whiskers, nano-/micro-fibrillated cellulose (NFC/MFC) based reinforcements are increasingly being used as sustainable alternatives without compromising the mechanical properties of the end product [18, 49-51]. It is noted that the most commonly used green reinforcements include NFC/MFC, nano-crystalline cellulose, cellulose whiskers, etc.

All the above mentioned forms of cellulose are obtained from various plant based sources as well as discarded biobased wastes and are isolated by mechanical methods and/or enzymatic/chemical hydrolysis. The processes for cellulose isolation include a few important steps for removal of other components such as lignin, pectin and hemicellulose. Therefore, it is usually a 3 to 5 step process involving chemical/enzymatic processing followed by mechanical shearing to obtain the desired dimensions. The conventional process to obtain the nano-/micro-fibrillated cellulose from multiple biobased sources can include the following steps:

1. Alkali treatment: The waxy substances on fibers (pectinic polysaccharides) and lignin influence the fiber wettability and adhesion characteristics making it resistant to solvent penetrations and processing [52]. Alkali treatment is an important step that helps solubilize the pectin and hemicellulose present in the fiber, making it swell and more accessible for further chemical treatments [53]. Though it may differ depending on the source of the cellulose, this treatment is usually carried out at elevated temperatures, as lignin removal is easier at or above its glass transition temperature. Solubilized components are then removed by washing and filtration.
2. Bleaching: Bleaching is optionally carried out to break down the phenolic compounds or chromophores and, thus, whitening the pulp [54].
3. Acid/Enzymatic hydrolysis: This is an important step where degradation of cellulose occurs in the presence of acids or enzymes that can cut the polymeric chain [55]. This

treatment is usually the final step which also results in some size reduction. Many studies have been carried out to analyze the effect of the acid hydrolysis treatment on cellulosic fibers including cotton, bagasse [19, 56], flax, etc., after which the pulp is subjected to mechanical degradation.

4. Mechanical treatments: Conventionally, this step is carried out to tailor and reduce the size of the cellulosic fibers by cleaving along their longitudinal axis and an effort is made to increase their aspect ratio. The cellulose microfiber pulp is diluted excessively and subjected to high speed high pressure homogenization causing the fiber to break down [57]. The extent of break down can be controlled by the imparted pressure and number of homogenization cycles.

In the current research, such micro-fibrillated cellulose referred to as (BFMC) was isolated from banana stem fibers making the RP resin a completely sustainable product derived from the *Musaceae* family of crops.

2.5 Natural and Synthetic Fibers

Fibers can be broadly defined as continuous or short length filaments of small diameters (approximately 3-25 μm) with a high aspect ratio obtained from natural or synthetic origin. They have multiple uses depending on their physical/mechanical properties, morphology and chemical structure and the use of natural fibers can be traced back to as long as 3000 years [58].

Figure 2.5 gives a detailed classification of fibers based on the origin. Fibers can be primarily categorized into two broad classes, natural and synthetic. As the names suggest, natural fibers are produced by nature through plants and animals, e.g., cotton, ramie, jute, sisal, wool, silk, etc.,

and can be further classified depending on their source as vegetable (mainly cellulose), animal (protein) and mineral fibers. The cellulosic vegetable fibers can be obtained from several parts of the plants including seed, bast (stem) or leaf.

Synthetic (man-made) fibers are further categorized into regenerated or semi-synthetics that are obtained by modifying naturally occurring fibers and synthetics that are obtained from fiber forming polymers and include polyester, nylon, carbon, polypropylene, Kevlar®, etc.

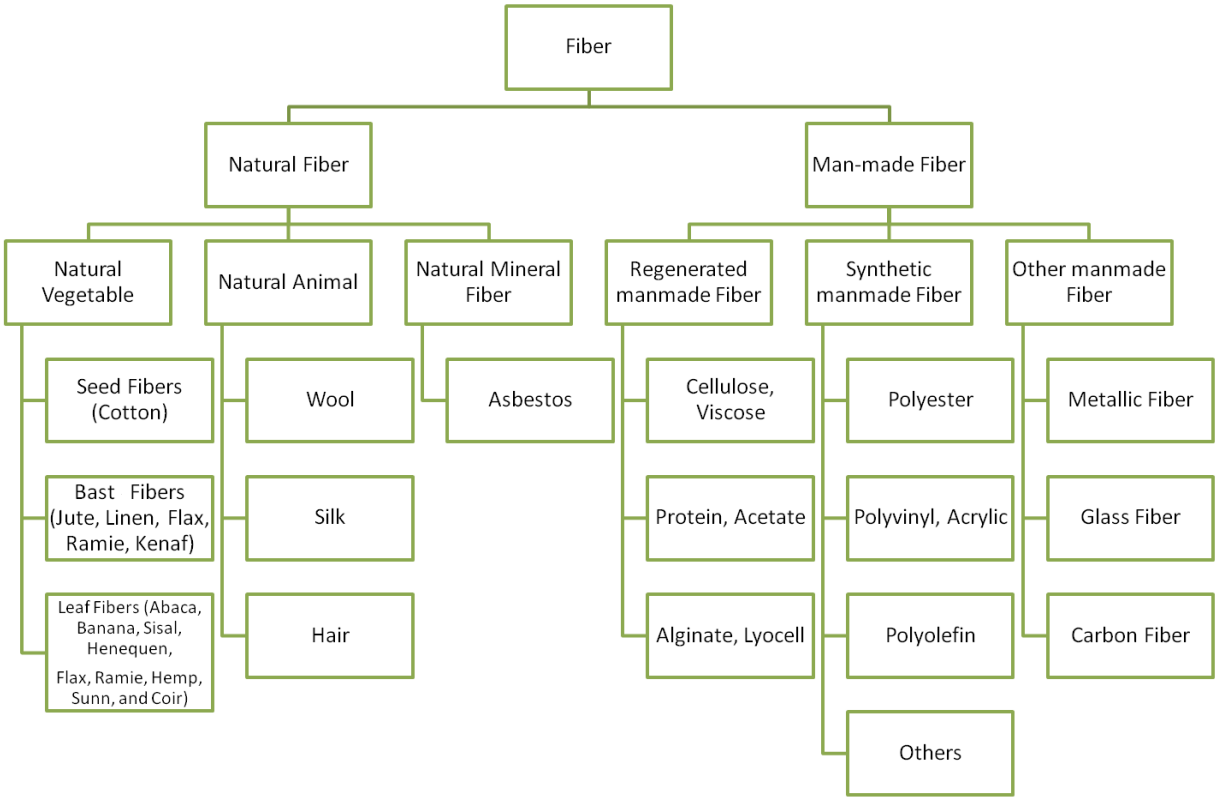

Figure 2.5 Classification of fibers based on their origin [59]

The largest use for fibers is in the textile and apparel industry, followed by their use in upholstery, or in industrial applications including reinforcing component in composites. The

rapid increase in their demand has necessitated invention and production of an increasing number of synthetic fibers with broad range of properties. Figure 2.6 shows the worldwide production of chemical and textile fibers over 40 years from 1975 till 2013 [60]. It can be clearly seen that the textile fiber production has increased 4 times over the past 40 years promising widening of its application fields beyond the traditional textile industry.

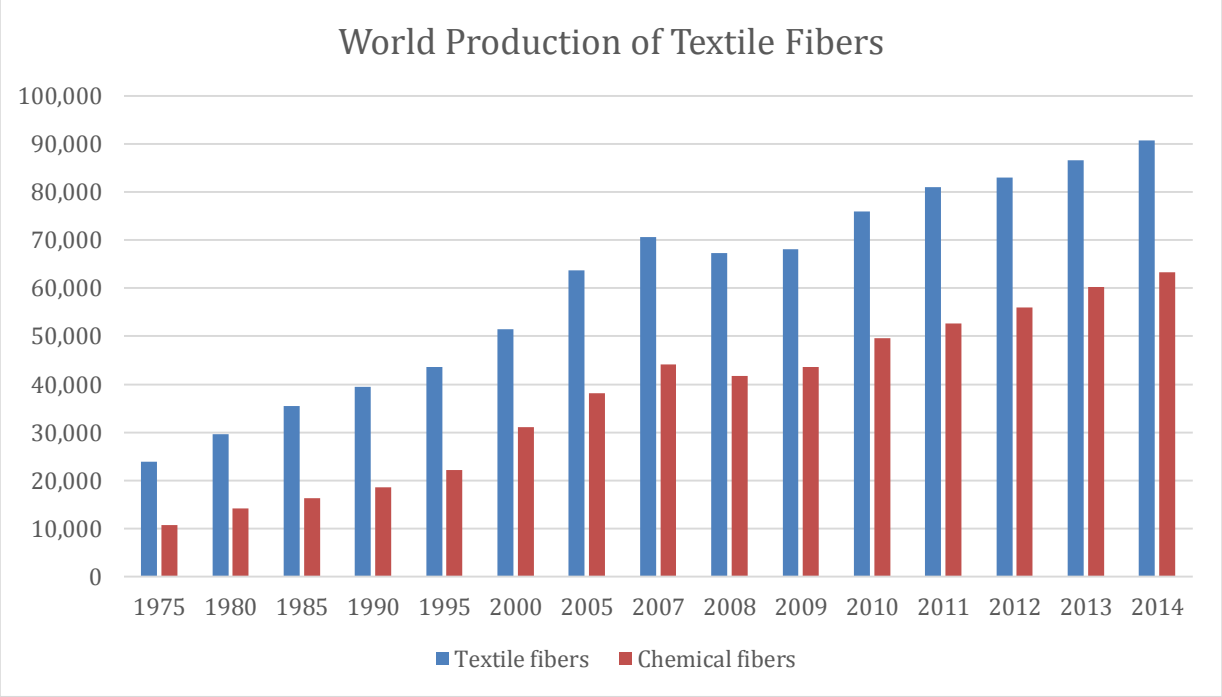

Figure 2.6 Worldwide production of chemical and textile fibers from 1975 to 2013 [60]

The growth rate of chemical/synthetic fibers is much higher compared to the rate of natural fiber production due to increase in their demand for advanced applications. Synthetic fibers such as aramid, (Kevlar®), graphite and others possess very high tensile strength and crystallinity leading to their extensive usage in industries ranging from sports gear to aerospace parts. Other synthetic fiber forming polymers include polyethylene (PE), polypropylene (PP), polyethylene

terephthalate (PET) or nylon, which can be extruded as per the end use giving extensive opportunity for modifications and versatile applications. Unfortunately, most of the synthetic fibers are obtained from petroleum which is an exhaustible (not sustainable) source and their disposal, is non compatible with the environment. Thus, through rising awareness and legislative demands, there is an increasing need to make use of the abundantly available natural fibers as a replacement for the currently used synthetic polymers.

2.5.1 Cellulose Based Fibers

Various forms of cellulose, together, constitute the largest categories of polymers utilized for industrial purposes worldwide [61]. Cellulose is a tasteless, odorless and hydrophilic polymer. It is insoluble in water and most organic solvents and biodegradable. The natural fibers derived from plant/vegetable sources are lignocellulosic in nature, i.e., they contain both cellulose and lignin. Such combination forms the most abundant biopolymer made through photosynthesis in trees, crops, etc. Cellulose based fibers are currently the most widely used natural fibers with applications as reinforcing composite fillers [62]. The natural cellulose in the form of Cellulose I with I_α is obtained mainly from bacteria and algae whereas I_β enriched cellulose is obtained in plants and other plant matter [63]. The net production of natural cellulose based fibers is considered to be 2×10^{11} metric tons per year whereas that of synthetic polymers is 1.5×10^{8} metric tons [6]. There have been many attempts by researchers to use the cellulose based fibers for industrial applications. However, plant based cellulose fibers show a significant variation in diameter and length as well as tensile properties which is undesirable for advanced applications where consistent properties are required.

Most of the natural cellulose fibers have Young's modulus ranging from 10 to 30 GPa and strength between 200 and 1000 MPa [64]. Some natural fibers, e.g., flax, when processed properly have shown Young's modulus of over 100 GPa and strengths of over 1200 MPa [65]. The low strength and Young's modulus values of natural cellulosic fibers, in general, can be attributed to the large microfibrillar angles with respect to fiber axis, high moisture absorption as well as fiber extraction processes used. The tensile strength of some of these fibers such as hemp, sisal, flax and ramie is comparable to that of commonly used glass fiber [64] and hence being used as replacements for glass fibers in various composite applications. Table 2.4 describes the mechanical properties of natural cellulose fibers in comparison to E-glass fibers.

Table 2.4 Mechanical properties of natural cellulose based fibers in comparison to glass fiber [66]

Fiber	Young's Modulus (GPa)	Ultimate Strength (MPa)	Strain (%)
E-glass	**73**	**2400**	**3**
Hemp	**70**	**500-900**	**1.6**
Jute	**10-30**	**400-800**	**1.8**
Ramie	**44**	**500**	**2**
Coir	**6**	**220**	**15-25**
Sisal	**38**	**600-700**	**2-3**
Cotton	**12**	**400**	**3-10**
Flax	**60-80**	**800-1400**	**1.3-1.7**

Some of the studies carried out with high strength natural cellulose fibers include the use of jute fibers [14, 67], sisal fibers [13, 68], flax fibers [34, 69, 70], bamboo fibers [50], pineapple fibers [71], kenaf fibers [72] and ramie fibers[73].

These naturally occurring cellulose fibers are known to have cellulose I conformation which possess intramolecular hydrogen bonding between successive units. The other conformation, cellulose II, is present in the regenerated cellulose fibers that possesses a bifurcated intramolecular hydrogen bonding [74]. Figure 2.7 shows the chain conformations of Cellulose (I) found in natural fibers and Cellulose (II) found in regenerated fibers respectively.

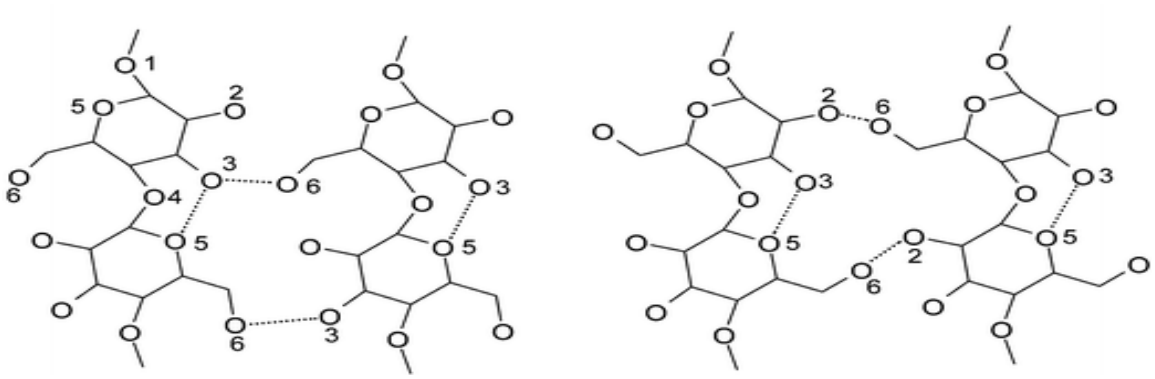

Figure 2.7 Chain conformations of Cellulose (I) (left) found in natural fibers and Cellulose (II) (right) found in regenerated fibers respectively [74]

Mechanical properties of fibers are greatly dependent on factors like diameter, morphology, chemical structure, microfibrillar angle, etc. These factors vary largely in the case of plant based cellulosic fibers, subsequently resulting in a large variation of mechanical properties. Other factors for variation in properties include soil conditions, weather (temperature, rain, drought, etc.). In order to increase the use of the plant based fibers in technical applications, it is necessary that they meet the prerequisite of consistent and enhanced mechanical properties. This

can be brought about by chemically and/or physically modifying the cellulose polymer to obtain regenerated cellulose fibers that are more uniform, moisture repellant and thermally or mechanically stable without compromising on their advantageous properties of biocompatibility and biodegradability.

2.5.2 Regenerated Cellulose Fibers

Regenerated cellulose fibers were the first artificial fibers ever discovered by Schönbein (1845, solubilizing nitro cellulose in organic solvents) and Shweizer (1857, cellulose in cuprammonium solution) [75]. These belong to the semisynthetic category of fibers derived by partially modifying naturally occurring cellulose in contrast to the completely synthetic fibers. The cellulose obtained in regenerated fibers is cellulose II. The conversion of cellulose I to II is an irreversible process. Therefore, cellulose II is considered a stable form whereas cellulose I is in metastable state.

Regenerated cellulose fibers also are in the continuous form unlike the natural fibers which are short (staple). As of today, there are many regenerated cellulose fibers being widely produced and used in the industrial world. They include viscose (rayon), modal, lyocell®, etc. Figure 2.8 is a graphical representation of the world production of regenerated cellulose fibers in 2006.

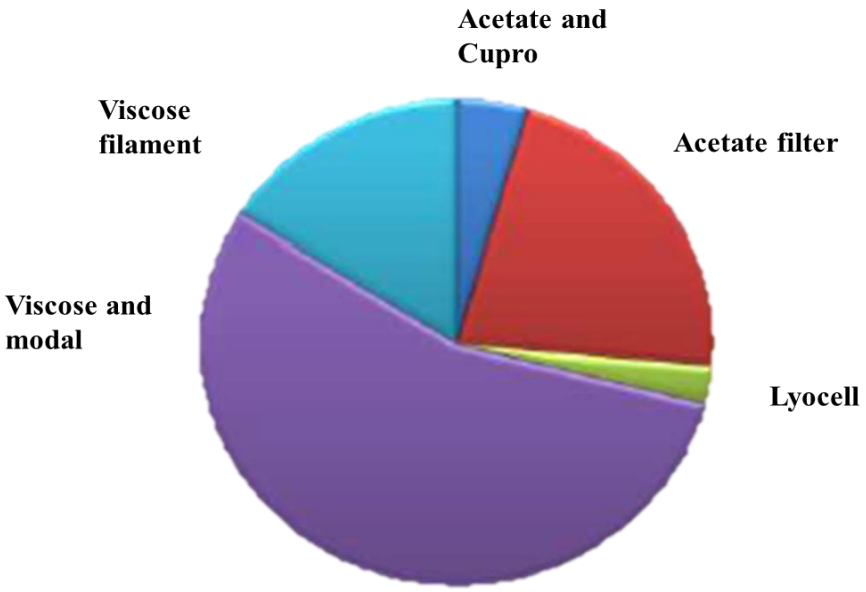

Figure 2.8 World production of regenerated cellulosic fibers in 2006 [76]

As seen in Figure 2.8, the most highly produced amongst the regenerated cellulose fibers is viscose [77].

Conventionally, the viscose fiber wet spinning process is an elaborate manufacturing procedure and involves multiple steps. Important processing steps are explained briefly as follows:

A. Slurry steeping and pressing

Suitably milled cellulose pulp is vigorously stirred with ~20% NaOH solution in a pulp mixer. The finely dispersed pulp slurry is passed to a slurry press to sieve out the fiber. In this phase cellulose reacts with soda to form a sodium salt (soda salt) as shown in reaction (1).

$$Cell - OH + NaOH \rightarrow Cell - ONa + H_2O \quad \text{-- (1)}$$

B. Alkali treatment

The treatment of alkaline cellulose is carried out in controlled temperature and humidity conditions. During this process, oxidative depolymerization of the cellulose occurs which reduces its molecular weight such that the final viscosity and concentration of the pulp are in acceptable ranges needed for spinning.

C. Xanthation

In this process, the alkali cellulose reacts with carbon disulfide, CS_2, forming a xanthate derivative of cellulose which is readily soluble in alkali.

$$CellO^-Na^+ + CS_2 \rightarrow CellOCS_2Na \quad \text{-- (2)}$$

D. Dissolving in caustic soda (Formation of soluble chemical derivative of cellulose)

Cellulose xanthate is dissolved readily in a cold alkali bath. Concentration of cellulose and NaOH in the xanthate, concentration of NaOH in the mixer, and the ratio of xanthate to NaOH in the mixer are the crucial parameters at this step. Similarly, delustrants and modifier chemicals are added at this step to obtain a homogenously mixed dope.

E. Aging, filtration and deaerating

The aging process takes up to 24 hr and is carried out in order to redistribute the xanthate groups in favorable positions for fiber spinning.

The filtration process involves numerous steps for filtering out the undissolved pulp and fibers and also to degenerate the gel like cellulose xanthate that is produced during aging.

Continuous deaerating is carried out to remove any air as well as to maintain homogeneity of the viscose pulp as it is warmed and pumped to the spinning cones in a vacuum tank.

F. Wet spinning and draw stretching

The filtered and deaerated viscose dope is pumped through a suitable spinneret into an acidic coagulating bath. The liquid filaments emerging from the spinnerets coagulate or regenerate cellulose at the interface of the acidic bath to form a cuticle and then the skin of the fiber which controls the rest of the regeneration. The formed fibers are pulled out through the bath by godet rolls that act as anchors for drawing the fibers. Zinc salts are added to the bath to retard the regeneration rate so that greater stretch can be applied to the fibers, thus obtaining high molecular orientation. The regeneration reactions take place simultaneously and are given as follows:

$$2\ \text{Cell} - OCS_2Na + H_2SO_4 \rightarrow 2\ \text{Cell} - OCS_2H + Na_2SO_4 \quad \text{-- (3)}$$

$$\text{Cell} - OCS_2H \rightarrow \text{Cell} - OH + CS_2 \quad \text{-- (4)}$$

G. Washing and drying

The regenerated fiber from the coagulating bath is contaminated with sulfuric acid, carbon disulfide and zinc sulfate. The contamination is removed through subsequent washing and drying to yield pure cellulose fibers. It is then lubricated suitably for the end use and dried to a moisture level of ~10%.

The regenerated cellulose has cellulose II form that has a bifurcated intramolecular hydrogen bonding as opposed to Cellulose I form that is found in natural fibers. Cellulose I and II forms have been shown in Figure 2.7 earlier. Some properties of regenerated cellulose fibers along with synthetic fibers (acrylic and polyolefin) are summarized in Table 2.5.

Table 2.5 Properties of Representative Regenerated Cellulose and Synthetic Fibers [58]

	Regenerated cellulose fibers		Synthetic fibers	
	Viscose	**Modal**	**Acrylics**	**Polyolefins (PE and PP)**
Specific Gravity (g/cm^3)	**1.5-1.52**	**-**	**1.14-1.18**	**0.9-0.95**
Degree Of Polymerization (%)	**200-400**	**600-800**	**2000**	**2500-3000**
Degree Of Crystallinity (%)	**35-40**	**40-50**	**70-80**	**85-90**
Moisture Regain (%)	**12-14**	**10**	**1.2-2.0**	**≤0.1**
Melting Range (°C)	**No Melting**	**No Melting**	**No Melting**	**115-179**
Extensibility (%) Dry	**15-30**	**5-10**	**25**	**10-20**
Handle	**Medium soft-Limp**	**Crisp**	**Soft, Waxy**	**Very Waxy**

It is known that there is a significant change in terms of thermal resistance and mechanical properties of regenerated cellulose fibers compared to natural cellulose based fibers. However, there is still room for improvement to obtain higher degree of crystallinity which the synthetic fibers possess to improve the regenerated cellulose properties. Liquid crystalline cellulose fibers are a class of fibers that possess high crystallinity and orientation comparable to the synthetic fibers. These fibers are discussed in the next section.

2.5.3 Liquid Crystalline Cellulose (LCC) Fibers

The first observation of liquid crystalline solution of cellulose derivative was made in 1976 by Gray and Werbowyj [78]. Liquid crystalline phase is considered a mesophase between solid

crystalline and liquid, i.e., these materials flow like liquids but show certain properties such as refractive index similar to that of solid crystals. The advantage of using liquid crystalline polymers is that their chain conformation can be transformed into highly oriented fibers without the necessity of post treatment [79].

Polymers possess two long range orders, namely center of mass of the molecules and molecular orientation on a three dimensional axis. Both the orders usually get disrupted beyond melting temperatures in common polymeric systems. However, in case of some polymers which form a liquid crystalline phase during this transition, the positional order related to the center of mass disappears but the molecular orientation order still remains intact [79]. Figure 2.9 illustrates the hydrogen bonding structure in the LCC fiber molecular chains. As seen, the hydrogen bonding is seen along the chain axis leading to unidirectional and well oriented molecular chains in the LCC fibers.

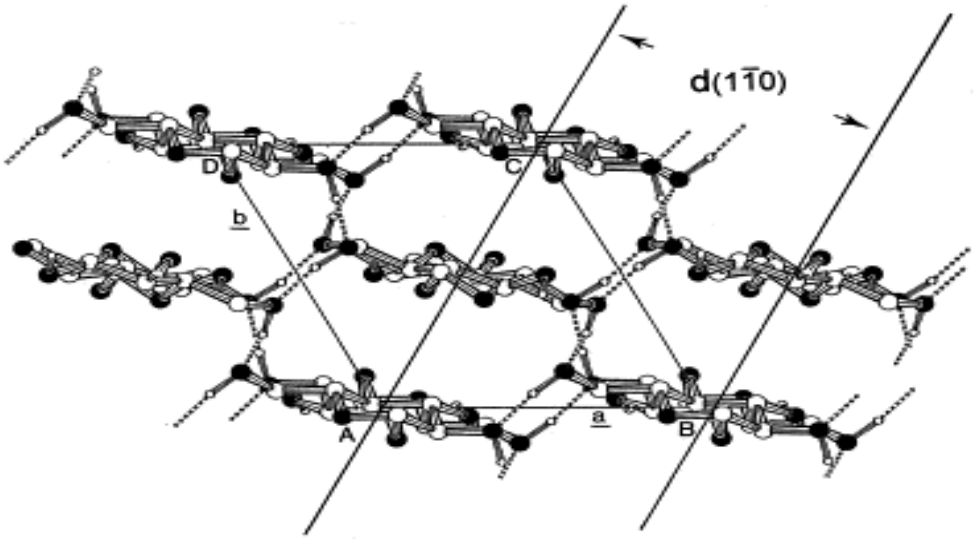

Figure 2.9 The hydrogen bonding structure in the LCC fiber molecular chains [80]

These novel liquid crystal solutions having unidirectionally oriented molecular chains, are known to be excellent precursors to spin high modulus and strength fibers, e.g., Twaron® by Akzo Nobel, Kevlar® by DuPont, respectively [80]. On similar lines many researchers are making use of strong polar solvents to create the mesophase and, in turn, form rigid chain polymers [81, 82].

Few direct solvents in which mesophase of cellulose may occur include N-Methylmorpholine-N-Oxide (NMMO), mixture of trifluoroacetic acid and dichloromethane, mixture of dimethylacetamide and ammonia [83], sulfuric acid and phosphoric acid [81].

However, very few solvents are known to be used for the dissolution of non-derivatized, i.e., pure cellulose and even fewer form anisotropic solutions. Of these, phosphoric acid is an inexpensive and environmentally friendly direct solvent that has a very strong dissolving power which allows the dissolution process to occur within a few minutes. As a result, it is more economical compared to the traditional viscose production process which has a residence time of 1-2 days in the plants due to the complicated aging process [83]. The method using phosphoric acid also eliminates the conventional means of using a co-solvent to form an anisotropic solution of phosphoric acid. Thus, this process makes it an efficient and easy process to scale up for spinning advanced LCC fibers.

In the present research, advanced LCC fibers spun from anisotropic phosphoric acid solution were used as composite fillers. They were further treated chemically and mechanically (under tension) to improve their tensile properties.

2.6 Advanced Fibers

High strength fibers are commonly used as reinforcing fillers to impart strength and stiffness to advanced composite materials. Some examples of advanced fibers include carbon/graphite, aramid, Kevlar®, glass, PBO (poly(p-phenylene-2,6-benzobisoxazole)) and metal fibers many of which are synthetic polymers that use petroleum as raw material source. They usually have Young's modulus values ranging from 50 GPa to as high as 850 GPa [84]. Table 2.6 gives a comparison of specific gravity and Young's moduli of some commercial high strength fibers.

Table 2.6 Comparison of specific gravity and Young's moduli of some high strength fibers used commercially

Fiber	Specific Gravity	Young's Modulus
Technora®	**1.39**	**70**
Kevlar® 49	**1.45**	**135**
Zylon®	**1.56**	**280**
Glass	**2.5**	**72**
Nextel® 610	**3.75**	**370**
Polyethylene	**0.96**	**117**
Carbon (Ultra High Modulus)®	**2.16**	**830**
Hi-Nicalon®	**2.74**	**265**

As these high strength fibers are the major strength imparting components of advanced composites, fiber selection is a crucial part of the composite fabrication procedure. It is carried out theoretically by using the rule of mixture depending on the desired strength of the end

product [85]. It is important that the fibers live up to the extremely high stresses and deformations during their use in automobile and aerospace industry parts or in sporting goods.

2.6.1 Factors Contributing to High Strength and Stiffness of Fibers

Mechanical properties of fibers are largely dependent on factors that can be broadly classified into structural or chemical composition. Factors that affect the strength and modulus of the fibers are as follows:

1. Degree of polymerization

   Higher the degree of polymerization (no. of monomer units in a single polymeric chain) of the fiber forming polymer, higher the strength of formed fibers. For example, ramie and flax are much stronger than cotton fibers.

   It is also known that only the polymers with a DP of more than 4,000 are spinnable, though this number is dependent on their chemistry. However, the spinnability and strength of formed fibers increases with increase in DP till about 20,000, again depending on their chemistry.

2. Molecular orientation

   Molecular orientation with the fiber axis is a crucial factor for high strength and modulus of fibers. The angle made by the molecular chains with the fiber axis has an inverse relationship to the tensile strength of the fibers. In cellulosic fibers, it is the microfibrillar angle that is important since the molecules are highly oriented within the microfibril.

3. Degree of crystallinity (phase structure and composition)

   High degree of crystallinity of a fiber leads to a closely packed molecular structure and lack of molecular chain mobility leading to a much stiffer (high modulus) fiber. Moreover, lower amorphous content reduces the reactive areas that may alter the fiber strength.

Though the size and nature of the crystals affect the strength of the fibers, the total percentage of crystallinity is directly correlated to the fiber strength.

4. Manufacturing process

In the case of synthetic and regenerated fibers, the manufacturing process can be altered greatly to obtain desired morphology that can result in high strength or 'advanced' fibers. Using air gap-wet spinning process, increasing the draw ratio, adjusting air gap lengths, addition of instant crystallization complexes in the spinning dope are some of the process modifications that affect the fiber strength and help in spinning of advanced fibers.

2.7 Treatments for Enhancing Fiber Strength and Young's Modulus

As stated above, there are many factors that ultimately contribute to the fiber tensile properties. Enhancing the mechanical properties of the fibers involves modifying one or more of the contributing parameters. Scientists and researchers have undertaken many approaches to this problem and the most widely used method is mercerization which involves a combination of simultaneous chemical and mechanical (tension) treatments on the cellulosic fibers.

Conventionally, the process of mercerization, invented by John Mercer in 1853, has been used in the textile industry to strengthen natural cellulose fibers, particularly cotton, with the help of mild alkalis, primarily NaOH. This is done by swelling the fiber with the help of Na^+ (or K^+) ion penetrations resulting in an increased and smoother surface area and reflectance of the fiber. Mercerization treatment also alters the crystal structure to a more thermodynamically stable form from cellulose I to II which leads to increase in the fiber strength.

Recently, there has been an increasing use of alkali treatment processes on regenerated cellulose fibers to study the change in their structure and properties [75, 86-88]. This is because, it is generally accepted that during the mercerization process of natural cellulosic fibers, the crystal lattice of cellulose I is replaced wholly or partially to the form of cellulose II. In the case of regenerated fibers, water destroys the weak hydrogen bonds in cellulose but cannot penetrate to the higher order (crystalline) regions [89]. This theory has been confirmed by the high strain/low modulus values of fibers in wet conditions. However, aqueous chemical solutions can penetrate into the higher order cellulosic regions leading to reorganization of cellulose structure and generation of reactive hydroxyl bonds [88]. As a result, the solution possessing the Na^+ (or K^+) ions is able to form Na-cellulose complex with the amorphous/semi crystalline cellulosic chains. The formed Na-cellulose has a high degree of orientation and crystallinity and it cannot be converted back to cellulose I due to its antiparallel structure similar to that of cellulose II. This may explain how cellulose I (parallel) gets altered to cellulose II (antiparallel) without solubilizing the cellulose [80].

When this chemical treatment is combined with the tension treatment, it produces a more pronounced effect on the fiber strength enhancement. Tension treatment is particularly known to alter the molecular orientation and associated crystallinity of the fibers making them stiffer and,

hence, efficient composite reinforcements. As the restructuring of the microfibrillar chains gets easier due to formation of reactive hydroxyl bonds, the applied stress allows the restructuring to occur along the direction of the applied stress. In case of natural fibers, the arrangement of microfibrils is one of the determining factors for their strength.

2.8 Starch Based 'Green' Resins

The use of starch in the manufacturing of resins began in the 1970's due to its cheap, abundant and renewable nature [90]. Resins formed from native and modified starches are increasingly being used in order to replace the petroleum based plastic products that cause adverse environmental effects. Starch is a versatile polymer that allows easy crosslinking with poly-carboxylic acids forming desirable resins for composites [91, 92]. Starch based materials and composites have been used for diverse applications ranging from disposable goods such as garbage bags, consumer goods including toothbrush and racket strings, food packaging [93] to tissue engineering [94].

Native starches derived from maize, rice, potato, etc., have been conventionally crosslinked using citric acid [95], sodium trimetaphosphate, epichlorohydrin [96] and phosphorous oxychloride to increase their film forming properties. In the procedure of crosslinking the starch molecules are interconnected by covalent bonding making it a thermoset resin. As such, the process not only increases the molecular weight of the material but also enhances the mechanical properties [31].

Many modified starches are produced by chemically substituting the hydroxyl groups attached to the starch molecules during the process of isolation. The type of isolation modification, degree of substitution and modification conditions are the factors that affect the characteristics of the

final modified starch [97]. However, use of native starches retain the 'green' nature of the process and also generate profit out of the unused produce that is otherwise wasted.

Native starches lack the desirable mechanical properties as seen in cases of the modified starches. Mechanical properties of starch based resins depend on the amylose and amylopectin ratio, plasticizer, moisture content and storage conditions. In order to enhance the mechanical properties of native starch based resins, certain post isolation modifications such as introduction of cellulose fibers and micro cellulose can be carried out [90]. Cellulose being less hydrophilic than starch increases the water resistance of the resin [90].

Table 2.7 gives the comparison between the environmental effect caused by starch based resins and LDPE. It is clear that significantly low use of energy resources and low ozone formation potential proves the advantageous nature of starch based resins [98]. As a result, starch based resins are now increasingly produced commercially all over the world as ideal replacements for petroleum based plastics.

Table 2.7 Comparison between the environmental effect caused by starch based resins and LDPE [98]

	Starch Based Resins	**LDPE**
Energy Resources Utilized (MJ)	**2550**	**9170**
Ozone Formation Potential (kg ethylene eq.)	**0.47**	**1.7**

* Values based on 100 kg base material

2.9 Fiber Reinforced 'Green' Composites

Fiber reinforced composites were first produced in 1908 with cellulose fiber and phenolics, and enhanced further using urea and melamine. They gained commercial status with glass fiber composites in unsaturated polyesters by 1940s [64].

Composites, conventionally, consist of two or more distinct phases namely, a resin (continuous phase) and a reinforcement (discontinuous phase) that are combined together in order to generate a material with completely unique properties that cannot be obtained by its components, individually.

'Green' composites are composite materials comprising of one or more phases of biobased origin. Coir, bamboo, jute, sisal and hemp fibers have been used as composite reinforcements [14, 66, 69, 99]. Regenerated cellulose fibers can also be counted in this definition of 'green' composites due to their basic cellulosic backbone and biocompatible nature. Similarly, resins made from biodegradable polymers such as starch, protein or lipids are used to form fully green composites. Such biobased composites made from components having a polysaccharide backbone do not face hindrances with respect to fiber/resin adhesion due to the common chemistry and large number of hydroxyl bonds that can readily react or form hydrogen bonds.

It can be inferred from the literature that 'green' composites are the best replacements for petroleum based composites in order to achieve full biodegradability and build sustainable products. Current research of fabricating fiber reinforced composites from fully biodegradable components such as RP starch, BFMC and LCC fibers is conducted in support of improving the functionality and maximizing the availability of 'green' composites.

3 EXPERIMENTAL METHODS

3.1 Materials

Raw green plantains were purchased from a local super market. Analytical grade potassium hydroxide (KOH), sodium hydroxide (NaOH), 1,2,3,4-butane tetracarboxylic acid (BTCA) and sodium hypophosphite monohydrate (NaHyp), were purchased from Sigma Aldrich (St. Louis, MO) and used as received. Acetic acid and sodium-bisulfite ($NaHSO_3$, 40%) solutions were also purchased from Sigma Aldrich and used as received.

Mechanically extracted banana stem fibers were obtained from CSIR- North East Institute of Science and Technology (NEIST), Jorhat, India. Air gap wet spun LCC multifilament yarns (~1000 filaments), made by dissolving cellulose in phosphoric acid, were kindly provided by Dr. H. Boerstoel, Teijin Twaron BV (Arnhem, The Netherlands).

3.2 Starch Isolation from Raw Plantain (Fruit and Peel)

In order to isolate starch from raw plantains (RP), they were first separated into fruit and peel. The RP fruit was cut into 2 cm thick slices. Slices of RP fruit weighing a total of 150 gm were added to 300 ml of a solvent containing either 1% $NaHSO_3$, 2.8% KOH or 2% NaOH, separately [36, 38]. The pH of the mixture was adjusted between 3 and 4 using dilute acetic acid. The mixture was blended for 12-15 min in a high speed kitchen blender to get a homogenous viscous paste of fine consistency. This paste was then subjected to magnetic stirring (200 rpm) for steeping for 3 hr at 27°C. The paste was then passed through a 250 μm mesh sieve to remove the fibrous and particulate matter still present in the mixture. The viscous

paste of starch pulp was washed thoroughly using DI (deionized) water to remove the water soluble solvent used during steeping. The filtered and washed starch pulp was subsequently dried in an air circulating oven at 65°C for 12-14 hr. The dried material was ground into fine powder to obtain plantain starch powder from the fruit. The process was repeated separately using different solvents (1% $NaHSO_3$ or 0.5M KOH or 0.5M NaOH) for the fruit as well as the peel. Figure 3.1 illustrates the schematic representation of the steps in the conversion of raw plantain fruit to isolated raw plantain (RP) starch powder.

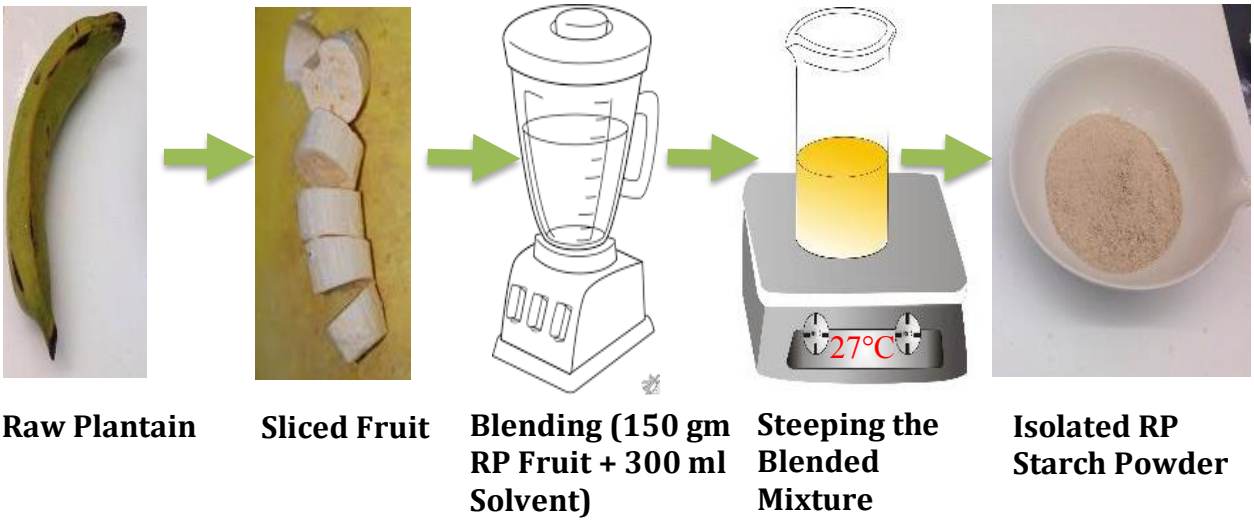

Figure 3.1 Schematic representation of the steps in the conversion of raw plantain fruit to isolated RP starch powder

3.3 Characterization of Raw Plantain (RP) Starch

The RP starch powder derived using (1%) $NaHSO_3$ was characterized to compare its properties to commercially available starches. Following subsections describe the characterization techniques used to obtain various properties and to make the comparisons.

3.3.1 Proximate Analysis

The starch specimen isolated from plantain fruit and peel, separately, using all the 4 solvents were analyzed for their starch content. Forage labs at Dairy One, Ithaca, NY, performed this analysis. The starch content was also studied as a function of pH 3-4 and number of washes 0-2.

3.3.2 Attenuated Total Reflectance - Fourier Transform Infrared Analysis (ATR-FTIR)

The ATR-FTIR spectra were collected using the spectrophotometer Nicolet Magna -560 FTIR (Nicolet, now Thermo, Waltham, MA, US) for native RP starch isolated from $NaHSO_3$ and commercially available corn starch for comparison. Each spectrum was recorded as an average of 64 scans in the range of 4000 to 550 cm^{-1}, wavenumbers.

3.3.3 Thermogravimetric Analysis (TGA)

The native RP starch and the crosslinked RP starch films were scanned on the thermogravimetric analyzer (TGA-2050, TA Instruments Inc., New Castle, DE) from 25°C to 500°C at the rate of 10°C/min in nitrogen atmosphere to determine their degradation temperature and thermal stability.

3.3.4 Differential Scanning Calorimetry (DSC)

The native RP starch was scanned in the differential scanning calorimeter (Q-500, TA Instruments Inc., New Castle, DE) to estimate the onset peak and conclusion temperatures of gelatinization. Additionally, DSC data were also used to determine the gelatinization enthalpy.

3.3.5 X-ray Diffraction (XRD)

The native RP starch powder was characterized on the Scintag theta-theta X-ray diffractometer (Scintag Inc., Cupertino, CA). The diffraction spectra were analyzed using the MDI-JADE, industry standard software for peak indexing. The data were used in determining the crystallinity of the starch.

3.3.6 Rheological Testing

A 5% starch solution in DI water was run on the Rheo 1000 (TA Instruments, New Castle, DE), using 60 mm parallel plates, as a function of increasing shear rate 0-250 (1/s). These measurements were made to characterize the gelatinization behavior of the RP starch, i.e. change in viscosity (Pa.s) of starch as a function of increasing temperature. The samples at 65, 75 and 85°C were characterized separately.

3.3.7 Scanning Electron Microscopy (SEM)

In order to observe the morphology of specimens during the process of gelatinization of starch, specimens of about 1 ml solution were extracted at 4 different temperatures (55, 65, 75 and 85°C) during the temperature ramp and observed on FESEM, Tescan Mira 3 (Tescan, Brno, Czech Republic). The specimens were mounted on standard aluminum SEM stubs with double sided electrically conductive adhesive tapes. The specimens were air dried at room temperature (RT) for 12 hr and sputter-coated using a gold target for 45 sec at 45 mA. The images were captured with 5 kV in resolution mode using an In-beam detector.

3.4 Isolation of Fibrillar Micro Cellulose from Banana Stem Fiber

Mechanically extracted banana stem fibers were obtained from CSIR- North East Institute of Science and Technology (NEIST), Jorhat, India. These fibers were used to extract fibrillar micro cellulose by the procedure used in earlier studies [100, 101]. They were gently combed and separated into small bunches. The cellulosic fibers were delignified with alkaline treatment using NaOH solution (10%) at RT. The delignified fibers were washed with DI water to remove the excess NaOH and air dried at room temperature. The washed and dried fibers were then chopped to about 2 cm length and subjected to a bleaching process using 10% hydrogen peroxide (H_2O_2) solution for 20 min at RT. This process led to whitening of chopped fibers, which were further prepared for acid hydrolysis by sieving and washing them. Acid hydrolysis was carried out with concentration and duration parameters optimized to 7% H_2SO_4 solution and 3 hr, respectively. The acid hydrolyzed chopped fibers were sieved and washed multiple times to remove traces of any sulfuric acid. Finally these were suspended in DI water and subjected to

high speed homogenization at 5000 rpm for 10 min. The fibrillar micro cellulose obtained at the end of this procedure were refrigerated as a DI water suspension and will be referred to in the subsequent sections as banana fiber micro cellulose (BFMC).

3.5 SEM Characterization of Banana Fiber Micro Cellulose

The BFMC derived from banana stem fibers were characterized using a scanning electron microscope FESEM, Tescan Mira 3 (Tescan, Brno, Czech Republic) to characterize their surface characteristics and aspect ratio. The BFMC specimens were sieved, dried and mounted on standard aluminum SEM stubs with double sided electrically conductive adhesive tapes. The specimens were air dried at RT for 12 hr and sputter-coated using a gold target for 45 sec at 45 mA. The images were captured with 5 kV in resolution mode using an Inbeam detector. Inbuilt scales were used to measure the diameters and lengths of the BFMC. An average of over 10 readings was used to calculate the aspect ratios of the specimens.

3.6 Crosslinking and Fabrication of RP Starch Resin Films

In order to obtain RP starch based crosslinked resin films, 8 gm of starch and BFMC in the ratio 3:1 were mixed with 150 ml DI water at RT and subjected to magnetic stirring while gradually increasing the temperature to 95°C. Change in the viscosity was continuously monitored visually. To obtain maximum gelatinization, the mixture was stirred for an additional 30 min at 95°C. BTCA (10% by weight of starch) was added to the gelatinized mixture as a crosslinker and $NaHSO_3$ (50% by weight of BTCA) was added as a catalyst. The mixture was stirred at

90°C for one hr to ensure homogenous mixing and crosslinking of the material. After cooling, the resin was poured onto Teflon® coated glass plates and heated in an oven chamber at 70°C for 24 hr. The dried and set films were then peeled off the Teflon® coated glass plate to obtain free standing films. The films were further heated in a carver hydraulic hot press for 20 min at 120°C under 2000 psi (13.79 MPa) pressure for curing and allowing complete crosslinking.

The cured films were cooled and washed with DI water for 5 min to remove traces of unreacted BTCA and Nahyp (catalyst). The process of resin film formation from RP starch is explained schematically in Figure 3.2

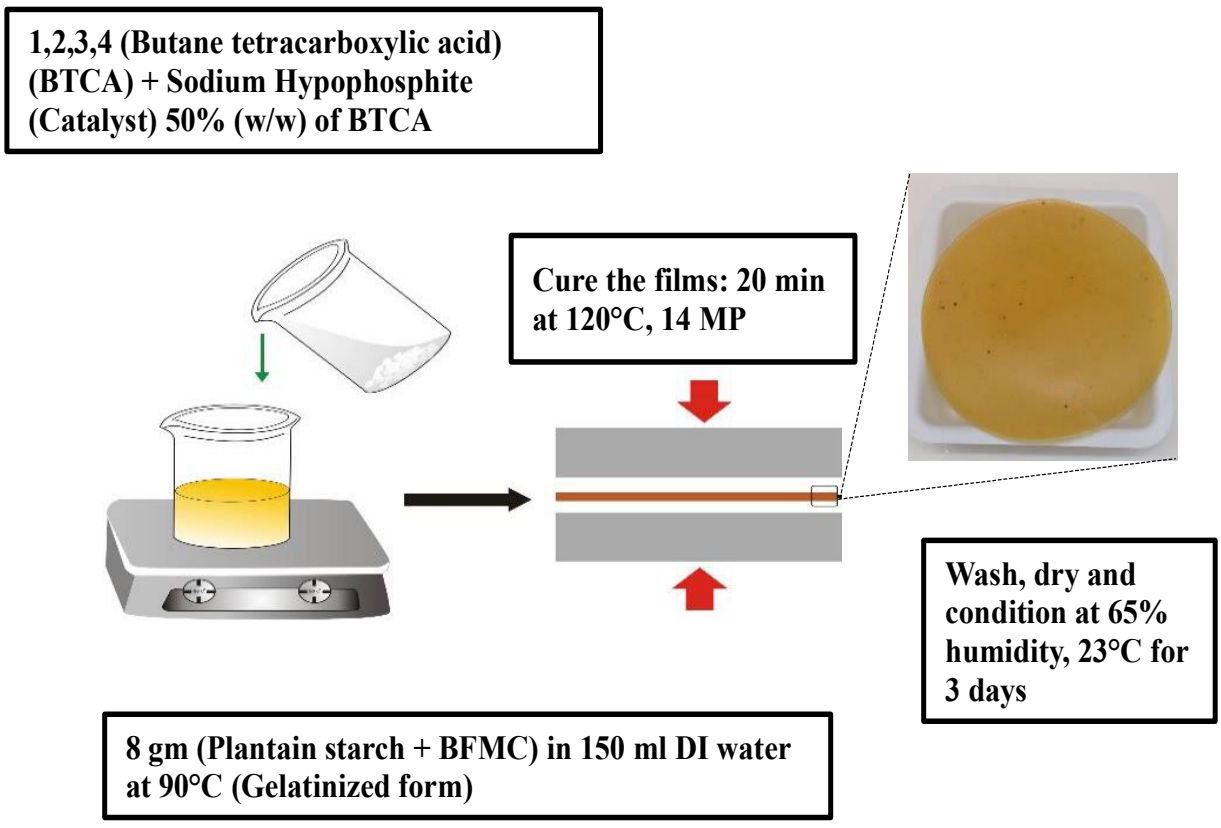

Figure 3.2 Schematic representation of resin film formation process for crosslinked RP starch

3.7 Characterization of Control and Modified Resin Films

The control (non-crosslinked) resin films prepared from RP starch and the films reinforced with BFMC and crosslinked with BTCA were characterized for changes in their physical and chemical properties as well as to confirm the crosslinking reactions. The characterization techniques used are briefly described below.

3.7.1 Attenuated Total Reflectance-Fourier Transform Infrared Analysis (ATR-FTIR)

The ATR-FTIR spectra were collected using the Nicolet Magna 560 FTIR spectrophotometer for RP starch isolated using sodium bisulfite, crosslinked starch (pre and post washing) and (pre and post) drying of starch films. Each spectrum was taken as an average of 64 scans and recorded from 4000 to 550 cm^{-1} wavenumbers. The spectrum helped in studying the crosslinking reaction in the resin films.

3.7.2 Moisture Testing

The moisture content of the resin films was measured by gravimetric (weight increase) method. The resin film specimens were weighed before and after conditioning for 3 days at 21°C and 65% relative humidity (RH) and moisture content was calculated using the following formula:

Moisture content of resin film (%):

$$\frac{[\text{wt. after conditioning } (w_2) - \text{wt. before conditioning } (w_1)] * 100\ (\%)}{\text{wt. after conditioning } (w_2)}$$

3.7.3 Tensile Characterization

The RP starch resin films were cut into rectangular pieces of size 1.5 cm × 7 cm to characterize their tensile properties. They were cut randomly from the films to ensure unbiased estimate of their tensile properties. The film thickness of each specimen was determined independently prior to tensile testing. These films were conditioned at 65% RH at 21°C for 24 hr prior to testing. A gauge length of 25 mm and a crosshead speed of 0.6 mm/min (strain rate of 0.024 min^{-1}) were used for all the specimens. The tests were carried out using Instron universal tester, model 5566, (Instron Co., Canton, MA).

3.8 Development of Tension Setup

To carry out the chemical treatments of LCC multifilament yarns, a customized apparatus was built using laser cut Plexiglas® plates with dimensions as shown in Figure 3.3. It consisted of an arrangement to apply desired loads to the yarns in case of chemical treatment with loads.

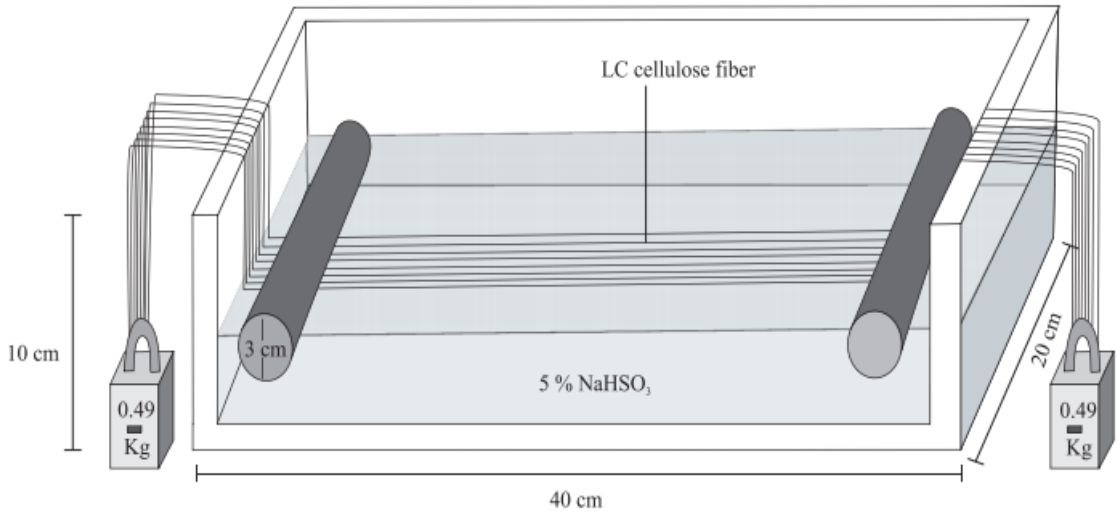

Figure 3.3 Plexiglas® setup for chemical and tension treatment of LCC yarns

3.9 Treatments to Enhance the Mechanical Properties of LCC Yarn

The LCC yarns were subjected to various treatments in order to enhance their tensile properties. Treated fibers were characterized to understand the morphological changes. Initially the LCC yarns were treated at RT in the slack form and the effect of solution concentration was studied. Four different solutions, NaOH, KOH, $NaHSO_3$ and NH_4OH were studied for comparing their effectiveness. In the second stage the effect of treatment under load was studied followed by effect of the treatment duration. The treatment parameters that were optimized in order to obtain the best possible tensile properties are discussed below:

3.9.1 Chemical Solvents:

For slack treatment of LCC yarns, the specimens were immersed in 2% solutions of NaOH, KOH, $NaHSO_3$ or NH_4OH without any load. The treatment was carried out for 120 min at RT.

3.9.2 Solvent Concentration:

The concentration of the selected solvents was then varied to 2, 5 and 10% for a constant duration of 2 hr while the temperature was maintained at RT.

3.9.3 Wet/Dry Testing:

The fibers were then characterized for tensile properties using Instron universal tester in wet as well as washed and dried conditions. The wet testing was carried out on the fiber specimen by mounting the individual fibers from LCC yarns treated with KOH or $NaHSO_3$ solvents separately on paper tabs without drying, for tension testing on Instron universal tester. This test was carried out in order to gain a better understanding of the load capacity, modulus, yield behavior, etc., of the fibers in wet condition. These values were used in deciding the treatment loads (stress) for the treatments carried under tension.

3.9.4 Chemical Treatment Load:

The yarns immersed in $NaHSO_3$ or KOH solutions were then kept under tension by suspending desired weights attached at the two ends of the yarns in the tension setup. The loads were derived as 10% and 25% of the fracture stress from the preliminary results of tensile properties of the wet LCC fiber.

3.9.5 Treatment Duration:

The duration of the treatment under load was varied from 30, 60 and 120 min to understand its effect on the tensile properties of the fibers. The best one of the four solvents used and the optimum values for concentration, load and treatment duration were decided based on the results obtained from the tensile modulus and the fracture stress of the fibers at various parameters.

After completing the treatments all fibers were rinsed with DI water to remove the traces of water soluble $NaHSO_3$ and KOH and dried in an air circulating oven at 50°C for 4 hr in each case except for the testing in wet condition. The number of LCC fibers in the yarn were counted after each treatment and were found to be unchanged (~1000) suggesting that no fibers broke during the treatment.

3.10 Characterization of Control and Treated LCC Yarns

The control and chemically treated LCC yarns (slack and under tension) were tested for their tensile properties, crystallinity, orientation and morphology using the following techniques.

3.10.1 X-Ray Diffraction Analysis

Scintag Theta-Theta X-Ray Diffractometer (XRD) (model LT-801, Scintag Inc., Cupertino, CA) was used to characterize the crystallinity of LCC yarns. Voltage of 45 kV and a current of 40 mA were applied during the X-ray scattering process and diffractograms from 5 to 40° were recorded. The obtained results were analyzed using the MDI-JADE analysis.

3.10.2 Scanning Electron Microscopy (SEM)

The treated and control LCC fiber morphologies and diameters were determined using a scanning electron microscope FESEM (Tescan Mira3, Tescan, Brno, Czech Republic). Single LCC fibers were attached with double sided carbon tape on SEM mounts. The specimens loaded on the mounts were gold coated using a sputter coater for 30 sec at 45 mA. The images were captured using an accelerating voltage of 5 kV in resolution mode with an Inbeam detector.

3.10.3 General Area Detector Diffraction (GADD) Spectra

The LCC multifilament yarns were tested for change in their molecular orientation before and after the treatments using the 2 dimensional area detecting diffractometer, Bruker GADDS, (Bruker-AXS, Inc., Madison, WI). The LCC yarns were mounted on a specimen plate parallel to the equator and adjusted using an automated laser video alignment system for its precise positioning.

3.10.4 Tensile Characterization

The tensile properties of the LC fibers including fracture stress (strength), modulus and tensile strain at fracture were measured using Instron, universal tensile tester (Model 5566, Instron Co., Canton, MA) following ASTM standard D 3822-01. Individual fibers were separated from the LCC yarn using sharp metal tweezers. Single fiber specimens were prepared using paper tabs of size (2 x 12.5) cm as shown in Figure 3.4. Round holes were punched equidistantly from the center of the paper tab to create a gauge length of 8.5 cm and fiber specimen were glued using commercially available Ethyl Cyanoacrylate based Krazyglue® on the paper tabs at the two ends of the holes. The paper tab was gripped vertically along the length using the rubber grippers of the Instron universal tester. Once the tab was set in a taut condition at the gauge length required, the tab was cut at the punched holes. This allowed the single LCC fiber to stand freely on the machine for accurate tensile characteristic measurements. The average fiber diameter obtained from the SEM micrographs was used to calculate the strength of the fibers. A load cell of 100 N and a crosshead speed of 0.1 mm/min (strain rate of $0.001 min^{-1}$) were utilized for these tests. At least 30 specimens were tested for each condition. The average values were calculated from the data using MS excel and statistical software JMP.

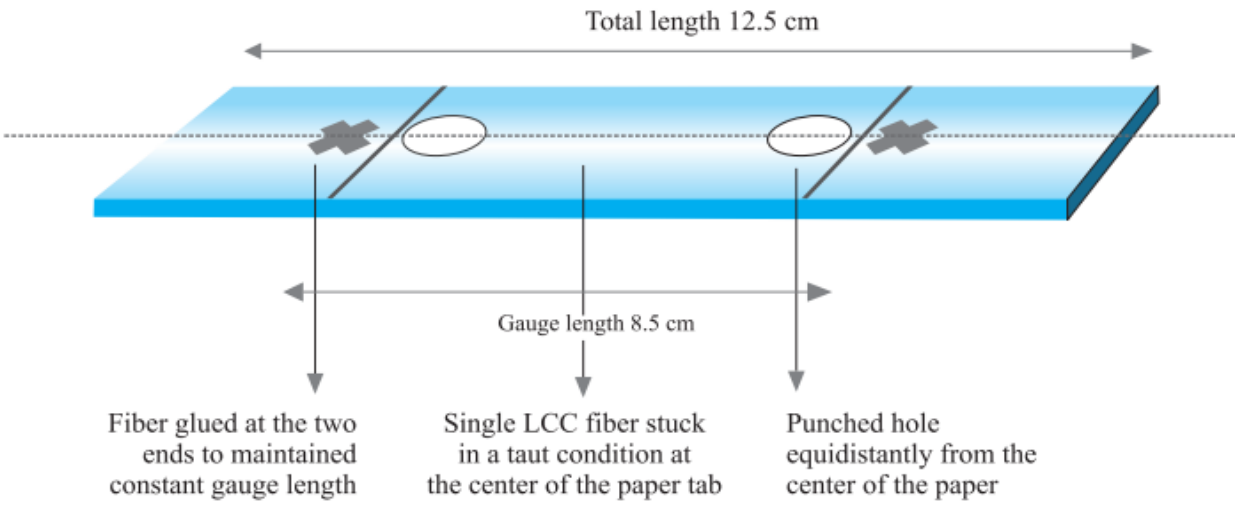

Figure 3.4 Design of paper tab used to test the tensile properties of the LCC fibers

3.11 LCC Fiber Reinforced RP Starch Based 'Green' Composite Fabrication

Resin prepared using 75% isolated raw plantain (RP) starch powder and 25% BFMC was used to fabricate 'green' composites by reinforcing it with control and slack and tension treated LCC yarns, separately. Thin layer of the resin was poured onto a glass plate coated with Teflon® sheet such that it does not flow to the edges. The yarns were completely soaked in the RP starch based resin to ensure maximum impregnation of resin onto the yarns. In order to obtain best possible alignment of the yarns on the glass plate, they were stretched and clipped on the edges of the glass plate using metal grippers. The excess resin was removed by hand from the sides and the composite was dried in an oven at 70°C for 14 hr to obtain heat set, uncured pre impregnated composites (prepregs). These prepregs were then hot pressed at 120°C for 20 min. The thickness and the dimensions of the composite were maintained around 0.25 mm and 5 mm x 40

mm, respectively. Similarly, the fiber mass fraction and volume fraction in the composite were maintained at around 23-26%.

3.11.1 Resin/Fiber Content Calculation and Rule of Mixtures

The resin content was calculated using the volume fraction of the yarns in the final composite. The total volume of the composite was calculated by measuring its dimensions, i.e., length of the composite using a ruler and the width and thickness using a vernier caliper. Similarly, the length of the yarns was measured using the ruler and fiber diameter on the scanning electron microscope as described previously in section. The measured dimensions were substituted in the following formulae to derive the total volume of the composite and the total volume of the fibers in the composite respectively:

Volume of the composite (V_c) = Length (L_c) × Breadth (B_c) × Height (H_c)

Total volume of the fibers (V_f) = 3.14 × Radius $(R_f)^2$ × Length (L_f) × 1000 × no. of yarns incorporated in the composite

The calculated volumes of the fibers and the total composite were subsequently used to predict the mechanical properties of the final composite using the rule of mixtures. This rule helps determine the weighted mean that can predict the upper bound of properties such as Young's modulus, thermal conductivity, and electric conductivity of a composite that consists of unidirectional parallel fibers and a resin.

The elastic modulus of the composite can be theoretically calculated using the rule of mixtures as below [102]:

Rule of mixtures:

Upper bound $E_c = f^* E_f + (1-f) *Er$

Where: E_f = Elastic modulus of fibers

E_r = Elastic modulus of the resin/matrix

f = Volume fraction of the fibers calculated as: $f = V_f / (V_f + V_r)$

V_f = Total volume of the fibers

V_r = Total volume of the resin.

Similarly, the expected lower bound of the property can also be calculated using the inverse rule of mixtures for tests in direction perpendicular to the fiber axis [102]:

Lower bound $E_c = (f/ E_f + (1-f)/Er)^{-1}$

In the present case, using the above explained rule of mixtures, the upper bound of the tensile modulus, tensile strength and the % strain was calculated for the fabricated composites and the calculated values were compared with those obtained experimentally. The mechanical properties of the fabricated composites primarily depend on the properties of the fiber reinforcements and the expected range of the elastic modulus can be calculated beforehand.

3.12 Tensile Characterization of Fiber Reinforced 'Green' Composites

The tensile properties of fiber reinforced green composites were tested using Instron, universal tensile tester (Model: 5566, Instron Co., Canton, MA) as per ASTM D 3039-00. A load cell of 10 KN was used for these tests. The composite specimens were conditioned for 24 hr at ASTM conditions of 21°C and 65% relative humidity. The tensile characterization was then carried out by gripping the two ends of specimens along the length by serrated grips of the Instron tester. Gauge length of 30 mm and crosshead speed of 10 mm/min (strain rate of 0.33 min^{-1}) was maintained for the tensile tests. At least 4 specimens were tested to determine the average values of the mechanical properties.

4 RESULTS AND DISCUSSION

4.1 Proximate Analysis of Raw Plantain (Fruit and Peel)

The proximate analysis of the RP starch specimens provided constituent percentage values of starch, crude fiber, crude fat, lignin, crude protein, simple sugars, water soluble carbohydrates (WSC) and ash. Table 4.1 presents a representative example of proximate analysis results of RP fruit starch specimen isolated using 1% solution of $NaHSO_3$ at pH 3 and after 2 washes. The percentage values of constituents in the specimen are shown for with and without moisture (dry matter only), separately. This analysis provided a better understanding of the contents in order to carry out further modifications to the RP starch isolation procedure. The analysis was repeated after every modification and the changes in the starch content were noted. Optimizing isolation parameters such as isolation solvent, pH and number of washes were carried out in order to obtain maximum starch content. Using the optimized parameters it was possible to isolate more than 80% starch from the RP fruit. Effects of various parameters are discussed below.

Table 4.1 Proximate analysis results of RP starch specimen isolated using 1% solution of $NaHSO_3$ at pH 3 and after 2 washes

Components	As Received (%)	Dry Matter (%)
Moisture	**19.8**	
Dry Matter	**80.2**	
Crude Protein	**1.7**	**2.1**
Adjusted Crude Protein	**1.7**	**2.1**
Lignin	**0.3**	**0.4**
Crude Fiber	**0.9**	**1.1**
Starch	**64.9**	**80.9**
Water Soluble Carbs.	**0**	**0**
Simple Sugars	**1.7**	**2.1**
Crude Fat	**0.9**	**1.1**
Ash	**0.3**	**0.4**

4.1.1 Effect of Solvents

Initially, the RP starch isolation procedure was carried out separately for the fruit and the peel using the following solvents:

a. NaOH (1% solution)

b. KOH (1% solution)

c. $NaHSO_3$ (1% solution)

It was observed that isolation with both $NaHSO_3$ and KOH was successful in obtaining more than 65% starch from the RP fruit. However, NaOH saponified the blended pulp making it foamy and rendering it difficult to use. The treatment with KOH also showed blackening of the mixture due to the process of delignification taking place during steeping [36]. Table 4.2 presents the starch content obtained from RP specimens isolated from pulp and peel, separately. The starch percentages from pulp and peel showed a considerable difference. Starch isolation from RP fruit was easier compared to that from peel due to its low content of fibrous matter, ash and pectinic impurities. Table 4.2 shows that the yield of starch isolated using KOH was much lower than that obtained using $NaHSO_3$. This is because during the process of steeping with $NaHSO_3$, the endogenous enzymes such as polygalacturonase, present in the RP fruit disintegrate the cellulosic cell walls allowing the starch granules to come into the aqueous solution [103]. Since the process of starch isolation from RP fruit using $NaHSO_3$ resulted in obtaining maximum starch percentage, this process was used for subsequent processing of gelatinization and crosslinking in this thesis. Moreover, $NaHSO_3$ being a food grade chemical, makes the process of starch isolation completely green.

Table 4.2 Starch content in RP specimens isolated from pulp and peel separately

	Fruit - $NaHSO_3$	**Peel - $NaHSO_3$**	**Fruit - KOH**	**Peel - KOH**
Starch % Based on Dry Matter	**74.2%**	**65.5%**	**69.8%**	**20.7%**

4.1.2 Effect of Washes

Washing with water can remove the soluble carbohydrates, simple sugars and some other impurities. The effect of number of washes was studied in order to observe the reduction in the percentages of water soluble compounds and other impurities and, thus, to increase the percentage of isolated starch. Figures 4.1 and 4.2 show the starch and ash contents, respectively, as a function of washes. It can be seen from Figure 4.1 that the starch percentage increased from 71.4 before washing to 77.5% after 2 washes and from Figure 4.2 it is clear that the decrease in ash percentage from 8.14 before washing to 1.62% after 2 washes.

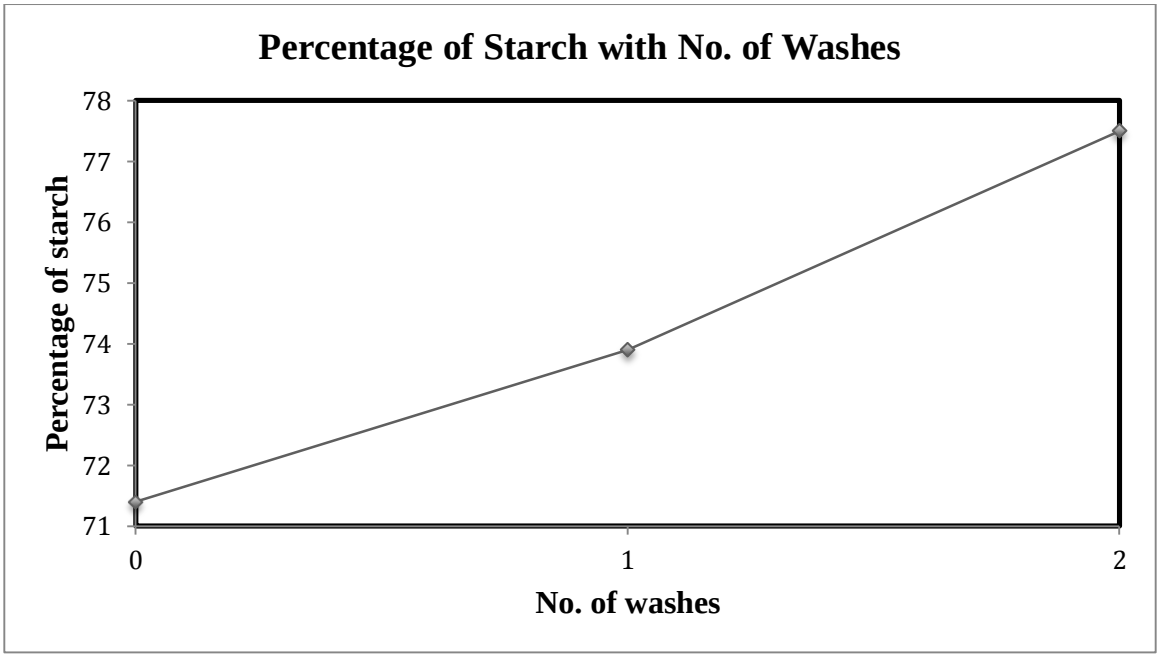

Figure 4.1 Starch percent as a function of number of washes

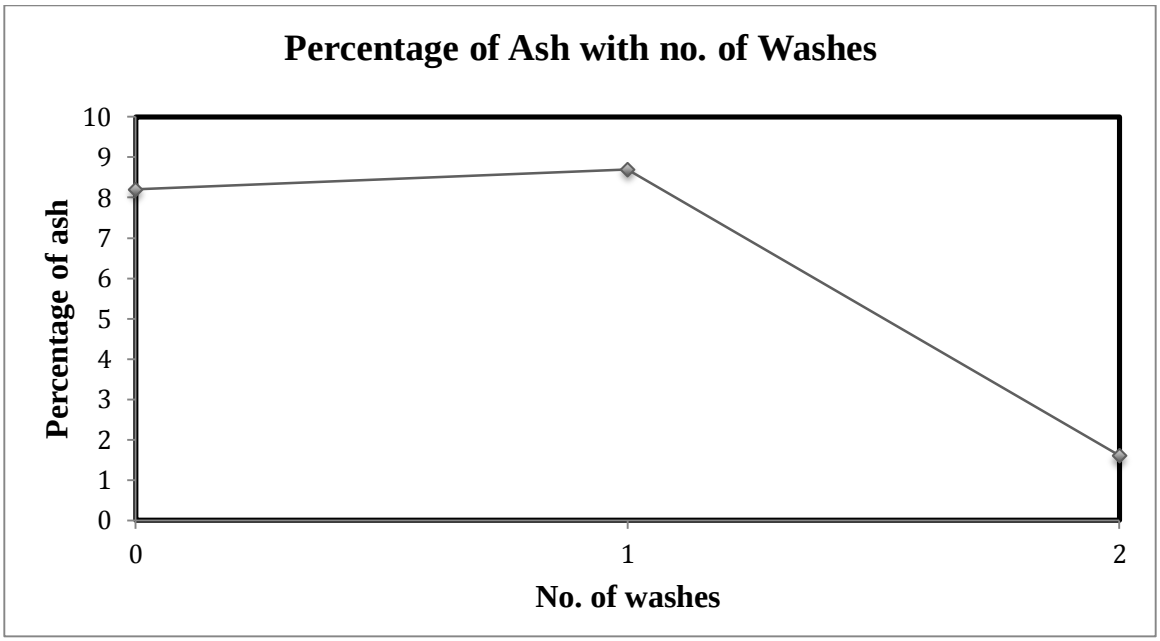

Figure 4.2 Ash percentage as a function of number of washes

4.1.3 Effect of pH

Conventionally, the starch isolation with $NaHSO_3$ takes place between pH 3 to 5 [36, 103]. The effect of $NaHSO_3$ solution pH was studied on the starch percentage obtained. Table 4.3 shows the proximate analysis results of RP starch specimen isolated at pH 3 and pH 5 on the basis of dry matter.

Table 4.3 Proximate analysis results of RP starch specimens isolated at pH 3 and pH 5

Components	pH-3 (DM)* (%)	pH-5 (DM) (%)
Crude Protein	**2.1**	**2.0**
Adjusted Crude Protein	**2.1**	**2.0**
Lignin	**0.4**	**1.0**
Crude Fiber	**1.1**	**1.3**
Starch	**80.9**	**77.6**
Water soluble Carbs.	**0**	**1.8**
Simple Sugars	**2.1**	**1.0**
Crude Fat	**1.1**	**0.7**
Ash	**0.38**	**1.62**

* Values indicate dry matter percentage

The results in Table 4.3 indicate that the variation of pH in the range of 3 to 5 did not show a significant effect on the percentage of starch. However, the process of starch isolation with 1% solution $NaHSO_3$ at pH 4 with two washes was used for further processing, characterization and resin formation. This method was followed as described in the earlier literature [103].

4.2 Characterization of Raw Plantain Starch

RP starch obtained from the fruit was fully characterized using several techniques including X-ray diffraction, thermal analysis (TGA, DSC), solution rheology and SEM. These results are discussed in the sections below.

4.2.1 X-ray Diffraction (XRD)

RP starch obtained from the fruit was characterized for its degree of crystallinity. Figure 4.3 shows the XRD pattern of RP starch. This perfectly matched the plantain starch XRD patterns in earlier literature [43]. The two characteristic crystalline peaks at 2θ values of 17 and 23 match the crystalline peaks of native cornstarch confirming its similarity to native starches [18, 104]. The percentage crystallinity of the RP starch was calculated as 57.4% from the XRD patterns by amorphous peak subtraction method.

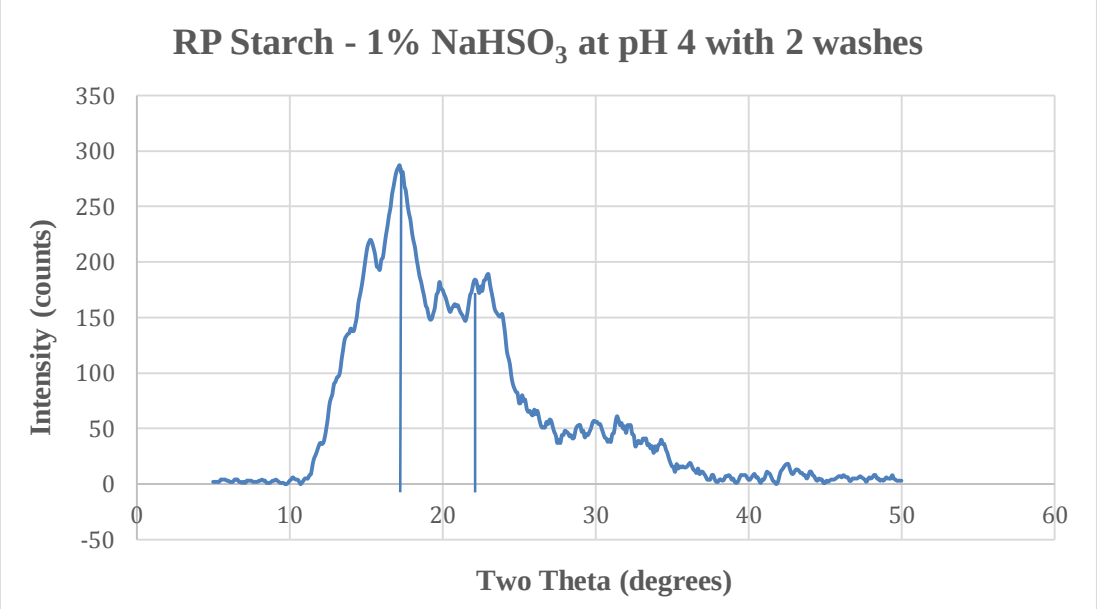

Figure 4.3 XRD spectrum of RP starch

4.2.2 Thermogravimetric Analysis (TGA)

Figure 4.4 shows a typical TGA thermogram of RP starch. The initial 10% weight loss up to 140°C accounts for the loss of moisture in the starch specimen. The total weight loss at 500°C was 67-70% when the starch gets charred and most other elements except carbon have been lost.

The starch degradation onset temperature was seen at 235°C which is identical to banana, corn and cassava starches in literature [104].

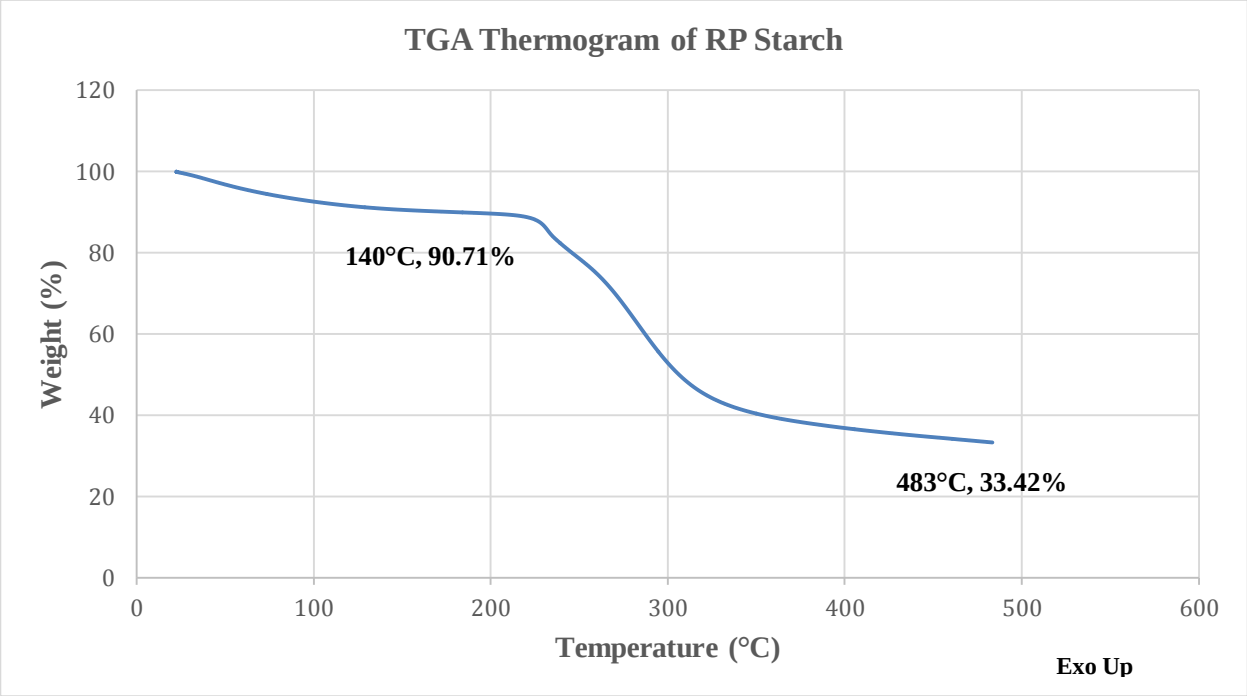

Figure 4.4 TGA thermogram of RP starch

4.2.3 Differential Scanning Calorimetry (DSC)

Figure 4.5 shows a typical DSC thermogram of 5% solution of RP starch. The enthalpy of gelatinization was calculated as 372.1 J/g by calculating the area under the endothermic peak. DSC characterization helped in other estimations related to the gelatinization of RP starch from the DSC thermogram. These are summarized as follows:

1. The onset (start) of gelatinization is at T_{onset} ~ 63°C.

2. The maximum endothermic reaction (peak) happens at T_{peak} i.e. gelatinization temperature ~ 80°C.
3. The gelatinization process completes at $T_{conclusion}$ ~ 84°C.

The gelatinization range estimated from the DSC thermogram matched the values in literature [37]

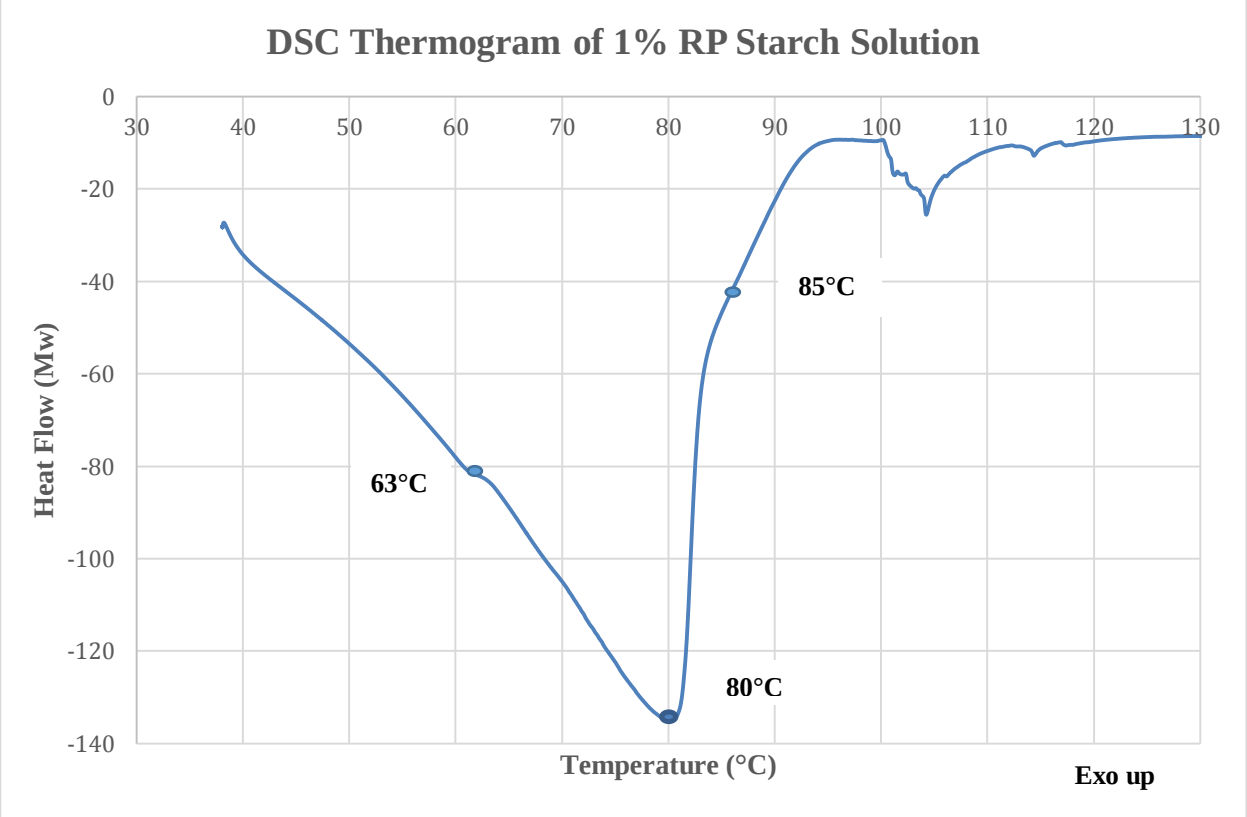

Figure 4.5 DSC thermogram of RP starch solution

4.2.4 Rheological Characterization

Figures 4.6 (A), (B) and (C) show the viscosity vs shear rate plots of 5% RP starch solution with increase in temperature, i.e. at 65, 75 and 85°C, respectively. These 3 temperatures were selected on the basis of the gelatinization range obtained from the DSC thermogram in Figure 4.5. All the 3 specimens were tested on the rheometer while gradually increasing the shear rate from 0 to 250 (1/s). At 65°C, Figure 4.6 (A), the viscosity vs shear rate plot showed a considerable fluctuation in viscosity with increase in shear rate. This was observed due to existence of starch powder and water in separate phases and the presence of some intact starch granules at this temperature.

Figure 4.6 (B) shows the viscosity vs shear rate plot of RP starch solution at 75°C. At this temperature, the mixture had passed the onset temperature of gelatinization as seen in Figure 4.5. As such, most starch granules do not exist as a separate phase, which is observed by the decrease in fluctuation of viscosity compared to that seen in Figure 4.6 (A). However, in Figure 4.6 (C), viscosity vs shear rate plot of RP starch solution tested at 85°C, the conclusion temperature of 83°C had been passed and the process of gelatinization was almost complete. As a result, a much smoother plot was seen which confirms that the mixture was in a homogenous phase.

Across the plots in Figures 4.6 (A), (B), and (C) a significant increase was observed in the initial viscosity i.e. viscosity at zero shear rate with increase in the temperature. This was due to the process of gradual gelatinization that takes place with increase in the temperature of the mixture leading to an increase in viscosity and homogeneous nature of the material.

From Figure 4.6 (C) an overall trend of shear thinning of RP starch as the viscosity decreases with increase in shear rate can be observed.

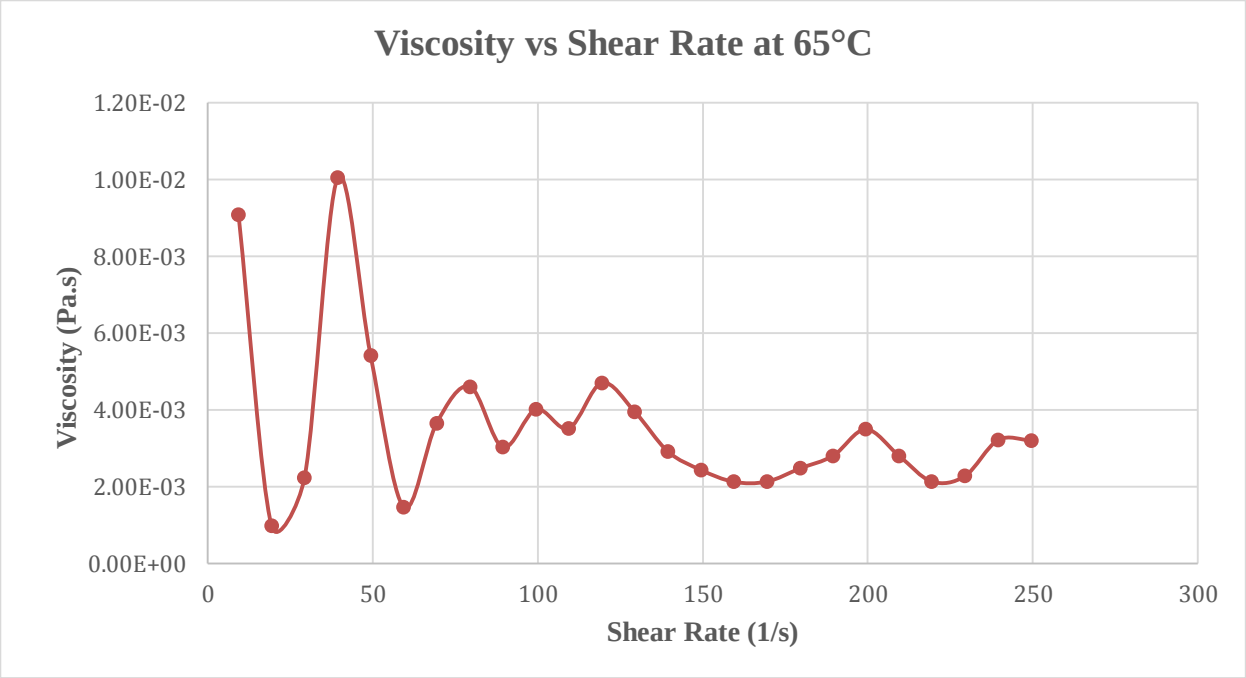

Figure 4.6 (A) Viscosity vs Shear rate plot of 5% RP starch solution at 65°C

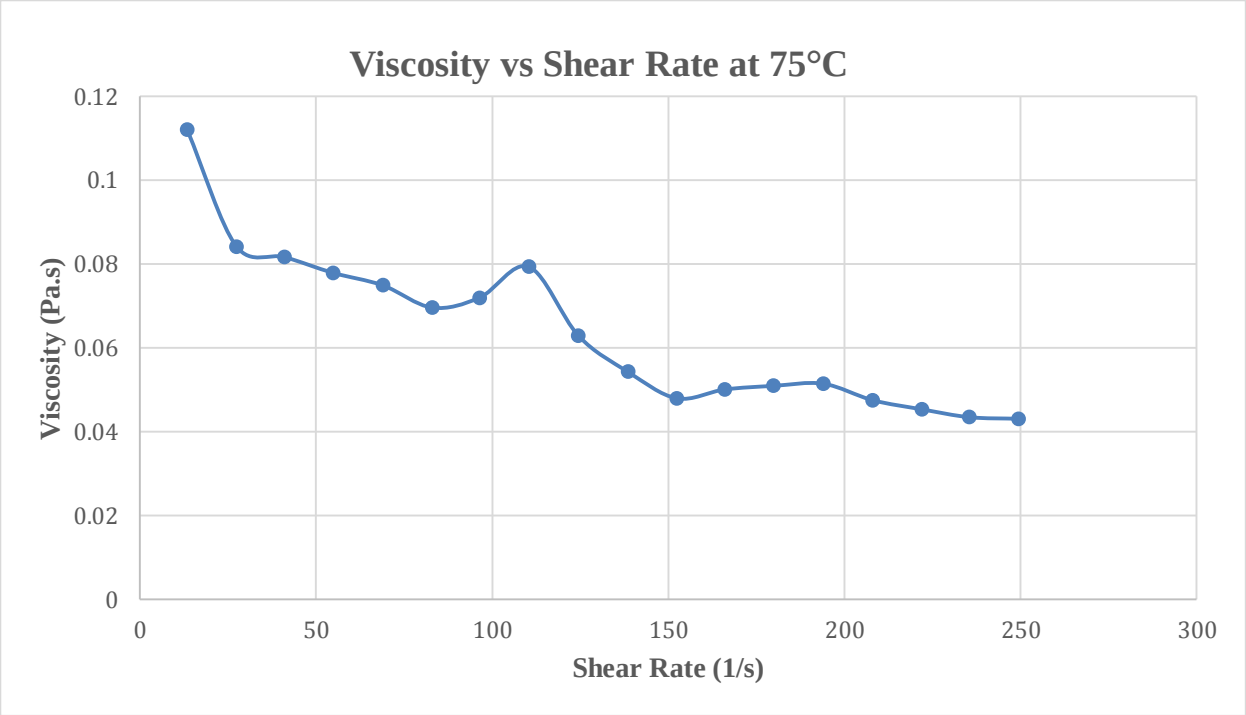

Figure 4.6 (B) Viscosity vs Shear rate plot of 5% RP starch solution at 75°C

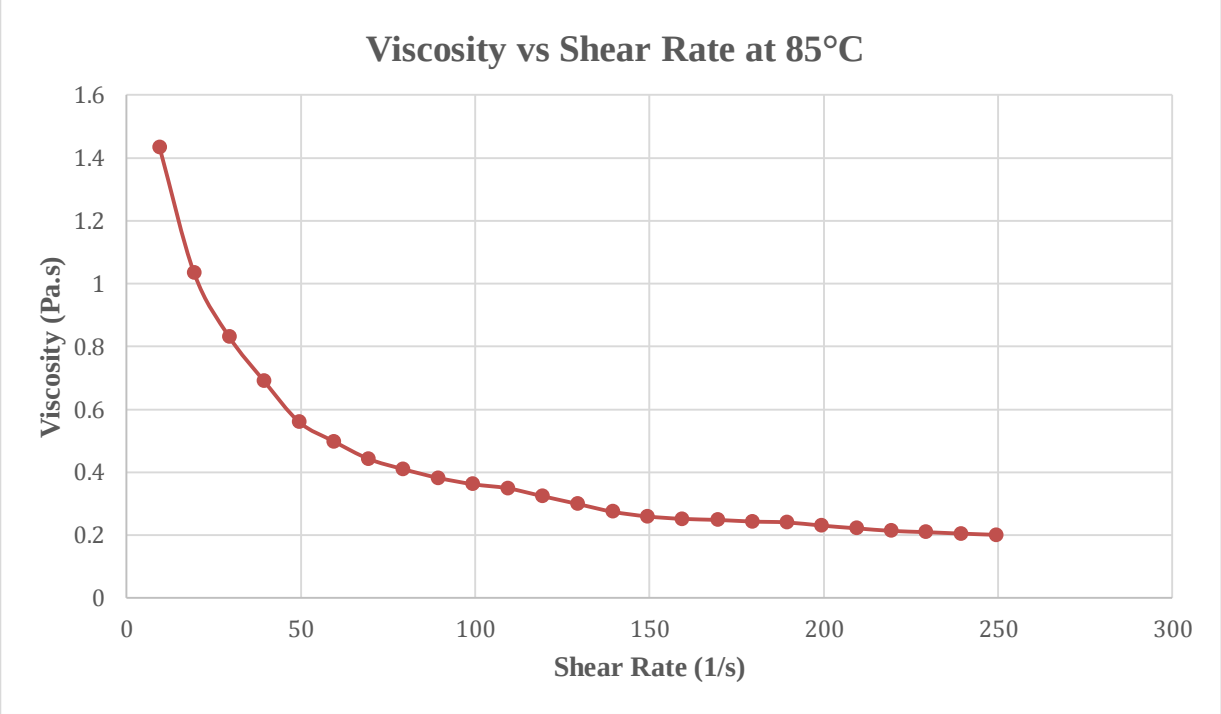

Figure 4.6 (C) Viscosity vs Shear rate of 5% RP starch solution at 85°C

4.2.5 Scanning Electron Microscopy (SEM)

Five percent starch solution was gradually heated with continuous stirring. 10 ml solution specimens were removed from the beaker as the temperature attained the values of 55, 65, 75 and 85°C, separately. These specimens were then observed under SEM to capture images to crosscheck with the gelatinizing results obtained from the rheometer. The data obtained from the rheometer was supported by SEM images of RP starch specimens captured at increasing temperatures of 55, 65, 75 and 85°C during the process of gelatinization. Figures 4.7 (A) and (B) show the granules of RP starch at 55°C that are intact and unaffected at that temperature. This is because the solution had not reached the gelatinization onset temperature of 63°C. SEM images in Figures 4.8 (A) and (B) show the RP starch specimens at 65°C. Partial gelling of the

RP starch granules can be seen in these images. Figures 4.9 (A) and (B) show SEM images of the RP starch solution specimens at 75°C which is semi gelatinized and has no intact granules. These SEM images show gelled granules in the form of large bumps. Figures 4.10 (A) and (B) show SEM images of completely gelatinized and homogenous RP starch specimens that are void of any traces of separate granules.

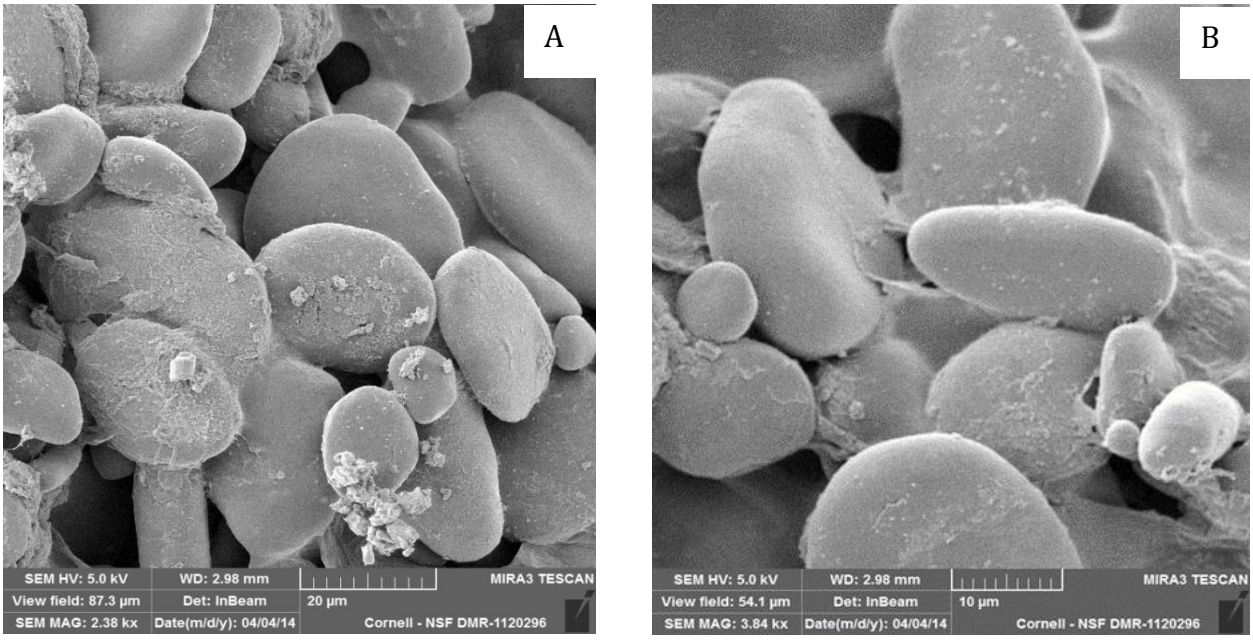

Figure 4.7 (A) and (B) SEM images of RP starch solution at 55°C

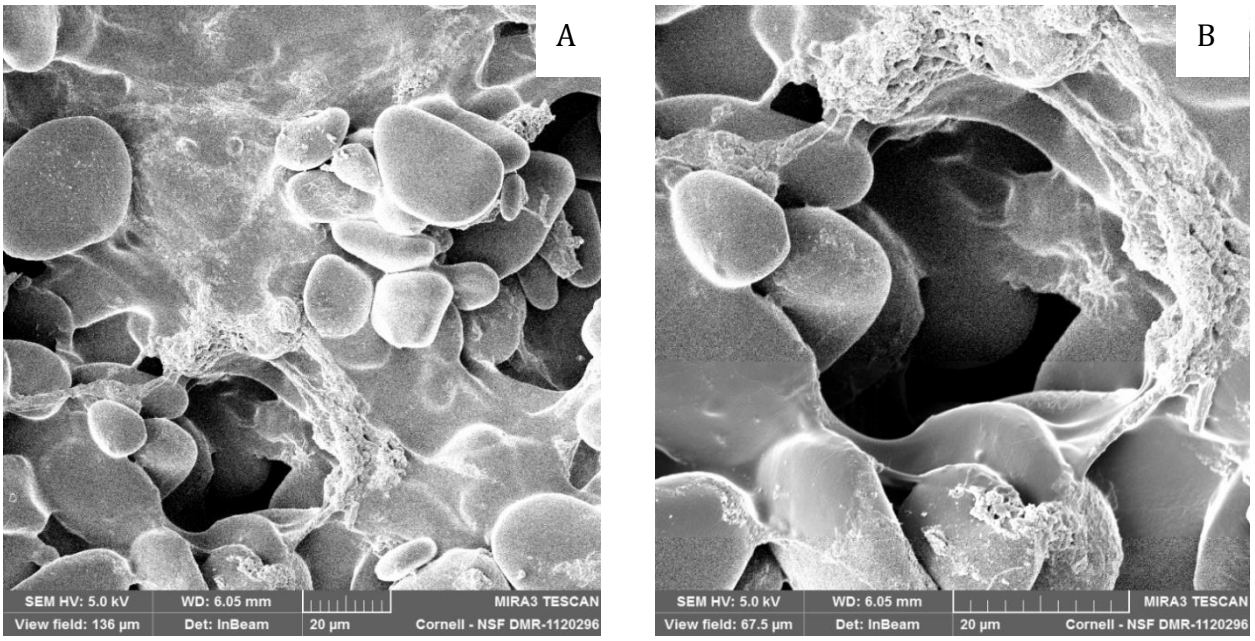

Figure 4.8 (A) and (B) SEM images of RP starch solution at 65°C

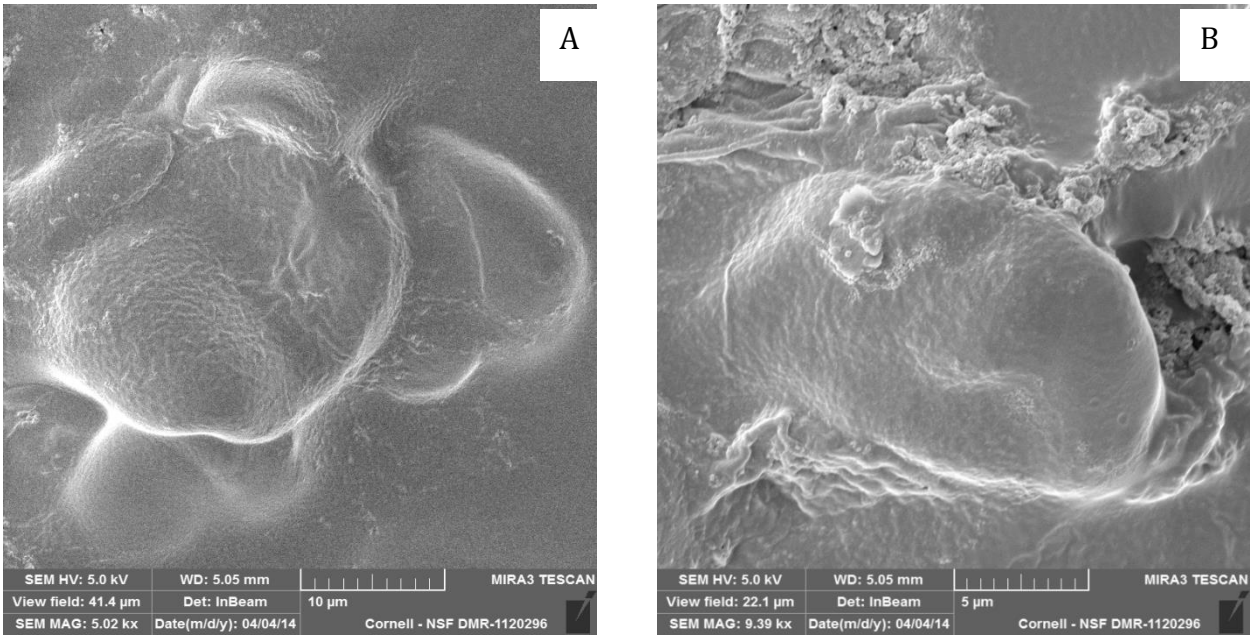

Figure 4.9 (A) and (B) SEM images of RP starch solution at 75°C

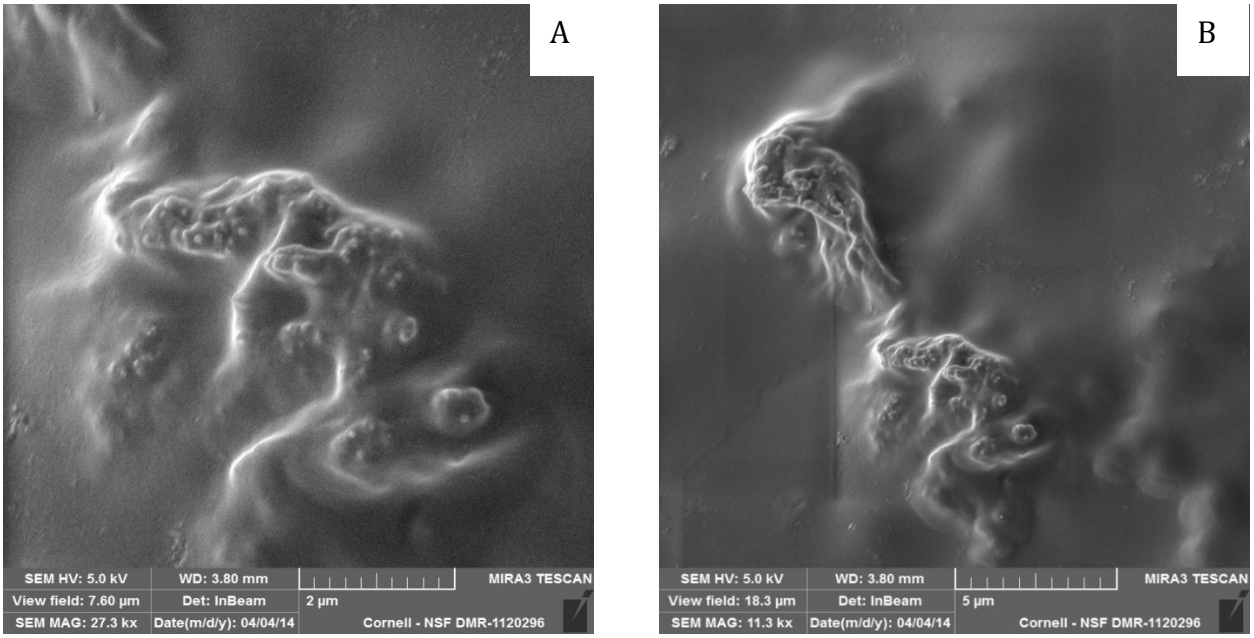

Figure 4.10 (A) and (B) SEM images of RP starch solution at 85°C

4.2.6 ATR-FTIR Study

Figure 4.11 shows the ATR-FTIR spectra of RP (blue) and native corn (orange) starches. Both show identical absorption peaks that confirm the RP starch is chemically comparable to commercially available starches. The absorption at 1336 (cm^{-1}) wavenumber corresponding to the bending mode of C-H bond for RP starch matched the starch spectra shown in literature for other starches [18, 31, 46]. This assures the good quality of the RP starch obtained in this study, at least qualitatively.

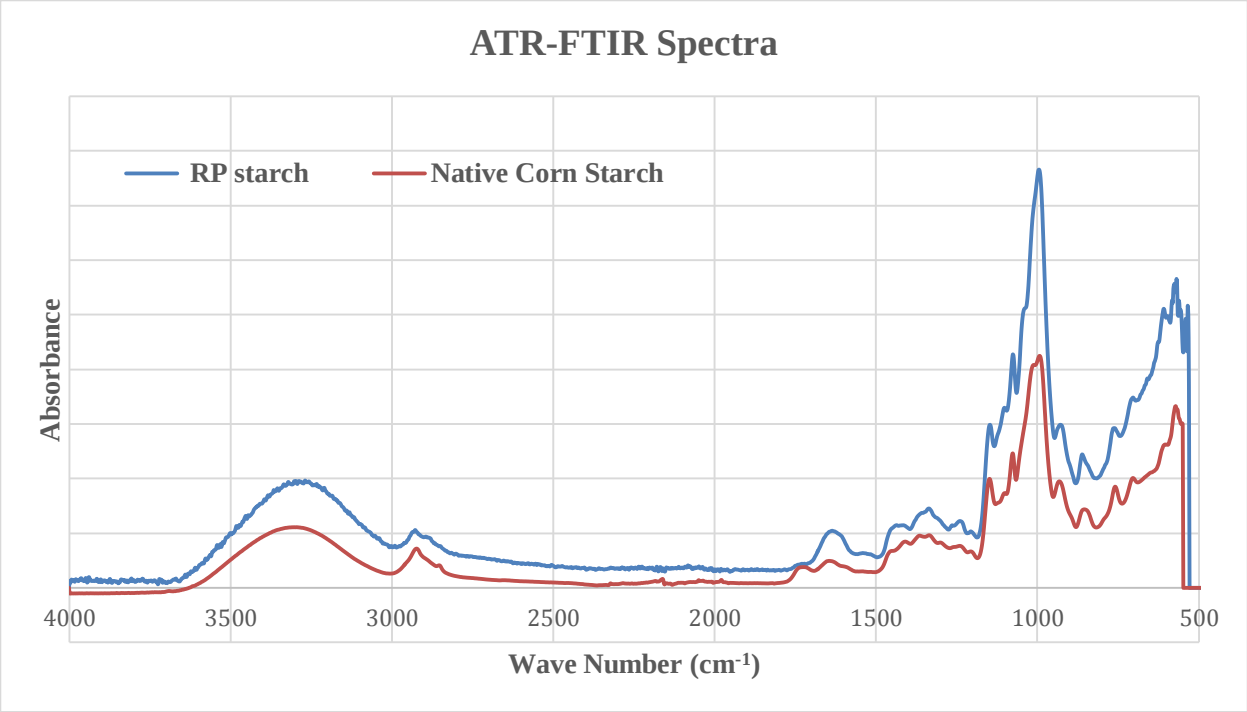

Figure 4.11 ATR-FTIR spectra of RP starch and native corn starch

4.3 Characterization of Fibrillar Micro Cellulose from Banana Stem Fiber (BFMC)

The BFMC was isolated from banana stem fibers by acid hydrolysis using H_2SO_4. It was further used as the reinforcing element in RP starch resin to enhance its strength and stiffness. In order to observe the surface morphology and aspect ratio (length and diameter) of the BFMC, it was characterized using SEM. The SEM images showed a decrease in the diameter of BFMC after acid hydrolysis and further decrease with high speed homogenization. Acid hydrolysis of cellulose is known to cleave and separate out the fibrillar structure, making it finer and subsequently increasing its aspect ratio [54]. This change can be seen through the successive images. Figures 4.12 (A) and (B) show SEM images of delignified and bleached banana fiber with an average diameter measured to be 120 µm. Figures 4.13 (A) and (B) show SEM images of BFMC obtained post acid hydrolysis and homogenization at 2000 rpm for 10 min and Figures

4.14 (A) and (B) show SEM images of further separation of BFMC fibrils after homogenization at 5000 rpm for 10 min. In comparison with the pre hydrolyzed banana fibers, high speed homogenization at 2000 rpm and 5000 rpm help in separating out singular fibrils from the entangled mesh-like structure. As per the results discussed later in section 4.4.4, introduction of BFMC in the resin evidently contributed to its strength and stiffness. Similar to MFC and nano-cellulose whiskers used in the earlier research [48, 49, 51], other nano scale components like BFMC with a high aspect ratio would impart strength and stiffness to the resin [54]. Use of BFMC made the resin a complete derivative of the *musaceae* family of crops.

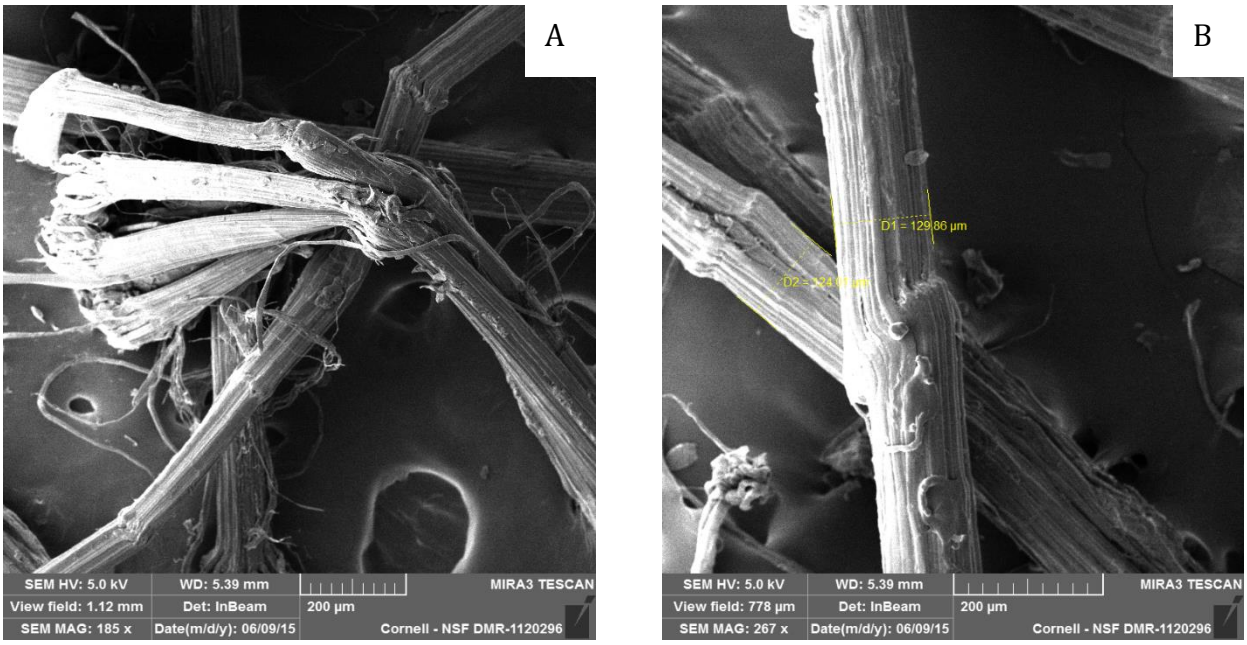

Figure 4.12 (A) and (B) SEM images of delignified and bleached banana fiber

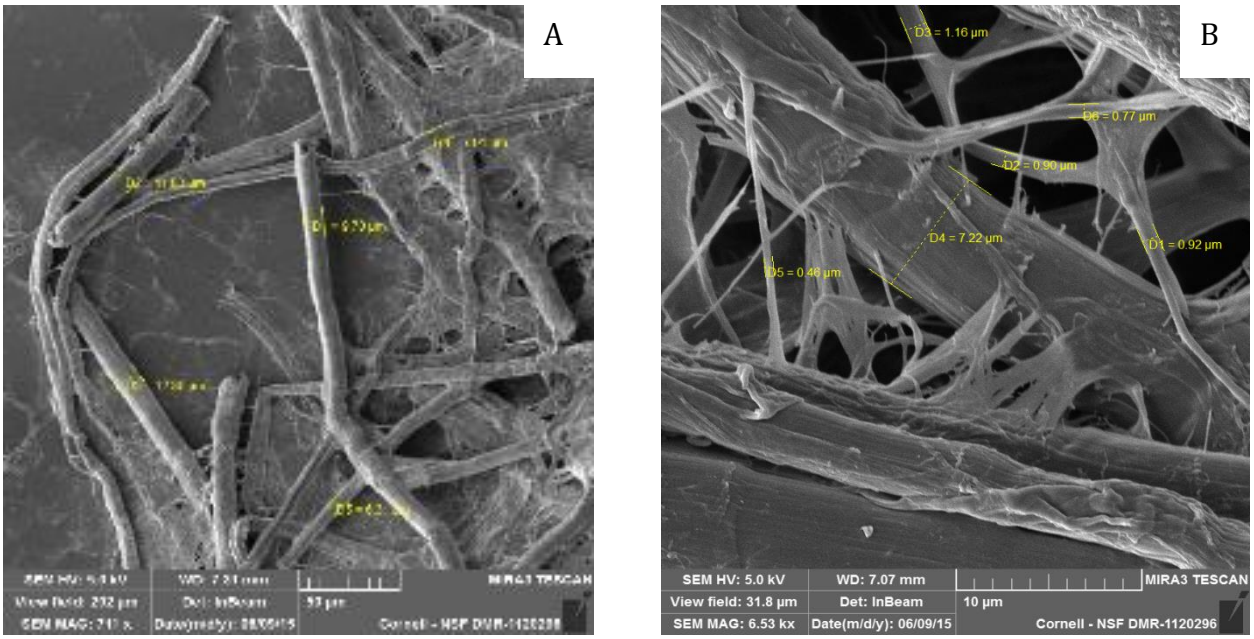

Figure 4.13 (A) and (B) SEM images of BFMC post acid hydrolysis and homogenization at 2000 rpm for 10 min

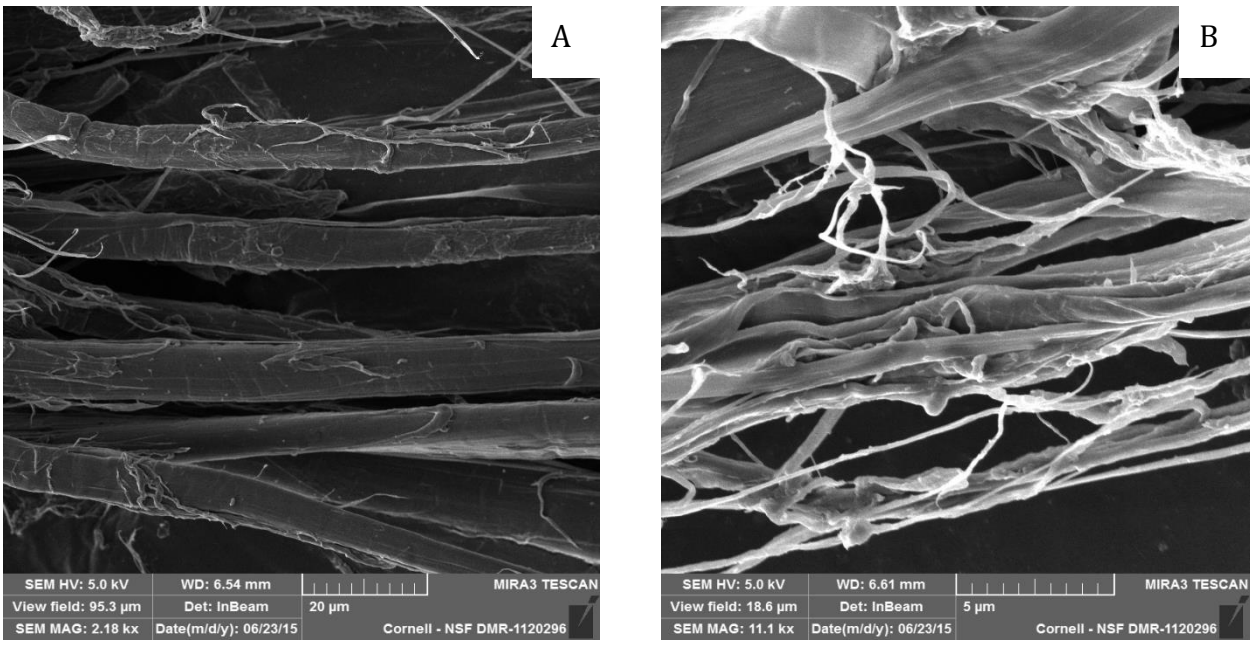

Figure 4.14 (A) and (B) SEM images of BFMC separated out further post acid hydrolysis and homogenization at 5000 rpm for 10 min

4.4 Characterization of Control and Modified Resin Films

The control resin films prepared from RP starch and the films reinforced with BFMC and crosslinked with BTCA were characterized for changes in physical and chemical properties. The results obtained are as follows:

4.4.1 ATR-FTIR Study

Figure 4.15 shows the ATR-FTIR spectra of RP starch (blue), pure BTCA (grey) and crosslinked RP resin (orange). The ATR-FTIR spectra of BTCA show a sharp characteristic absorption at 1691 cm^{-1} assigned to the carboxyl-carbonyl stretching vibration. The spectra of crosslinked resin with BTCA, showed a distinct vibration (absorption) at 1719 cm^{-1} corresponding to C=O (ester carbonyl) stretching peak which was not seen in the native RP starch spectra. It has been previously shown that corn and potato starches crosslinked with carboxylic acids show ester peaks at 1724 cm^{-1} and 1726 cm^{-1} respectively [18]. The crosslinking reaction proceeds through an esterification via formation of a cyclic anhydride intermediate aided by the catalyst [105]. The presence of above mentioned peaks in the crosslinked resin film and BTCA confirms the crosslinking reaction between RP starch and BTCA with the help of sodium hypophosphite as a catalyst.

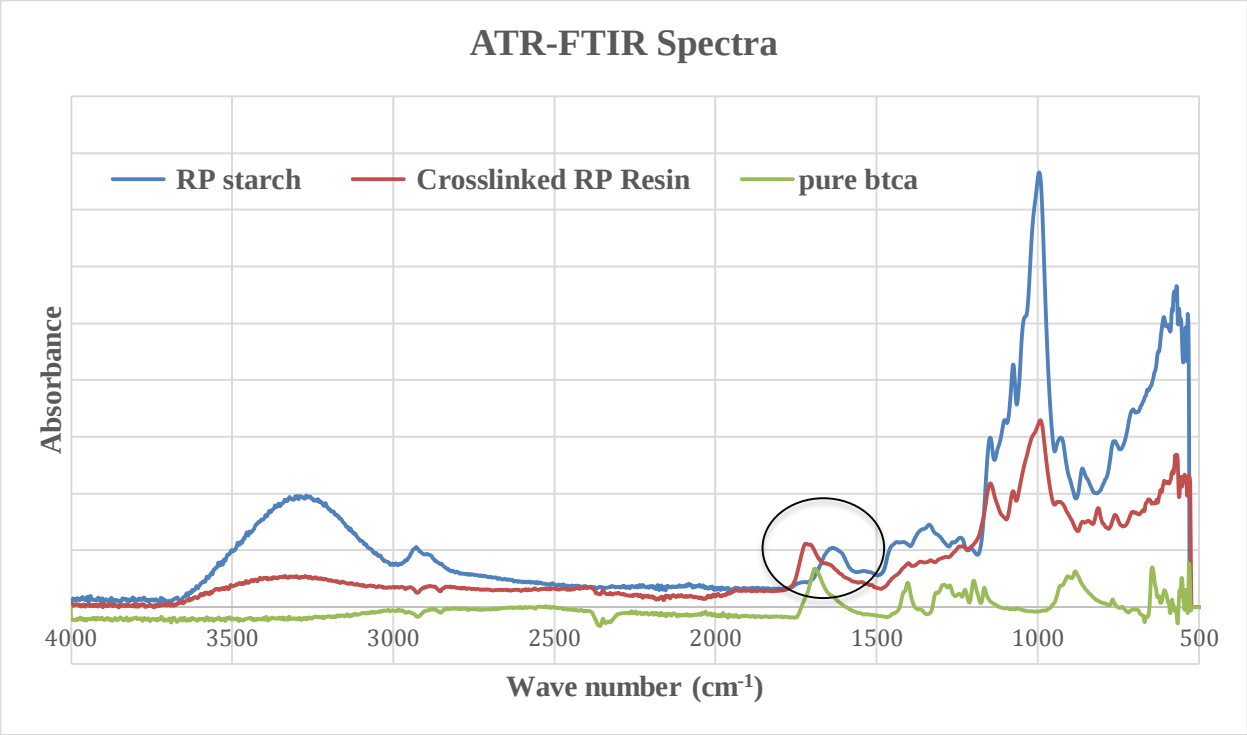

Figure 4.15 ATR-FTIR spectra of starch (blue), crosslinked RP resin (orange) and pure BTCA (grey) confirming the crosslinking reaction of RP starch with BTCA

4.4.2 Thermogravimetric Analysis (TGA)

Figure 4.16 shows a typical TGA thermogram for crosslinked RP resin. Weight loss of only 1% was observed around 140°C which can be assumed to be the loss of moisture from the specimen. This value is significantly lower than the moisture loss (~10%) seen in native RP starch at the same temperature (Figure 4.4). However, both native and crosslinked starch showed a high thermal degradation onset temperature around 235°C that remained unchanged. Around 59-60% of total weight loss was observed at 500°C. This was much less in comparison to about 67% weight loss obtained for RP starch. This is clearly a function of starch crosslinking with BTCA and is expected because of the compact network.

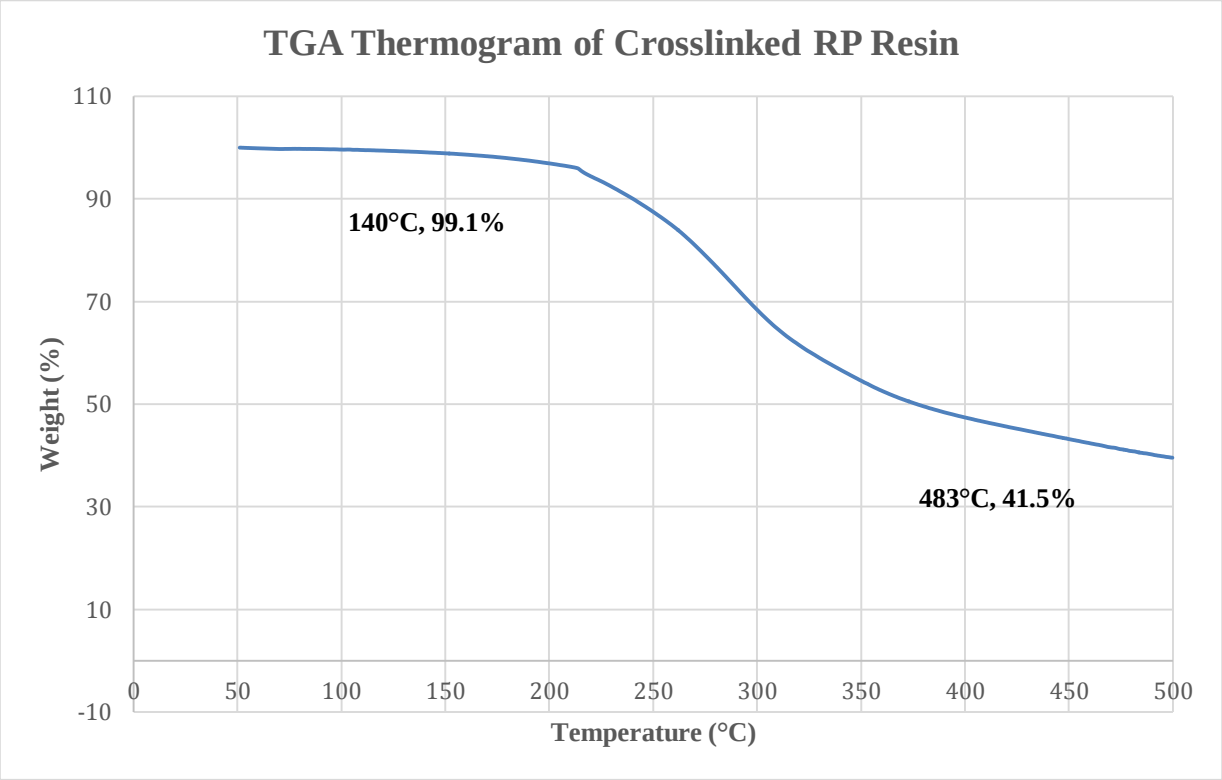

Figure 4.16 TGA thermogram of crosslinked RP resin

4.4.3 Moisture Absorption

The moisture absorption of crosslinked resin was calculated as an average of 3 specimens by weight addition (gravimetric) method after conditioning the samples at 65% humidity for 24 hr at RT compared to their dry weight. The moisture content of RP starch resin was calculated to be 13.3% whereas the moisture content of crosslinked and modified (reinforced with BFMC) resin was calculated to be 9.5%. The reduction in moisture content was due to crosslinking of RP starch that led to a reduction in the number of reactive hydroxyl groups present in the resin as well as to the compact network formed by crosslinking that pulls the molecules together and

reduces the space for water [18, 31]. In addition, BFMC being mostly crystalline, absorbs less moisture.

4.4.4 Tensile Property Characterization

Table 4.4 presents the tensile properties of the control (native RP starch), crosslinked and modified RP resin films. These were tested for their tensile modulus, fracture strain and fracture stress (strength). As can be expected, crosslinking of the RP starch resin with BTCA, leads to a more compact structure pulling the molecules closer. This, in turn, provides better H-bonding between the RP starch molecules leading to higher stiffness of the resin. In case of modified starches reinforced with MFC which has a Young's modulus of 140 GPa, the strength and Young's modulus of the resin can be as high as 39 MPa and 2.34 GPa, respectively [18]. This is seen due to the presence of 4 carboxyl groups present in BTCA making it highly reactive with hydroxyl bonds in RP starch. As a result, crosslinking of RP starch lead to a 100% increase in the resin modulus from 85 MPa to 178.6 MPa. Moreover, due to the chemical similarity between BFMC and RP starch, a high interfacial interactions through hydrogen bonding (high adhesion) can be expected between the two components. This was confirmed by significant increase in the modulus and strength of the crosslinked resins consisting of 25% BFMC compared to the resins without BFMC. Another factor for the high Young's modulus of crosslinked RP resin with BFMC (430 MPa) compared to crosslinked RP resin without BFMC (178.6 MPa) is the high modulus of BFMC itself. Although the Young's modulus of BFMC could not be measured, the fibrils are expected to have very high strength. For example, Young's modulus of industrial grade MFC is estimated at about 140 GPa [18]. The reason for

combining BFMC with RP resin was indeed to obtain high resin strength, while keeping it inexpensive. Figure 4.17 summarizes the increase in Young's modulus with crosslinking and modification (addition of BFMC) of control RP resin.

Table 4.4 Tensile properties of control, crosslinked and modified RP resin films

	Control RP Resin	Crosslinked RP Resin: 10% BTCA	Control RP + 25% BFMC Resin	Crosslinked RP + 25% BFMC Resin: 10% BTCA
Modulus (MPa)	**85.1 (17.4)***	**178.6 (38)**	**372.8 (47.1)**	**430.6 (72.6)**
Strength (MPa)	**3.65 (0.6)**	**6.1 (0.49)**	**9.41(1.57)**	**8.7 (2.25)**
Strain (%)	**18.9 (3.4)**	**21.7 (4.7)**	**8.3 (3.8)**	**4.1 (2.4)**

* Values in parentheses denote standard deviation

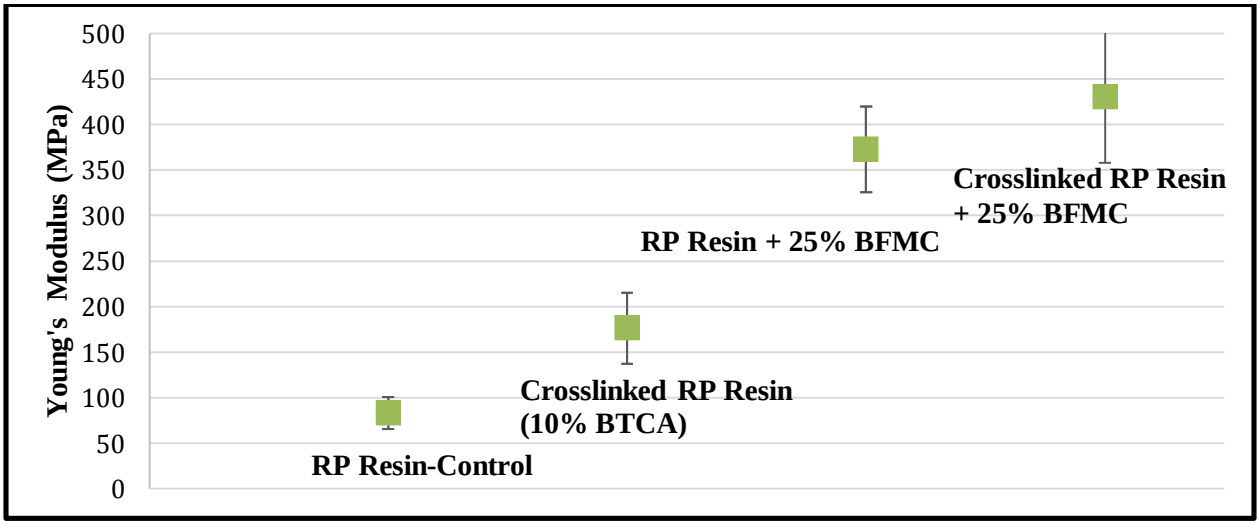

Figure 4.17 Summary of Young's moduli with crosslinking and modifications of RP resin

4.5 Characterization of Control and Treated LCC Yarns and Fibers

Control and treated (with $NaHSO_3$ and KOH solutions) LCC fibers were characterized for their tensile properties and significant changes were seen in the physical and mechanical properties of the fibers post treatments. The results are discussed below.

4.5.1 Fiber Diameter and Surface Morphology

Single LCC fibers were characterized using SEM to study their surface morphology and diameter pre and post treatments. Figures 4.18 (A) and (B) show typical SEM images of control (untreated) LCC single fibers with a somewhat smooth surface and uniformity along their axis unlike natural cellulosic fibers which show a large degree of variation and roughness. The average fiber diameter was calculated as 10.7 µm.

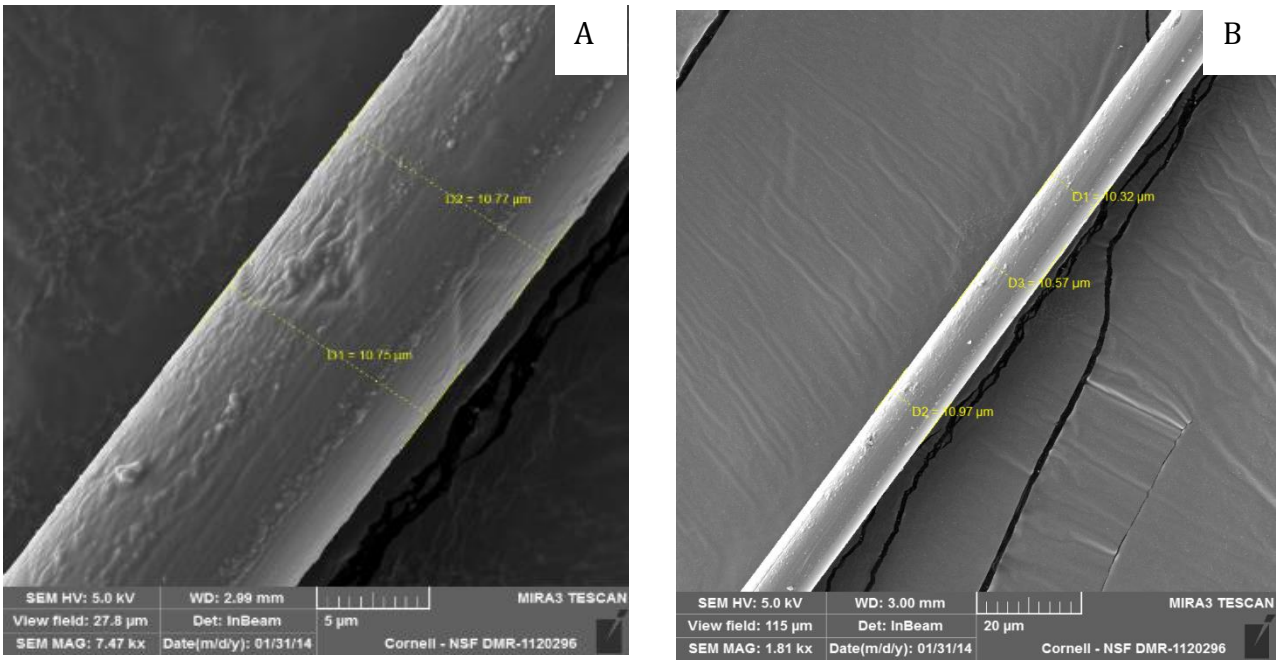

Figure 4.18 (A) and (B) SEM images of control LCC single fibers at different magnifications

Figures 4.19 (A) and (B) show typical SEM images LCC fibers treated with 5% $NaHSO_3$ solution under 0.98 kg and 2.42 kg load, respectively, and Figures 4.20 (A) and (B) show typical SEM images LCC fibers treated with 10% KOH solution under 0.98 kg and 2.42 kg load, respectively. Chemical and tension treatments with $NaHSO_3$ did not show any change in the fiber surface. However, treatments with KOH led to scaling of the fiber surface as shown in Figure 4.20 (A) and further led to degradation of the fiber surface with increase in load 2.42 kg as can be seen in Figure 4.20 (B). Previously, researchers had successfully shown an increase in the mechanical properties of LCC fiber under tension at lower concentrations of KOH [15]. This degeneration of fiber surface was attributed to the high concentration of KOH that made the fiber incapable of withstanding the load treatment. The tension treatment with $NaHSO_3$ at small loads (0.98 kg), i.e., with fiber stress of 112 MPa led to a reduction in the fiber diameter as expected. This reduction was observed due to rearrangement of molecular chains and better alignment along the fiber axis i.e. longitudinal direction in which tension was applied [15]. The change in molecular orientation was been further confirmed by GADD testing and is discussed in section 4.5.3.

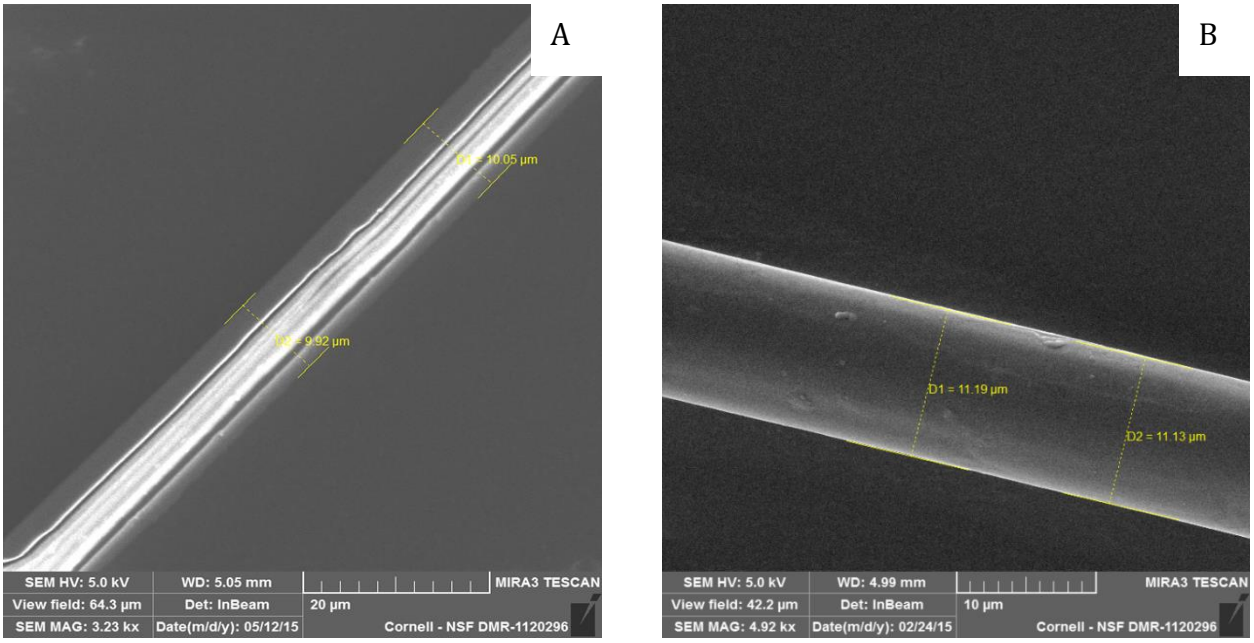

Figure 4.19 SEM images of single LCC fibers treated with 5% $NaHSO_3$ solution (A) 60 min under 0.98 kg load (B) 120 min under 2.42 kg load

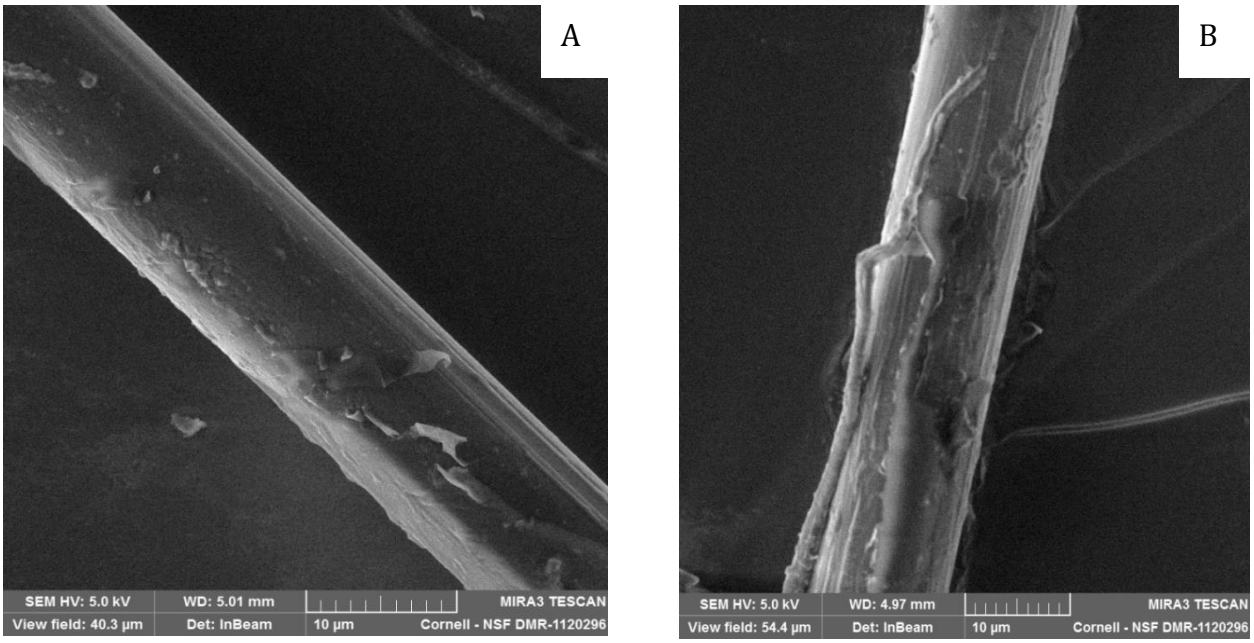

Figure 4.20 SEM images of single LCC fibers treated with 10% KOH solution (A) 120 min under 0.98 kg load (B) 120 min under 2.42 kg load

4.5.2 X-Ray Diffraction

The crystallinity of LCC fibers was tested using the most common method of X-ray diffraction. The percent crystallinity of the LCC yarn pre and post treatments was calculated by initially subtracting the background from the spectra [13, 15]. Figure 4.21 shows the XRD spectra of control LCC yarns for amorphous peak subtraction method. This method included calculation of crystalline peak area by subtracting the amorphous ground from the total peak area. Similarly, Figures 4.22 and 4.23 show the XRD spectra of LCC yarns for amorphous peak subtraction method treated with 10% KOH and 5% $NaHSO_3$ solutions. The results of crystallinity from Figure 4.21 (A) control and Figure 4.22 KOH treated yarns matched the literature accurately [15]. Table 4.5 presents the crystallinity of the LCC yarns pre and post chemical treatment. The values ensure that percent crystallinity of the fibers increased significantly, reducing the amorphous part in the fibers after the chemical treatments. Higher crystallinity can be expected to result in higher fiber strength and stiffness.

Table 4.5 Crystallinity (%) values of LCC yarns pre and post chemical treatment

	Amorphous Peak Subtraction Method
Control	**57.8%**
10% KOH	**78.6%**
5% $NaHSO_3$	**80.1%**

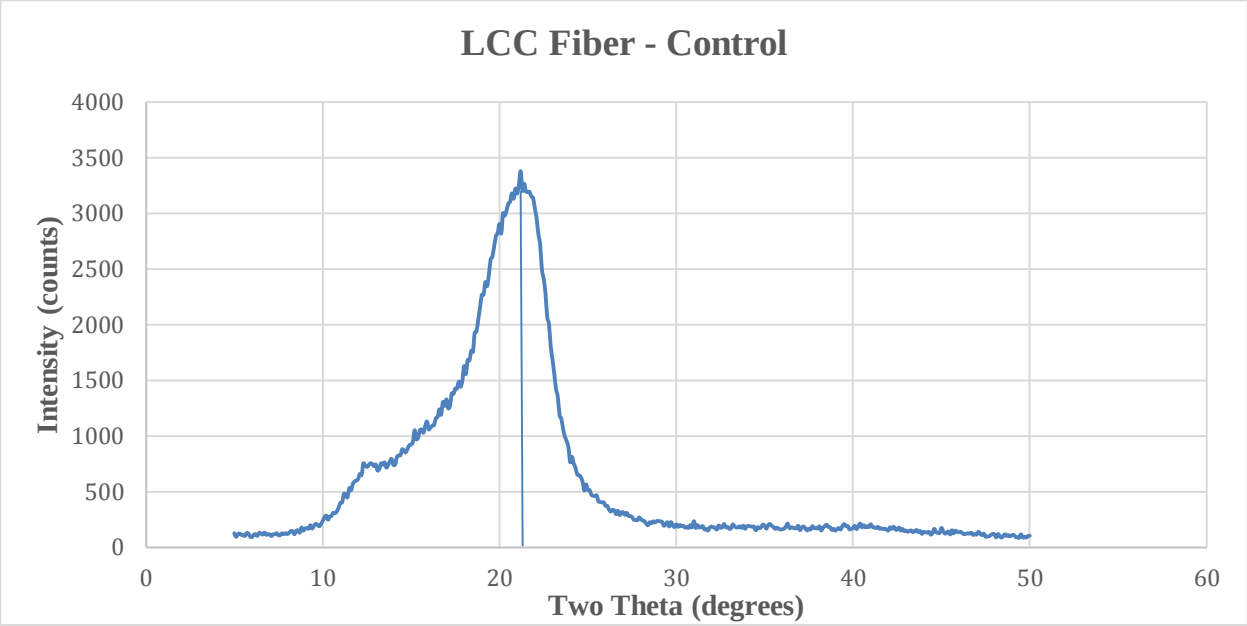

Figure 4.21 XRD spectrum of Control LCC yarns

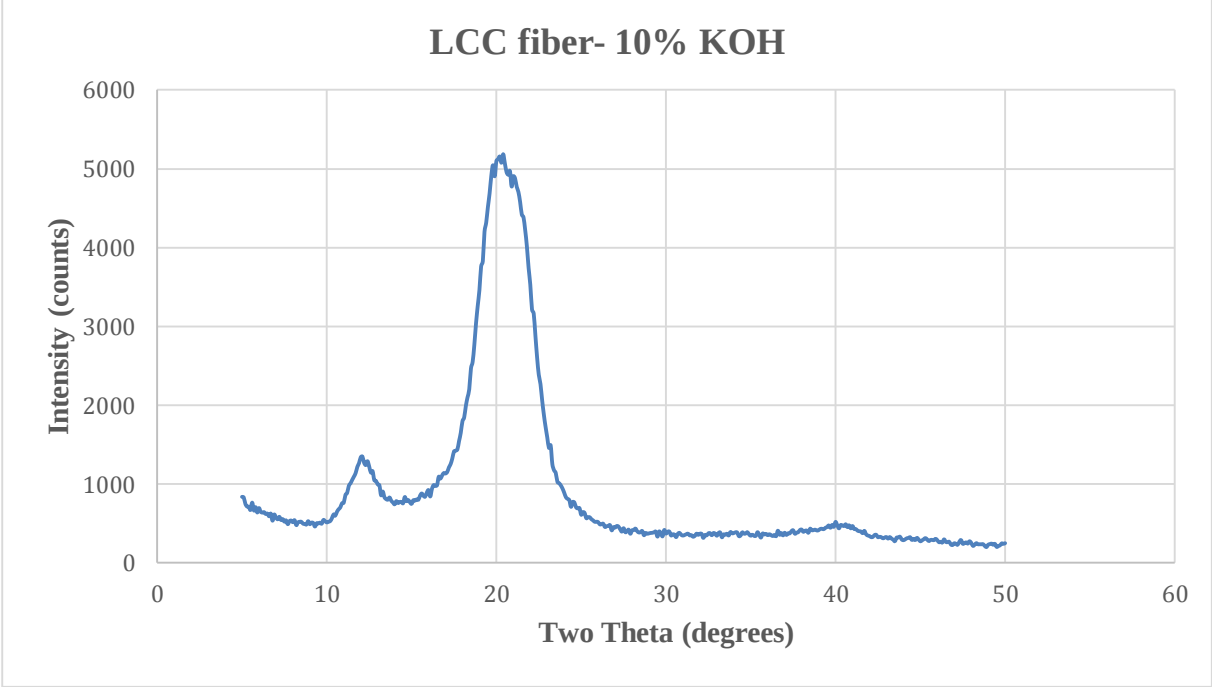

Figure 4.22 XRD spectrum of LCC yarns treated with 10% KOH solution

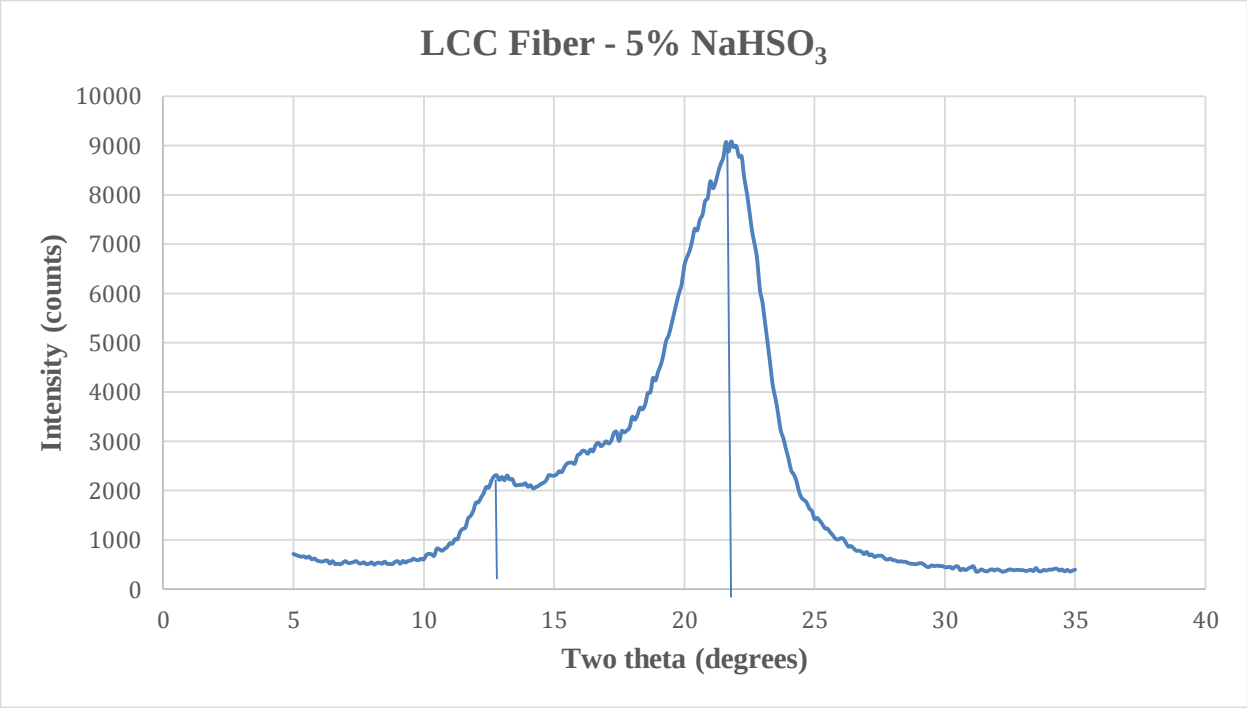

Figure 4.23 XRD spectrum of LCC yarns treated with 5% $NaHSO_3$ solution

4.5.3 General Area Detector Diffraction (GADD) Spectra

The LCC yarns were tested for change in the molecular orientation post the tension treatment. Figures 4.24 (A) and (B) show the GADD spectra of control LCC yarns and LCC yarns treated with 5% $NaHSO_3$ for 60 min under 0.98 kg load, respectively. The sharp peaks treated LCC yarns indicated a significant increase in the molecular orientation of the fiber along its axis after the treatment with the load. This was clearly observed through the GADD spectra showing a reduction in detected area post treatment. Table 4.6 presents the full width at half maximum (FWHM) values of control and treated LCC yarns derived from the GADD spectra. The narrowing in FWHM values from 17.9 to 10.2 confirmed the formation of highly oriented LCC

fibers post tension treatment. This was desired as higher orientation can be expected to result in better fiber alignment and finally increase in fiber strength.

Table 4.6 FWHM values of control and treated and LCC yarns derived from the GADD spectra

	FWHM
Control	**17.9**
$NaHSO_3$ 60 min 0.98 kg	**10.2**

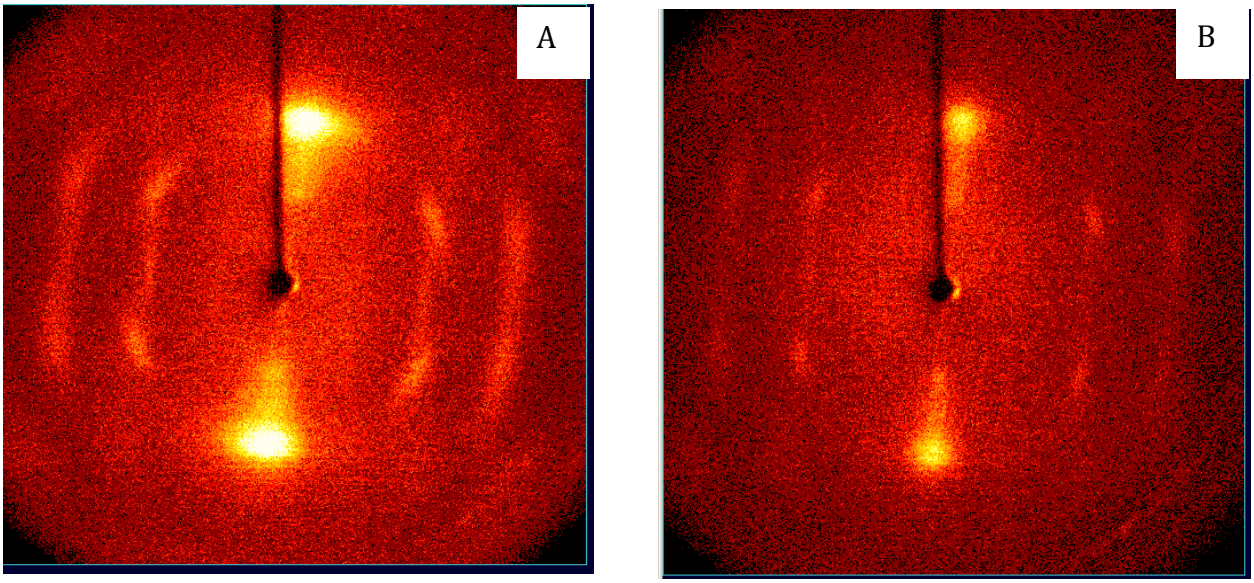

Figure 4.24 GADD spectra of (A) Control LCC yarns and (B) LCC yarns treated with 5% $NaHSO_3$ solution for 60 min under 0.98 kg load

4.5.4 Tensile properties of LCC fibers

The LCC fibers were expected to possess high tensile modulus and strength as shown by Kim and Netravali due to their inherent high degree of crystallinity [15]. Table 4.7 shows the tensile

properties of control LCC fibers. The fibers were tested using Instron universal tester and did not show yielding with increase in stress. Figure 4.25 shows a representative stress vs strain plot of the control LCC single fiber.

Table. 4.7 Tensile properties of control LCC fibers

	Control LCC Fibers
Young's Modulus (GPa)	**45.6 (14)***
Strength (MPa)	**1250 (252)**
Strain (%)	**4.6 (0.89)**

* Values in parentheses indicate standard deviation

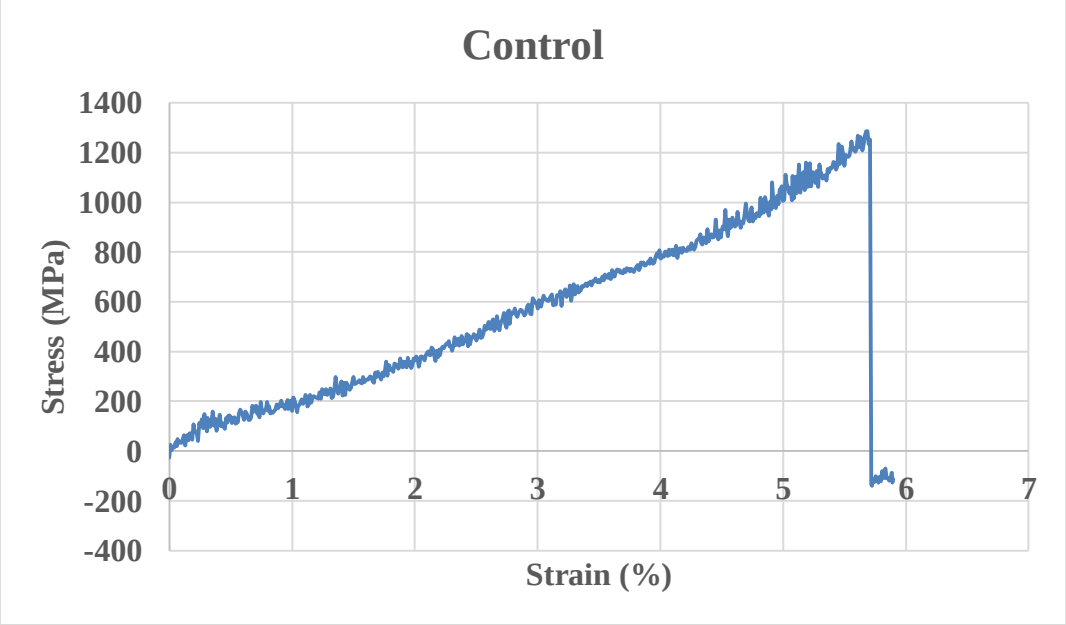

Figure 4.25 Representative stress vs strain plot of control LCC single fiber

4.5.4.1 Effect of Solvent

In order to enhance the mechanical properties of the LCC fibers, they were subjected to a chemical treatment using various solvents. The preliminary results indicated that treatment with NaOH was strong and had negative effects on the fiber leading to disintegration of the fiber structure. Previous experiments of LCC fiber treatment with NaOH had also resulted in loss of tensile strength and break down of fibrils [15].

Table 4.8 summarizes the results of tensile properties of LCC fibers as a function of the treatment solvents used. A comparison of the tensile properties showed KOH and NaHSO3 treatments resulted in stiffer and stronger fibers. As a result, 2% solutions of KOH and $NaHSO_3$ were chosen as the desired solvents for further treatments.

In order to get a better understanding of the obtained results from the Instron universal tester, Figure 4.26 shows the representative stress vs strain plots as a function of treatments with different solvents.

Table 4.8 Tensile properties of LCC fibers as a function of the treatment solvent

	Control	KOH (2%)	$NaHSO_3$ (2%)	NH_4OH (2%)
Modulus (GPa)	**45.6 (14)***	**47.4 (8.9)**	**52.9 (18.4)**	**35.2 (8.1)**
Strength (MPa)	**1250 (252)**	**1295 (406)**	**1347 (399)**	**1286 (208)**
Strain (%)	**4.65**	**6.06**	**5.11**	**5.38**

* Values in parentheses indicate standard deviation

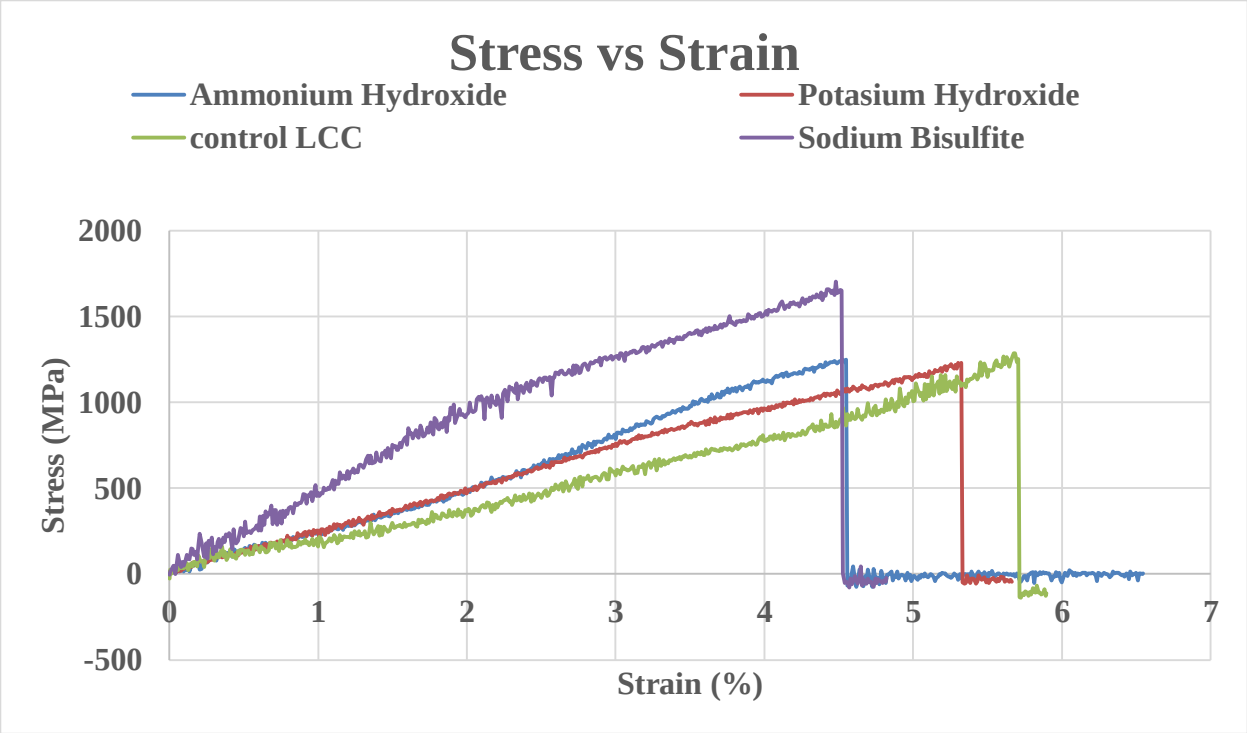

Figure 4.26 Representative stress vs strain plots of LCC fibers as a function of solvent

4.5.4.2 Effect of Solvent Concentration

The change in mechanical properties of LCC fibers was studied as a function of concentration of KOH and $NaHSO_3$ which had given the best improvements in the tensile properties. Three concentrations of the selected solvents, 2%, 5% and 10%, were used for the treatment. A constant duration of 2 hr treatment time was used while the temperature was maintained at RT.

As expected, with the increase in the solvent concentration, there was greater availability of the solvent to penetrate into the fiber. This led to a reduction in the amorphous phase of the fiber making it stiffer and increasing its modulus. This assumption was supported by the gradual decrease in fracture strain values with increase in concentration for both the solutions.

Table 4.9 presents the tensile properties of LCC fibers treated with the KOH and $NaHSO_3$ at different concentrations. Figure 4.27 gives a comparative summary of change in young's modulus of the fibers as a function of KOH or $NaHSO_3$ concentrations. In case of KOH, the modulus showed a linear increase with concentration i.e. 47.3, 52.3 and 56.8 GPa with concentrations of 2, 5 and 10 %, respectively, giving best results with 10% KOH solution. These results matched literature where tensile properties of LCC fibers treated in slack conditions with 2M KOH solution [15].

However, in the case of $NaHSO_3$, the Young's modulus values did not show a considerable difference in the 5% and 10% solutions. Under these conditions the highest strength and Young's modulus were achieved. As a result, 5% $NaHSO_3$ treatment was chosen for further tests to avoid excessive usage of chemicals without compromising on the fiber strength.

Table 4.9 Tensile properties of LCC fibers treated with KOH and $NaHSO_3$ at different concentrations

	Control	KOH			$NaHSO_3$		
Concentration		**2%**	**5%**	**10%**	**2%**	**5%**	**10%**
Young's Modulus (GPa)	**45.4 (14)***	**47.4 (8.9)**	**52.3 (21.0)**	**56.8 (11.2)**	**52.9 (18.4)**	**54.5 (19.5)**	**54.8 (17.9)**
Strength (MPa)	**1250 (252)**	**1295 (406)**	**1374 (333)**	**1439 (147)**	**1347 (399)**	**1449 (435)**	**1283 (376)**
Strain (%)	**4.65**	**6.06**	**5.36**	**5.09**	**5.11**	**5.13**	**4.17**

* Values in parentheses indicate standard deviation

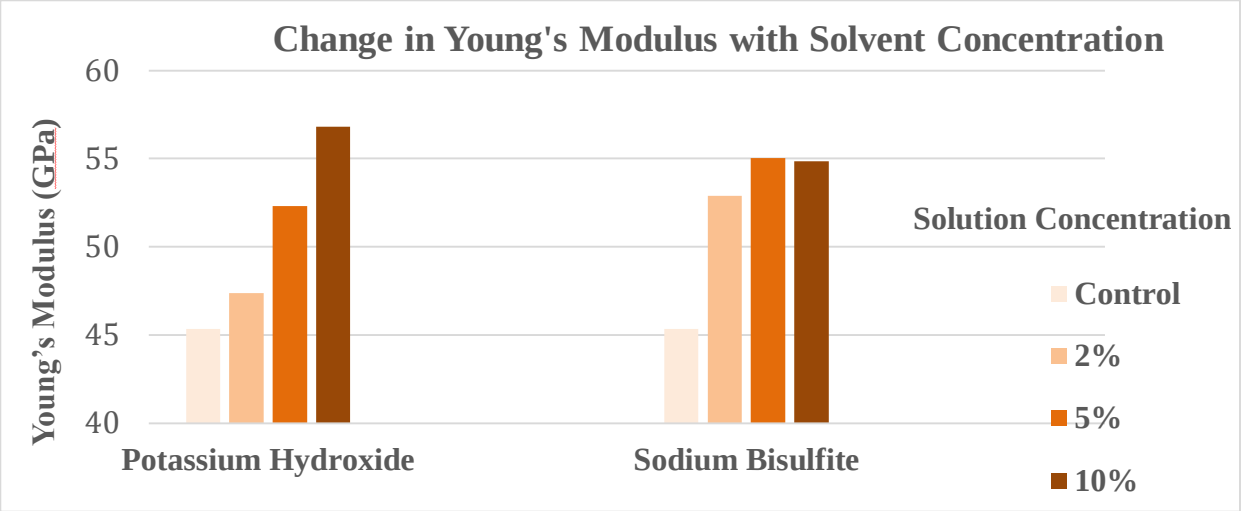

Figure 4.27 Comparative summary of change in young's modulus of the fibers as a function of KOH or $NaHSO_3$ concentrations

4.5.4.3 Wet/ Dry Testing

The tensile properties of LCC fibers were tested in wet conditions to obtain reference values for the loads to be imparted for chemical treatment. Water absorption is a characteristic behavior of cellulose based substrates which causes swelling and alters the dimensions resulting in significant changes in physical and tensile properties of the material [106]. As a result, it was important to understand the changes in mechanical properties of the fiber in wet state.

Table 4.10 presents the tensile properties of LCC fiber under dry and wet conditions. The data confirm that there is a considerable decrease in the modulus of the fibers in wet condition. However, the difference is more significant in the specimens wetted with chemical solvents compared to control. This can be explained by the cellulose water interaction behavior [75]. On drying the fibers, there is subsequent reduction in the swelling causing a zip up of the voids [86]. Recrystallization or spot wise bridging on drying of the swollen wetted substrate causes the zip-up. Moreover, the amorphous substrate may also recrystallize on drying [76].

Table 4.10 Tensile properties of LCC fibers in dry and wet conditions

	Control		KOH (10%)		$NaHSO_3$ (5%)	
	Dry	**Wet**	**Dry**	**Wet**	**Dry**	**Wet**
Young's Modulus (GPa)	**45.4 (14)***	**43.7 (17.3)**	**53.5 (11.23)**	**30.6 (8.89)**	**54.5 (19.5)**	**37.9 (13.9)**
Strength (MPa)	**1250 (252)**	**1169 (169)**	**1439 (147)**	**982 (180)**	**1449 (435)**	**1085 (264)**
Strain (%)	**4.65**	**5.34**	**5.09**	**5.01**	**5.13**	**4.83**

* Values in parentheses indicate standard deviation

4.5.4.4 Effect of Load

Imparting load along the fiber axis is a part of the conventional mercerization practice. It is conducted to strengthen the fiber and make it a stiffer material to be used in textiles/composites and other advanced applications [13, 75, 88].

As the load is imparted along with the chemical treatment, the combined effect results in better orientation of the molecular chains of the fiber and a rearrangement of the crystal structure [15]. It may also result in increase in degree of crystallinity due to conversion of the amorphous region due to zip up phenomenon [88].

Table 4.11 presents the tensile properties of LCC fibers as a function of load for KOH and $NaHSO_3$ treatments. However, the obtained results for LCC fibers treated with a load of 10% (0.98 kg) and 25% (2.42 kg) of wetted fiber fracture stress showed a considerable decrease in the tensile properties. This was assumed to be due to degradation of cellulose or significant molecular slippage under high load and concentration of treatment solvents for prolonged

periods (120 min) of time. As a result, the treatment with 2.42 kg load was considered too harsh for LCC fibers and discontinued for further processing.

Although KOH and $NaHSO_3$ showed similar stiffness and strength values, there was a clear degradation of fiber surface seen with KOH treatments through the SEM images. Moreover, $NaHSO_3$ being a food grade chemical retained the 'green' nature of the processes. Keeping the process green was one of the objectives of this study. As a result, treatment with $NaHSO_3$ under 0.98 kg load was selected as the desired treatment for subsequent modifications.

Table 4.11 Tensile properties of LCC fibers as a function of load for KOH and $NaHSO_3$ treatments

	Control			KOH (10%)			$NaHSO_3$ (5%)		
Load (kg)	**Dry**	**Load 0.98**	**Load 2.4**	**No Load**	**Load 0.98**	**Load 2.4**	**No Load**	**Load 0.98**	**Load 2.4**
Young's Modulus (GPa)	**45.4 (14.0)***	**47.2 (13.1)**	**45.5 (18.9)**	**53.5 (11.2)**	**45.9 (10.3)**	**31.6 (10.4)**	**54.5 (19.5)**	**46.7 (15.1)**	**33.1 (8.8)**
Strength (MPa)	**1250 (252)**	**1517 (447)**	**1446 (388)**	**1439 (147)**	**1460 (247)**	**1291 (337)**	**1449 (435)**	**1480 (534)**	**1286 (255)**
Strain (%)	**4.65**	**5.71**	**5.58**	**5.09**	**5.90**	**5.54**	**5.13**	**5.72**	**5.58**

* Values in parentheses indicate standard deviation

4.5.4.5 Effect of Treatment Duration

To assess the effect of $NaHSO_3$ treatment time on the tensile properties of LCC fibers, the time was varied between 30 min and 120 min. Table 4.12 presents the tensile properties of LCC fibers as a function of duration of the $NaHSO_3$ treatment with load. The reduction in the

duration of load application showed clear evidence of increase in the tensile modulus. This supported the assumption that the initial load treatments for 120 min were too high for the cellulose structure of the fiber leading to a breakdown of chains or molecular slippage and even possible solubilization in the aqueous medium. Based on the results obtained, load application for 60 min was selected as the optimum treatment to obtain enhanced tensile properties of LCC fibers for composite applications.

Figure 4.28 summarizes the change in Young's modulus of LCC fibers with various $NaHSO_3$ treatments. The final tensile results received from Instron universal tester were in agreement with the data obtained by GADD, XRD and SEM characterizations discussed earlier. Increase in degree of crystallinity, molecular orientation and reduction in the fiber diameter resulted in more than 40% increase the Young's modulus and more than 30% increase in the tensile strength of LCC fibers.

Table 4.12 Tensile properties of LCC fibers as a function of duration of load during the $NaHSO_3$ treatment

	Control	**5% $NaHSO_3$**			
	Dry	**No Load**	**Load 0.98 kg (30 min)**	**Load 0.98 kg (60 min)**	**Load 0.98 kg (120 min)**
Young's Modulus (GPa)	**45.4 (14.0)***	**54.5 (19.5)**	**54.2 (10.7)**	**65.6 (15.4)**	**46.7 (15.1)**
Strength (MPa)	**1250 (252)**	**1449 (435)**	**1522 (220)**	**1588 (291)**	**1480 (534)**
Strain (%)	**4.65**	**5.13**	**5.18**	**6.66**	**5.72**

* Values in parentheses indicate standard deviation

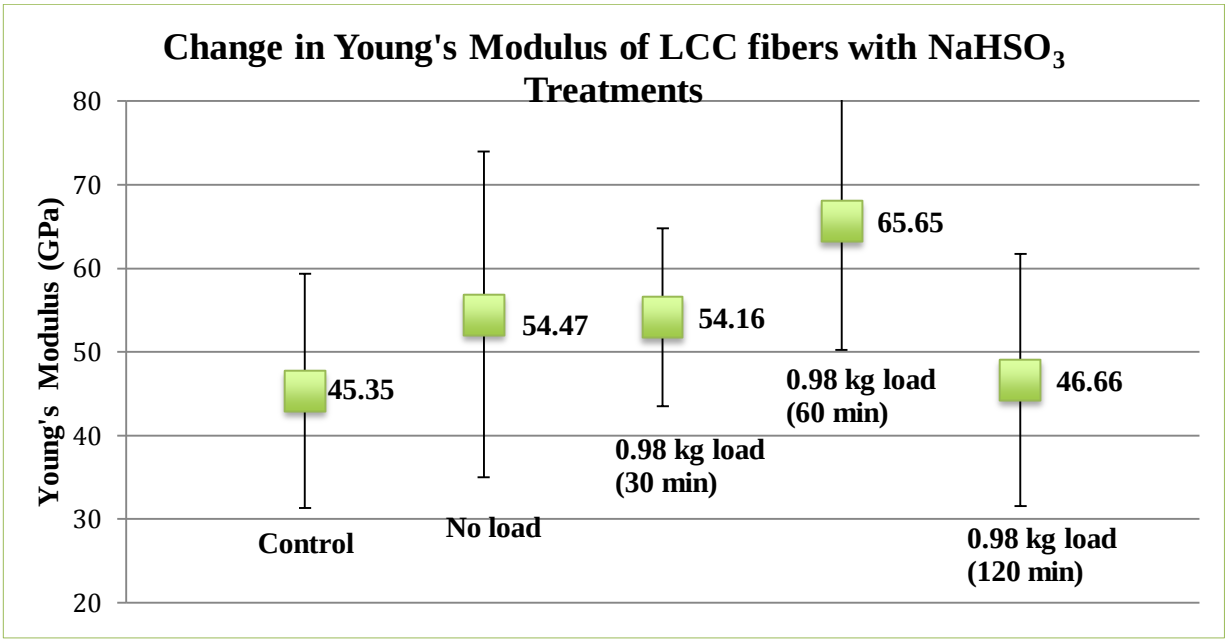

Figure 4.28 Summary of Young's moduli of LCC fibers with various $NaHSO_3$ treatments

4.6 Tensile Characterization of LCC Fiber Reinforced RP Starch Based Composites

Unidirectional green composites were fabricated using LCC fibers and RP starch resin. The fiber content in the composites was maintained around 23-26 % while fabrication. Since the composites were hand prepared, higher fiber content was difficult to process. Preliminary composites indicated that the resin could not penetrate completely inside the LCC yarns which is critical for their good mechanical performance. Lack of resin penetration resulted in poor composite properties. The maximum tensile strength achieved was 150 MPa whereas the Young's modulus values were restricted at 5 GPa. For the fibers treated under different conditions and used in composites, the results are presented in Table 4.13. The results are significantly lower than the theoretical values for several reasons. However, if the fiber fraction is increased to 0.65, commonly found in many composites, the strength of 848.04 MPa and Young's modulus of 42.83 GPa could be achieved, making them advanced green composites.

Table 4.13 Young's modulus and tensile strength (experimental values) of RP starch based LCC fiber reinforced composites

	Control	$NaHSO_3$ (No load)	$NaHSO_3$ 0.98 kg load
Young's Modulus (GPa)	**10.2 (2.7)***	**7.98 (3.2)**	**9.84 (0.8)**
Strength (MPa)	**223.5 (14.23)**	**170.5 (23.05)**	**165.7 (15.03)**

* Values in parentheses indicate standard deviation

The experimental values for tensile strength and young's modulus of composites fabricated using control (untreated) LCC yarns were 223.5 MPa and 10.2 GPa, respectively. However, the experimental values were not consistent and rather reduced for the composites made from treated yarns. The theoretical values of tensile strength and Young's modulus were calculated using the rule of mixtures and average fiber volume fraction of 0.255. Table 4.14 presents the young's modulus and tensile strength (theoretical values) of RP starch based LCC fiber reinforced composites.

Table 4.14 Young's modulus and tensile strength (theoretical values) of RP starch based LCC fiber reinforced composites (for fiber content of 25.5%)

	Control	$NaHSO_3$ (No load)	$NaHSO_3$ 0.98 kg load
Young's Modulus (GPa)	**11.66**	**13.95**	**16.74**
Strength (MPa)	**318.75**	**369.5**	**404.95**

Fabrication of composites using treated LCC yarns was a challenge as the fibers were difficult to separate from each other using manual methods.

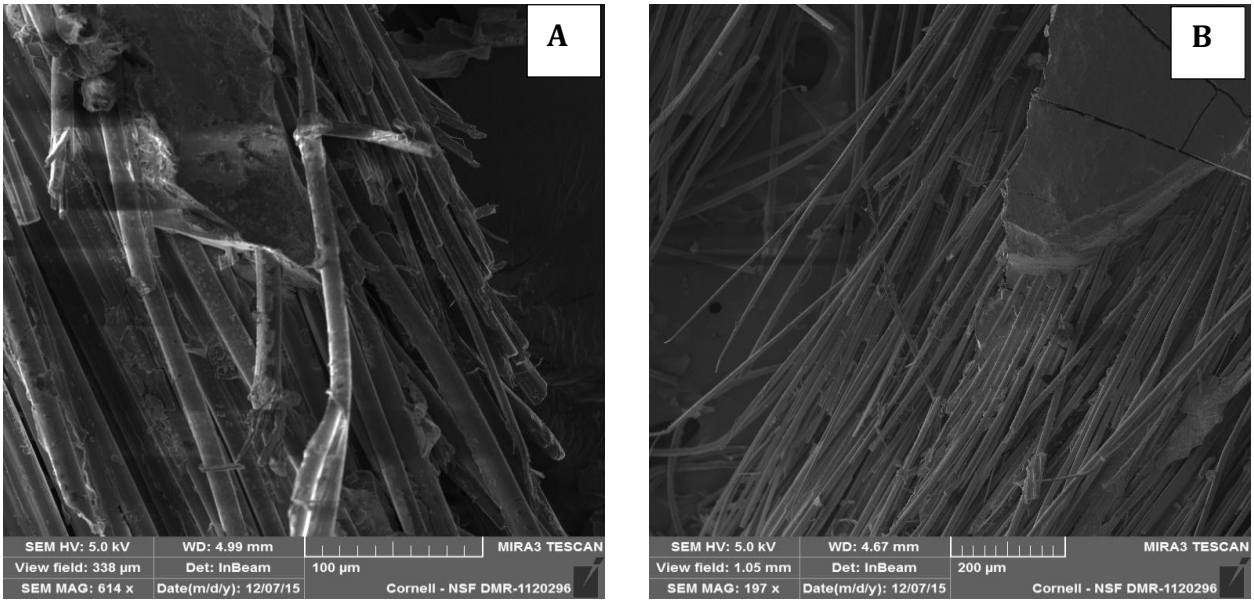

Figure 4.29 SEM images of tensile tested composite fracture surfaces, control (A) and treated (B) LCC fibers

The fracture surface of the tested composites with LCC yarns, showed fiber pull out from the resin indicating little penetration of the resin into the LCC yarn. At some locations no resin was seen because the highly viscous RP starch based resin was unable to reach the individual fibers of the treated LCC yarns, ultimately not allowing the fibers to contribute to the composite strength. Efforts were made to reduce the viscosity of the resin. As a result, some techniques such as manual separation, high speed sonication and air drying of the treated yarns were carried out with the expectation that these processes will separate the individual fibers within the yarn. While these yarns did look better, they did not allow adequate resin penetration in the treated and dried LCC yarn consisting 1000 fibers with ~10 µm diameter. Previous research has shown that fiber reinforced composites have been successfully fabricated using LCC yarns with low viscosity soy protein isolate resin. However, in order to successfully reinforce LCC yarns with high viscosity starch based resins, without compromising on the fiber orientation, mechanized

techniques like high speed air drying of treated fibers or high frequency sonication should be used for yarn separation or resin penetration respectively.

5. CONCLUSIONS

In this research an easy to scale up and convenient method was devised to obtain starch from the naturally available raw plantain fruit. The starch was crosslinked to enhance its mechanical properties. In addition, further enhancement of the properties were obtained by adding BFMC to the starch. The property-enhanced starch was then combined with LCC fibers to fabricate 'green' composites. From the observations and analysis of the processes undertaken and the results obtained following conclusions can be drawn:

5.1 Starch Isolation and Characterization

i. Starch was successfully isolated from raw plantain fruits using multiple solvents. The desired method was selected based upon the proximate analysis results and the environment friendliness of the end product.

ii. The method involving steeping of raw plantain pulp with 1% $NaHSO_3$ solution, not only was a green process involving nontoxic, water soluble, food grade chemical but also gave the best comparative results of isolated starch content of above 80%.

iii. The ATR-FTIR characterization of this native RP starch yielded functional groups matching to that of commercially available cornstarch.

iv. The XRD and DSC analysis gave an idea of the starch composition and preliminary data related to the enthalpy and temperatures of gelatinization respectively.

v. The RP starch exhibited an onset of gelatinization behavior at about 65°C and completion of gelatinization at about 83°C.

vi. This result was also supported by the rheometry results of 5% starch solution at increasing temperatures as a function of shear rate. The starch showed increase in initial

viscosity with increase in temperature. The homogeneity of the starch was also observed to increase with temperature due to the lack of fluctuations derived with increase in shear rate.

vii. RP starch showed physical and chemical properties comparable to the commercially available starches and was selected to be used as resin for fabricating green composites.

5.2 Resin Formation and Characterization

i. RP starch based resin was successfully formed using a nontoxic, green organic crosslinker 1,2,3,4-butane tetracarboxylic acid using sodium hypophosphite as the catalyst.

ii. Cellulose microfibrils (BFMC) were derived from banana stem fibers using acid hydrolysis method and used as reinforcing elements for the resin.

iii. In order to obtain best mechanical properties, the (BFMC) and crosslinker contents were optimized to 25% of total polysaccharide and 10% of total polysaccharide, respectively.

iv. The RP resin showed excellent adhesion due to the presence of a large number of reactive hydroxyl groups in each of the constituents. The process of crosslinking was confirmed by the reduction in moisture absorbance and the formation of characteristic peak at 1719 cm^{-1} in the ATR-FTIR spectrum, which is attributed to the ester carbonyl group (C=O).

v. The incorporation of cellulose microfibrils (BFMC) proved successful in imparting stiffness to the resin by increasing its Young's modulus by about 500% and reduction of strain to 20% of the control resin strain.

5.3 Strength and Modulus Enhancement Treatments on LLC Fibers

LCC fiber, an inherently strong fiber, was subjected to multiple chemical and mechanical strength enhancement treatments. These showed a gradual increase in the stiffness with optimization of each parameter. The changes observed as a function of each parameter are as follows:

5.3.1 Solvent

i. The chemical treatment with various aqueous solvents of NaOH, KOH, $NaHSO_3$, NH_4OH showed interesting but differing results on the morphology and strength of the fiber.

ii. NaOH solution degraded the fiber due to deep penetration leading to a breakdown of microfibrils. This observation was consistent with the previous literature.

iii. The treatments with KOH and $NaHSO_3$ showed a considerable increase the strength of the LCC fibers, which was assumed due to the aqueous ion penetration and reordering of phase structure.

5.3.2 Concentration

i. With increase in concentration of KOH and $NaHSO_3$ solutions it was observed that the stiffness increased. This was possibly due the presence of increased number of ions to penetrate the fiber structure.

ii. However, in the case $NaHSO_3$, 5% and 10% solutions did not show a considerable difference in the fiber properties. This may be due the fiber reaching a saturation state at the given concentration after which the cellulose structure begins to degrade the structure. This phenomenon is consistent with the earlier literature.

iii. There was a clear decrease in the strain of LCC fibers with increase in the concentration of the solvent. This clarified that the aqueous ions led to restructuring of the fiber phases, converting the amorphous region into semi-crystalline/crystalline region leading to a stiffer material desirable for use in composites.

iv. The change in phases was seen clearly in the XRD results. The degree of crystallinity increased from ~58% to almost 80% after the treatment.

v. After a considerable analysis of the data and literature review, treatments with 5% $NaHSO_3$ and 10% KOH seemed most suitable for further processing.

5.3.3 Dry/ Wet State

i. The tests carried out in wet state generated preliminary data required to select loads for mechanical treatment of LCC fibers.

ii. As expected the strength of the fibers in wet state was lesser by 40% compared to the dry state. This confirmed the hypothesis that there is a phase rearrangement in LCC fibers on alkali treatment.

iii. The difference in the wet test values between control and solvent treatment can be explained by the cellulose water interaction mechanism. While water is capable of only partially disintegrating the weak hydroxyl bonds of cellulose, it can penetrate into the crystalline structures with the aid of aqueous ionic solvents.

5.3.4 Load

i. This was a crucial fiber treatment that was responsible for molecular alignment and orientation along the fiber axis.

ii. This was supported by the GADD spectra of fibers that showed a significant decrease in the FWHM value from 17.9 to 10.2.

iii. However, results showed that loads beyond 15% of fracture load may be too harsh for LCC fibers in wet condition. This may be due to the process of phase restructuring that it undergoes before drying, which leads to temporary weakening of fibers making them incapable to withstand loads for a prolonged period.

iv. The degradation of fiber structure was observed with KOH treatment for 120 min due to which it was discontinued for further testing.

5.3.5 Duration

i. Reduction in treatment time showed a dramatic increase in the mechanical properties of LCC fibers.

ii. 5% $NaHSO_3$ treatment carried out with 0.98 kg load for 0, 30, 60 and 120 min showed a linear increase in the modulus and strength with increase in time. However, the treatment for 120 min was longer than needed and degraded the fiber which could be seen through the reduced Young's modulus.

5.4 Fabrication of LCC Fiber Reinforced RP Starch Based Composites

i. Unidirectional green composites were fabricated using LCC fibers and RP starch resin. The fiber content in the composites was maintained around 23-26% while fabrication.

ii. Preliminary composites indicated that the resin could not penetrate completely inside the LCC yarns which is critical for their good mechanical performance. Lack of resin penetration due to its high viscosity resulted in poor composite properties.

iii. Fabrication of composites using treated LCC yarns was a challenge as the fibers were difficult to separate from each other using manual methods. The fracture surface of the tested composites with control yarns, showed significant fiber pull out from the resin indicating little penetration of the resin into the LCC yarn.

iv. Efforts were made to reduce the viscosity of the resin. However, reduction of resin viscosity led to disintegration of the final composite. As a result, some techniques such as manual separation, high speed sonication and air drying of the treated yarns were carried out with the expectation that these processes will separate the individual fibers within the yarn. While these yarns did look better, they still did not allow adequate resin penetration in the treated and dried LCC yarn consisting 1000 fibers with ~10 µm diameter.

v. Previous research has shown that fiber reinforced composites have been successfully fabricated using LCC yarns with low viscosity soy protein isolate resin. However, in order to successfully reinforce LCC yarns with high viscosity starch based resins, without compromising on fiber orientation, mechanized techniques like high speed air drying of treated fibers or high frequency sonication may be used for yarn separation and resin penetration, respectively.

Other Comments

The use of fiber reinforced biobased composites has created a renaissance in almost all the fields which conventionally use petroleum based composites. Many researchers are now working on these materials to create innovative and competitive replacements for car components, airplane components, sporting goods, construction components, disposables and packing goods.

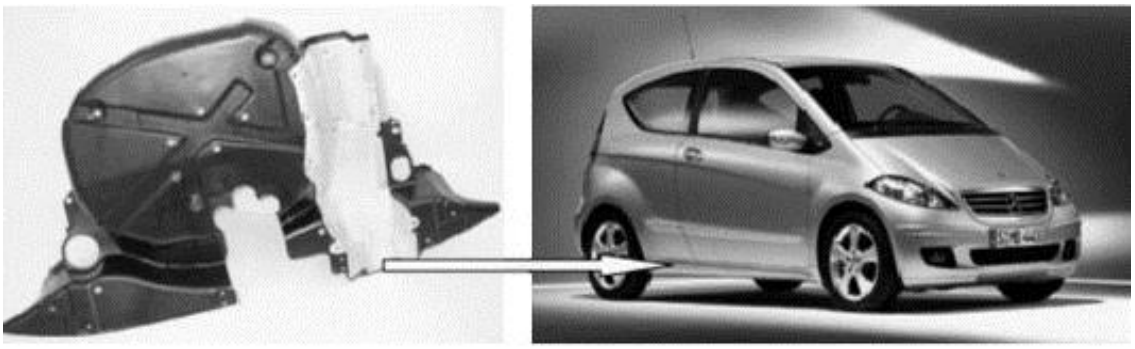

Figure 5.1 Under floor protection trim of Mercedes A class made from banana fiber reinforced composites

As shown in Figure 5.1, more and more premium auto brands like BMW, Tesla, Audi, Ford are now using biobased composites in various components such as door panels, dash boards, etc. Daimler-Benz has been using jute based door panels since 1996 in Mercedes cars and have been working with flax fiber composites to replace glass fiber materials since 1991 [107]. Added advantage of using these materials is weight savings of the car.

Recent work has also demonstrated the entire air plane body made using advanced hemp fiber along with other uses in auto applications requiring high specific stiffness [12].

In summary, this research using novel green starch based resin and high strength fibers is an attempt to contribute to the field of biobased ‘green’ composites, which possess a large potential for further growth and progress penetrating every untapped market.

BIBLIOGRAPHY

1. Matthews, F.L., Rawlings, R.D., *Composite Materials: Engineering and Science*. 1994, Woodhead Publishing Ltd.: Cambridge, UK.
2. Council, A.C., *U.S. Resin Production, Sales and Captive use*. 2015.
3. Mohanty, A.K., Misra, M., Drzal, L. T., *Sustainable composites from renewable resources.* Polymers and environment, 2002. **10**(Nos. 1/2): p. 19-26.
4. Bernhard, J., Witten, E. *Composites Market Report 2013*. 2013.
5. Netravali, A.N., *Green materials and process in fibers and fabrics* 2015, Cornell University
6. Mohanty, A.K., Misra, M., Hinrichsen, G., *Biofibers, biodegradable polymers and biocomposites: An overview.* Macromolecular Materials and engineering, 2000. **276-277,**(1): p. 1-24.
7. *The technology roadmap for plant/crop based renewable resources 2020*
8. Karnani, R., Krishnan, M., Narayan, R., *Biofiber reinforce popropylene composites.* Polymer Engineering and science, 1997. **37**(2): p. 476-483.
9. Morris, D.J. and I. Ahmed *The carbohydrate economy: Making chemicals and industrial materials from plant matter*. 1992.
10. Appiah, P. *50% waste of plantain production every week in Agogo*. 2014.
11. Shu, C., *Taiwan tries to revive its banana export industry*, in *The new york times* 2013.
12. Muhammad, P., Sain, M., *Sheet-Molded Polyolefin Natural Fiber Composites for Automotive Applications.* Macromolecular Materials and engineering, 2003. **288**(7): p. 553-557.
13. Kim, J.T., Netravali, A. N., *Mercerization of sisal fibers: Effect of tension on mechanical properties of sisal fiber and fiber-reinforced composites.* Composites Part A: Applied Science and Manufacturing, 2010. **41**(9): p. 1245-1252.
14. Plackett, D., Andersen, T., Batsberg, P. W., Nielsen, L.,, *Biodegradable composites based on l-polylactide and jute fibres.* Composites Science and Technology, 2003. **63**(9): p. 1287-1296.
15. Kim, J.T., Netravali, A. N.,, *Fabrication of advanced "green" composites using potassium hydroxide (KOH) treated liquid crystalline (LC) cellulose fibers.* Journal of Materials Science, 2013. **48**(11): p. 3950-3957.
16. Mathews, K., Van Hole, E., Kevin, A., *Biochemistry*. 2000, Benjamin Cummings: San Francisco, Claifornia
17. Blamier, J. *The macromolecules Polysaccharides*. 2004.
18. Ghosh Dastidar, T., Netravali, A N., *Cross-Linked Waxy Maize Starch-Based "Green" Composites.* ACS Sustainable Chemistry & Engineering, 2013. **1**(12): p. 1537-1544.
19. Viet, D., Stephanie, B., Gray, D., *Dispersion of cellulose nanocrystals in polar organic solvents.* Cellulose, 2007. **14**(2): p. 109-113.
20. Swinkels, J. *Sources of starch, its chemistry and physics*. 1985.
21. Whistler, R.L., *CHAPTER I - HISTORY AND FUTURE EXPECTATION OF STARCH USE*, in *Starch: Chemistry and Technology (Second Edition)*, R.L.W.N.B.F. Paschall, Editor. 1984, Academic Press: San Diego. p. 1-9.
22. Eliasson, A.-C., ed. *Starch in Food*. 2004, Woodhead publishing LImited: Cambridge, UK.

23. International, L., *Evaluation of the Community policy for starch and starch products* 2014.
24. Institute, I.s., *World starch production by crop*. 2010.
25. Santacruz, S., et al., *Three underutilised sources of starch from the Andean region in Ecuador Part I. Physico-chemical characterisation.* Carbohydrate Polymers, 2002. **49**(1): p. 63-70.
26. Satin, M., *Functional properties of starches.*
27. Du, X., Jia, Jianhua., Xu, Shiying., Zhou, Yibin, *Molecular Structure of Starch from Pueraria lobata (Willd.) Ohwi Relative to Kuzu Starch.* Starch - Stärke, 2007. **59**(12): p. 609-613.
28. Gallant, D.J., B. Bouchet, and P.M. Baldwin, *Microscopy of starch: evidence of a new level of granule organization.* Carbohydrate Polymers, 1997. **32**(3–4): p. 177-191.
29. Eggleston, G., R. Swennen, and S. Akoni, *Physicochemical Studies on Starches Isolated from Plantain Cultivars, Plantain Hybrids and Cooking Bananas.* Starch - Stärke, 1992. **44**(4): p. 121-128.
30. Jane, J., Chen, Y. Y., Lee, L. F., McPherson, A. E., et al., *Effects of Amylopectin Branch Chain Length and Amylose Content on the Gelatinization and Pasting Properties of Starch.* Cereal Chemistry Journal, 1999. **76**(5): p. 629-637.
31. Ghosh Dastidar, T., Netravali, A N., *'Green' crosslinking of native starches with malonic acid and their properties.* Carbohydrate Polymers, 2012. **90**(4): p. 1620-1628.
32. Biliaderis, C.G., *The structure and interactions of starch with food constituents.* Canadian Journal of Physiology and Pharmacology, 1991. **69**(1): p. 60-78.
33. Oates, C.G., *Towards an understanding of starch granule structure and hydrolysis.* Trends in Food Science & Technology, 1997. **8**(11): p. 375-382.
34. Chabba, S., Netravali, A. N., *'Green' composites Part 1: Characterization of flax fabric and glutaraldehyde modified soy protein concentrate composites.* Journal of Materials Science, 2005. **40**(23): p. 6263-6273.
35. La Mantia, F.P. and M. Morreale, *Green composites: A brief review.* Composites Part A: Applied Science and Manufacturing, 2011. **42**(6): p. 579-588.
36. Zhang, P., Whistler, R. L., BeMiller, J. N., Hamaker, B. R., *Banana starch: production, physicochemical properties, and digestibility—a review.* Carbohydrate Polymers, 2005. **59**(4): p. 443-458.
37. Lii, C.-Y., S.-M. Chang, and Y.-L. Young, *Investigation of the Physical and Chemical Properties of Banana Starches.* Journal of Food Science, 1982. **47**(5): p. 1493-1497.
38. Chiang, B.H., W.C. Chu, and C.L. Chu, *A Pilot Scale Study for Banana Starch Production.* Starch - Stärke, 1987. **39**(1): p. 5-8.
39. Kayisu, K., L.F. Hood, and P.J. Vansoest, *Characterization of Starch and Fiber of Banana Fruit.* Journal of Food Science, 1981. **46**(6): p. 1885-1890.
40. Madson, M., *Method of isolating a banana starch from green bananas.* 2013, Google Patents.
41. Pérez-Sira, E., *Characterization of Starch Isolated from Plantain (Musa paradisiaca normalis).* Starch - Stärke, 1997. **49**(2): p. 45-49.
42. Garcia, E. and F.M. Lajolo, *Starch Transformation During Banana Ripening: The Amylase and Glucosidase Behavior.* Journal of Food Science, 1988. **53**(4): p. 1181-1186.

43. Waliszewski K.N., A.M.A., Bello L. A., Monroy J. A., *Changes in banana starch by chemical and physical modifications.* Carbohydrate Polymers 2003. **52**: p. 237-242.
44. Jane, J.-l., *Current Understanding on Starch Granule Structures.* Journal of Applied Glycoscience, 2006. **53**(3): p. 205-213.
45. Hernández-Jaimes, C., Bello-Pérez, L. A., Vernon-Carter, E. J., Alvarez-Ramirez, J., *Plantain starch granules morphology, crystallinity, structure transition, and size evolution upon acid hydrolysis.* Carbohydrate Polymers, 2013. **95**(1): p. 207-213.
46. Núñez-Santiago, M.C., L.A. Bello-Pérez, and A. Tecante, *Swelling-solubility characteristics, granule size distribution and rheological behavior of banana (Musa paradisiaca) starch.* Carbohydrate Polymers, 2004. **56**(1): p. 65-75.
47. Von Loesecke, H.W. *Bananas*. Interscience Publishers, NY 1950. **2**.
48. Netravali, A.N., Huang, X., Mizuta, Kazuhiro, *Advanced 'green' composites.* Advanced Composite Materials, 2007. **16**(4): p. 269-282.
49. Qui, K., Netravali, A. N., *Fabrication and characterization of biodegradable composites based on microfibrillated cellulose and polyvinyl alcohol.* Composites Science and Technology, 2012. **72**(13): p. 1588-1594.
50. Xiaosong, H., Netravali, A. N., *Biodegradable green composites made using bamboo micro/nano-fibrils and chemically modified soy protein resin.* Composites Science and Technology, 2009. **69**(7–8): p. 1009-1015.
51. Nakamura, R., Netravali, A. N., et al., *Effect of halloysite nanotubes on mechanical properties and flammability of soy protein based green composites.* Fire and Materials, 2013. **37**(1): p. 75-90.
52. Safonov, V., *Treatment of textile materials.* Moscow: Legprombitizdat, 1991.
53. Bailie, C., ed. *Green Composites*. 1993, Woodhead Publishing Limited Cambridge, UK.
54. Elanthikkal, S., et al., *Cellulose microfibres produced from banana plant wastes: Isolation and characterization.* Carbohydrate Polymers, 2010. **80**(3): p. 852-859.
55. Walker, L.P., Wilson, D. B., *Enzymatic hydrolysis of cellulose: An overview.* Bioresource Technology, 1991. **36**(1): p. 3-14.
56. Bhattacharya, D., Germinario, L. T., Winter, W. T., *Isolation, preparation and characterization of cellulose microfibers obtained from bagasse.* Carbohydrate Polymers, 2008. **73**(3): p. 371-377.
57. Pelissari, F., Sobral, P. A., Menegalli, FlorenciaCecilia, *Isolation and characterization of cellulose nanofibers from banana peels.* Cellulose, 2014. **21**(1): p. 417-432.
58. Robertson, J.R., *Forensic examination of fibers*. 2003, Taylor and Francis Group.
59. Frompo, *Physical classification of fibers.*
60. Chemiefaser, I., *world wide production volume of chemical and textile fibers* 2014: Statista.
61. Maldas, D. and B.V. Kokta, *Interfacial adhesion of lignocellulosic materials in polymer composites: an overview.* Composite Interfaces, 1993. **1**(1): p. 87-108.
62. Averous, L. and N. Boquillon, *Biocomposites based on plasticized starch: thermal and mechanical behaviours.* Carbohydrate Polymers, 2004. **56**(2): p. 111-122.
63. Perez S., M.W., *Structure and morphology of cellulose* CERMAV-CNRS, 2001. **IV**.
64. Mohanty, A.K., Misra, M., Hinrichsen, G., *Biofibres, biodegradable polymers and biocomposites: An overview.* Macromolecular Materials and engineering, 2000. **276-277**(1): p. 1-24.

65. Netravali, A.N., Chabba, S., *Composites get greener.* Materials Today, 2003. **6**(4): p. 22-29.
66. Wambua, P., J. Ivens, and I. Verpoest, *Natural fibres: can they replace glass in fibre reinforced plastics?* Composites Science and Technology, 2003. **63**(9): p. 1259-1264.
67. Wollerdorfer, M. and H. Bader, *Influence of natural fibres on the mechanical properties of biodegradable polymers.* Industrial Crops and Products, 1998. **8**(2): p. 105-112.
68. C. K. Ruseckaite, A.J., *Thermal Degradation of mixtures of Polycaprolactone with cellulose derivatives.* Polymer Degradation and stability, 2003. **81 (2)**.
69. Oksman, K., M. Skrifvars, and J.F. Selin, *Natural fibres as reinforcement in polylactic acid (PLA) composites.* Composites Science and Technology, 2003. **63**(9): p. 1317-1324.
70. Liu, Z., et al., *"Green" Composites from Renewable Resources: Preparation of Epoxidized Soybean Oil and Flax Fiber Composites.* Journal of Agricultural and Food Chemistry, 2006. **54**(6): p. 2134-2137.
71. Luo, S., Netravali, A. N., *Interfacial and mechanical properties of environment-friendly "green" composites made from pineapple fibers and poly(hydroxybutyrate-co-valerate) resin.* Journal of Materials Science, 1999. **34**(15): p. 3709-3719.
72. Nishino, T., et al., *Kenaf reinforced biodegradable composite.* Composites Science and Technology, 2003. **63**(9): p. 1281-1286.
73. Lodha, P., Netravali, A. N., *Characterization of interfacial and mechanical properties of "green" composites with soy protein isolate and ramie fiber.* Journal of Materials Science, 2002. **37**(17): p. 3657-3665.
74. Kontturi, E., T. Tammelin, and M. Osterberg, *Cellulose-model films and the fundamental approach.* Chemical Society Reviews, 2006. **35**(12): p. 1287-1304.
75. Jan Sirosky, B.S., and T. Bechtold, *Alkali treatment of woven cellulose fabrics*, in *Intechopen.*
76. Abu-Rous, *Characterisation of wet state pore structure of lyocell and other man made cellulosic fibers by fluoroscence and electron microscopy*, in *University of innsbruk*. 2006.
77. Woodings, C., *Regenerated Cellulose fibers*. 2001, Woodhead Publishings Ltd. .
78. Werbowyj, R.S. and D.G. Gray, *Liquid Crystalline Structure In Aqueous Hydroxypropyl Cellulose Solutions.* Molecular Crystals and Liquid Crystals, 1976. **34**(4): p. 97-103.
79. Boerstoel, H., *Liquid Crystalline solutions of cellulose in phosphoric acid*. 1962.
80. Northolt, M.G., et al., *The structure and properties of cellulose fibres spun from an anisotropic phosphoric acid solution.* Polymer, 2001. **42**(19): p. 8249-8264.
81. Kamide, K., I. Miyamoto, and K. Okajima, *Formation and Properties of the Lyotropic Mesophase of the Cellulose/Mixed Inorganic Acid System.* Polym J, 1993. **25**(5): p. 453-461.
82. Gray, D.G., *Chemical characteristics of cellulosic liquid crystals.* Faraday Discussions of the Chemical Society, 1985. **79**(0): p. 257-264.
83. Boerstoel, H., et al., *Liquid crystalline solutions of cellulose in phosphoric acid.* Polymer, 2001. **42**(17): p. 7371-7379.
84. Bledzki, A.K. and J. Gassan, *Composites reinforced with cellulose based fibres.* Progress in Polymer Science, 1999. **24**(2): p. 221-274.

85. Galasso, F.S., *Advanced fibers and composites*. 1989, Gordon and Breach Science Publishers: NY, USA.
86. Crawshaw, J. and R.E. Cameron, *A small angle X-ray scattering study of pore structure in Tencel® cellulose fibres and the effects of physical treatments.* Polymer, 2000. **41**(12): p. 4691-4698.
87. Zhu, Y., X. Ren, and C. Wu, *Influence of alkali treatment on the structure of newcell fibers.* Journal of Applied Polymer Science, 2004. **93**(4): p. 1731-1735.
88. Okano, T. and A. Sarko, *Mercerization of cellulose. II. Alkali–cellulose intermediates and a possible mercerization mechanism.* Journal of Applied Polymer Science, 1985. **30**(1): p. 325-332.
89. Yawei Zhu, X.R.e.a., *Influence of alkali treatment on the structure of newcell fibers.* Applied polymer science, 2004. **93** p. 1731-1735.
90. Vilpoux, O. and L. Averous, *Starch-based plastics.* Technology, use and potentialities of Latin American starchy tubers, 2004: p. 521-553.
91. Lan, C., et al., *Design, Preparation and Characterization of Self-Reinforced Starch Films through Chemical Modification.* Macromolecular Materials and Engineering, 2010. **295**(11): p. 1025-1030.
92. Pashkuleva, I., H.S. Azevedo, and R.L. Reis, *Surface Structural Investigation of Starch-Based Biomaterials.* Macromolecular Bioscience, 2008. **8**(2): p. 210-219.
93. Ochi, S., *Development of high strength biodegradable composites using Manila hemp fiber and starch-based biodegradable resin.* Composites Part A: Applied Science and Manufacturing, 2006. **37**(11): p. 1879-1883.
94. Reddy, N. and Y. Yang, *Preparation and properties of starch acetate fibers for potential tissue engineering applications.* Biotechnology and Bioengineering, 2009. **103**(5): p. 1016-1022.
95. Passauer, L., F. Liebner, and K. Fischer, *Starch Phosphate Hydrogels. Part I: Synthesis by Mono-phosphorylation and Cross-linking of Starch.* Starch - Stärke, 2009. **61**(11): p. 621-627.
96. Chen, Y. and G. Wang, *Synthesis of crosslinked oxidized starch and its adsorption behavior for calcium ion.* Journal of Applied Polymer Science, 2006. **102**(2): p. 1539-1546.
97. Wool, R., Xiuzhi, S. S., *Biobased polymers and composites* 2005: Elsevier Academic press.
98. Lörcks, J., *Properties and applications of compostable starch-based plastic material.* Polymer Degradation and Stability, 1998. **59**(1–3): p. 245-249.
99. Yan, L., N. Chouw, and K. Jayaraman, *Flax fibre and its composites – A review.* Composites Part B: Engineering, 2014. **56**: p. 296-317.
100. Roman, M., Winter, W. T., *Effect of Sulfate groups from sulfuric acid hydrolysis on the thermal degration behavior of bacterial cellulose.* Biomacromolecules, 2004. **5(5)**.
101. Dong X. M., R.J.F., Gray D. G. , *Effect of microcrystalite preparation conditions on the formation of colloid crystals of cellulose* Cellulose, 1998. **5(1)**.
102. Alger mark, S.M. Polymer Science dictionary, 1997. **2**.
103. Whistler, R.L., *Banana starch production*. 1998, Google Patents.
104. Ramírez, M.G.L., et al., *Preparation and characterization of biodegradable composites based on Brazilian cassava starch, corn starch and green coconut fibers.* Matéria (Rio de Janeiro), 2010. **15**: p. 330-337.

105. Yang, C., *FTIR spectroscopy study of ester crosslinking of cotton cellulose catalysed by SHP.* Textile research journal, 2001. **71**.
106. Químicos., S.I.d.P., *Morton, WE, Hearle, WS Physical Properties of Textile Fibres.* Editors: Morton, WE, Hearle, WS, Published: The Textile Institute, England, 1993. **717**.
107. John, M.J. and S. Thomas, *Biofibres and biocomposites.* Carbohydrate Polymers, 2008. **71**(3): p. 343-364.